Chapter 1

Introduction to D-π-A systems: Applications in photovoltaics and nonlinear optics

Contents

1.1. Introduction

Organic molecules with π-conjugated scaffolds end-capped with electron donor and acceptor groups are widely investigated due to their immense application potentials and hence they belong to a promising area of organic chemistry. In these types of systems, the intra molecular charge transfer will occur from the donor unit (D) to the acceptor unit (A) (Figure 1.1).

Figure 1.1. Schematic representation of Donor-π-Acceptor molecule

Due to the interaction between the donor unit and acceptor unit a set of new low-energy molecular orbitals (MO) are generated, which shift the absorption maximum to longer wavelengths in comparison to the individual uncoupled systems. Such systems are generally referred as charge-transfer chromophores.[1-4] The interaction between the donor and acceptor can occur in a through bond or through space fashion. Stronger electronic coupling is observed when the donor and acceptor groups are in conjugation with each other. Such conjugated electron donor-acceptor (D-A) molecules are termed as "push-pull" systems. They have received increasing attention in the area of research focussing the development of organic materials for nonlinear optics,[5-10] electro-optics,[11-12] piezochromism,[13] solvatochromism[14-17] and photovoltaics.[18-28] In such D-A frameworks, HOMO and LUMO energies can be easily tuned by appropriate structural modifications. By careful optimization of structural motifs the morphology of the self-assemblies in the solid-state can be tuned to the requirement of the application scenario. The extent of electronic coupling between the donor and acceptor groups govern the HOMO–LUMO energy gap and thereby control the first order linear optical properties and higher order nonlinear optical (NLO) properties. Some of the structural features that

control these properties are (i) ionization potential of the donor and electron affinity of the acceptor (ii) extent of D-A interaction, (iii) topology of π-conjugation, (iv) degree of π-conjugation and (v) planarity of the molecule structure.

Mostly used electron acceptors (A) involve substituent's with -M/-I effects such as NO_2, CN, CHO and electron deficient heterocyclic systems such as diazines,[29-31] benzothiazole[32-33] imidazole etc., Typical electron donors (D) involved in the construction of D-A systems are molecules which are suitably substituted with +M/+I effects such as, OH, NH_2, OR, NR_2, heterocyclic moieties such as, thiophene,[34] carbazole, phenothiazine, phenoxazine, porphyrine, proaromatic pyran-4-ylidines,[35-38] metallocenes[39-44] etc., whereas the π-spacers involved are phenyl, thiophenyl, furanyl etc., Some of the representative's donors, acceptors and typical π-bridges are given in Chart 1.1.

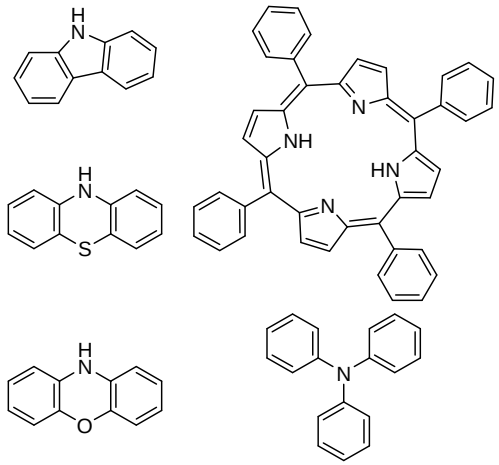

Donors

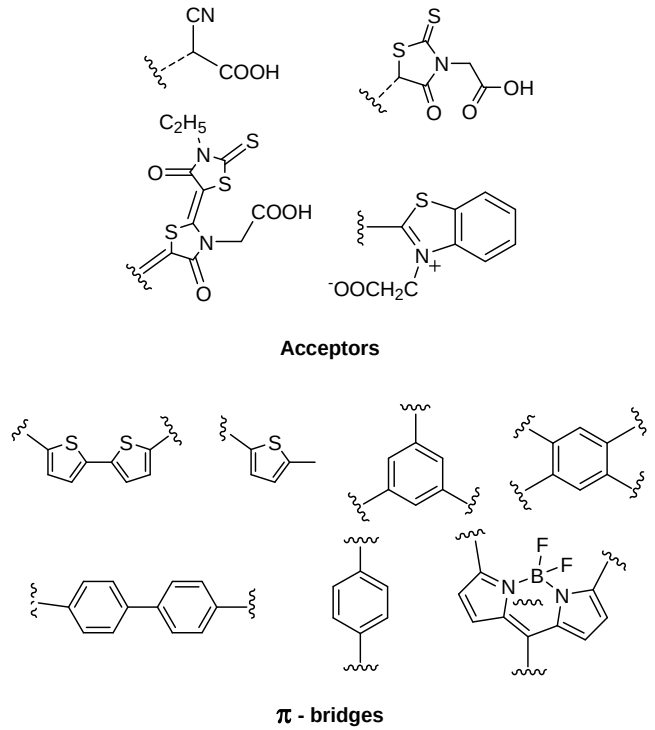

Chart 1.1. Donors, Acceptors and typical π-bridges

The presence of a permanent dipole moment in the ground state makes these molecules to respond to the environmental changes especially the polarity changes in the medium. This property of these molecules finds application in the development of solvatochromic probes. Based on the electronic nature of the donor and the acceptor groups they either show negative solvatochromism *ie.*, a hypsochromic shift to the absorption maximum with increased polarity of the medium or the opposite termed as positive solvatochromism. The well-known ET-30 solvent polarity scale is developed using the pyridinium betain dye (**1**) (Chart 1.2).[45]

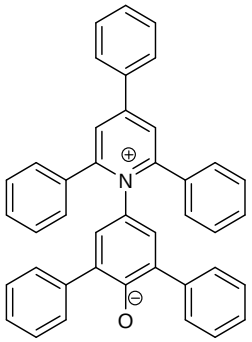

1

Chart 1.2. Molecular structure of pyridinium betain dye

The present thesis work focuses its attention on two major applications of donor-acceptor systems, the photovoltaic property and the nonlinear optical properties. The preceding section is a review on the application of organic molecules in photovoltaics and nonlinear optics.

1.2. Donor-Acceptor molecules in photovoltaics

The photoconductivity, the phenomenon that led to the discovery of photovoltaics is the increase in the electrical conductivity of an insulating molecule/material upon exposure to light.[46] This property is generally exhibited by semiconductors and was first observed for Selenium by Smith in 1873.[47] About 30 years later, photoconductivity was observed in an organic compound such as anthracene, by Pottchono.[48] In 1957, the first photoconducting polymer, poly (N-vinylcarbazole), was reported by H. Hoegl.[49] In the same era, Bell laboratories developed the first crystalline silicon based photovoltaic device with efficiency about

6%, there by opening up an era of solar power generation and its further developments. Now the efficiency of photovoltaic cells has reached 24.4% which uses crystalline silicon and 19% for copper-indium-gallium-selenide (CIGS) thin films.[50-51] One of the major drawbacks here is, the cost involved in the fabrication, which require high temperature and vacuum. Moreover, use of toxic heavy metals as components raises the concern of environmental damage. Therefore, researchers are in the search of new materials that are comparably less expensive with lesser environmental concern.[52]

First generation solar cells include conventional solar cells such as Silicon cells. The second generation cells involve thin film solar cells having one or more layers of photovoltaic materials such as cadmium telluride (CdTe), copper indium gallium diselenide (CIGS), and amorphous thin-film silicon on a substrate such as glass, plastic or metal. The third generation of emerging photovoltaic technology involve photoelectrochemcial cells such as dye sensitized solar cells, organic or polymer solar cells and perovskites solar cells. A recent development in solar cell research is the introduction of up conversion solar cells where the untapped near infrared (NIR) region of the solar spectrum is exploited to enhance the efficiency of an existing photoelectrochemical DSSC or bulkheterojunction device.

1.2.1. Silicon based solar cells

It is the most commonly known solar cell and is generally called as a p-n junction solar cell. It is formed by allowing the

diffusion of an n-type dopant on a p-type silicon wafer or vice versa. The photons of appropriate energy generate charge carriers by promoting a valence electron to the conduction band there by creating the electron hole pair or exciton. Photogenerated electrons migrate to the p-type side of the silicon and the holes migrate to the opposite side where the metal electrode collect them and route to an external load. The cost of the silicon solar cell technology has reduced significantly from US$76/Watt in 1977 to US$0.30/Watt in 2015. Today 90% of the solar energy conversions are made from silicon based devices. As far as the power generation efficiencies are concerned, cells employing silicon single crystals and bulk polycrystalline wafers reached efficiency up to 25% and 21.3 % respectively.[53]

1.2.2. Organic and polymer solar cells

Organic and polymer solar cells are thin film cells made from organic molecules or semiconducting polymers based on poly (phenylene) vinylene, phthalocyanines, fullerenes, etc. A major advantage is the potential reduction in the cost of processing as these materials offer easy solution processing or fabrication by roll-to-roll printing. Moreover, it is possible to manufacture mechanically flexible solar cell systems.[54]

Single layer devices

They are the simplest first generation organic photovoltaic cells. These devices are fabricated by sandwiching a layer of a

donor-acceptor type organic molecular or polymer material between two metallic conductors of different work function. Typically used conductors are indium tin oxide (ITO) with high work function and a layer of metals with low work function, such as aluminium, magnesium or calcium. The schematic representation of a single layer device is given in Figure 1.2. The power conversion efficiencies reported were poor (10^{-3}-10^{-2} %) and a high value of 0.7% was achieved when merocyanine dyes were used as the active layer.[55]

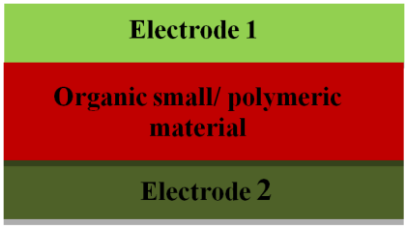

Figure 1.2.

Bilayer heterojunction devices

In this solar cell architecture, the electron donor material with hole transporting properties and an acceptor material with electron carrier properties are sandwiched between the two electrodes having different work functions. The photogenerated excitons are dissociated at the interface of acceptor layer and donor layer, after which, the electrons diffuse to the anode and holes towards the cathode.[56] The device structure is illustrated in Figure 1.3. About 1% power conversion efficiency has been achieved for a phthalocyanine based p-type materials in conjunction with an n-type perylene derivative.[57]

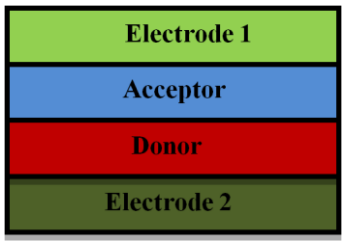

Figure 1.3.

Bulk heterojunction

The bulk heterojunction devices were introduced to improvise the efficiency of the bilayer heterojunction devices. In a bulk heterojuntion device, a blend of the donor polymer (p-type) and the acceptor polymer (n-type) in solution is spin coated forming a solid binary solution. Such binary solid solutions were also prepared by laminating two polymer types or by coevaporation and deposition.[58] The schematic representation of bulk heterojunction device is given in Figure 1.4. A major advantage of this type of cells is the increase in the interfacial area between the donor and acceptor materials.[59] Thus, the number of excitons generated is generally higher and expected to improve the overall efficiency. Highest efficiencies have been achieved when triads of type D-A-A based on merocyanine or triphenylamine dyes or oligothiophenes having Donor-Acceptor groups in conjunction with C_{60} and C_{70} derivatives were used as the acceptor.[60] Efficiencies over 6% have been reported for this architecture[61-64] whereas National Renewable Energy Laboratory (NREL) reported

efficiency upto 11.5 % for organic photovoltaic cells with a tandem architecture.[65]

Figure 1.4.

1.2.3. Perovskite solar cells

The perovskite solar cell is one of the latest introductions to the thin film photovoltaic devices and they are low cost technology for the future. In these type of cells, methylammonium lead halide ($MAPbX_3$, X=halide) or mixed halides serve as the light harvesting layer which injects electrons to the conduction band of the semiconductor such as TiO_2. The layered assembly of the cell consists of a bottom TiO_2 blocking layer on a conducting FTO glass, the light harvesting $MAPbX_3$ followed by the hole transport material (HTM) such as PEDOT-PSS, Spiro-OMETAD or simple electron rich organic compounds in contact with an external transparent FTO glass or noble metal electrode.[66-67] The block diagram and the energy level diagram for a typical perovskite cell is shown in Figure 1.5. Efficiency of over 12% has been achieved for these types of cells.[68] The major disadvantage is the lack of long term stability and the use of toxic metal ions in the construction of these types of cells. The future research in this area is directed towards development of alternate perovskite light

harvesting materials which is devoid of toxic metals, possessing long term stability and having higher efficiency.

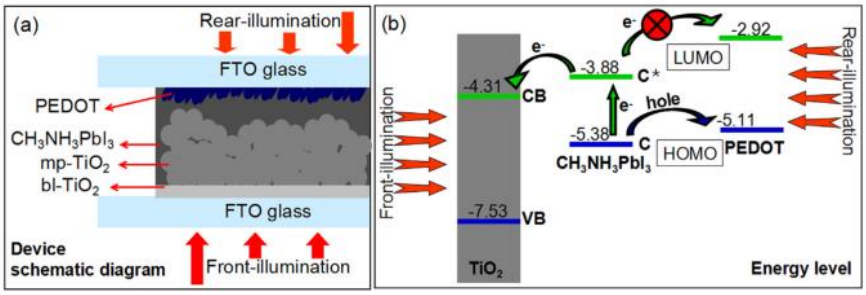

Figure 1.5. The schematic representation of perovskite cell

1.2.4. Photoelectrochemical cells - Organic dye sensitized solar cells (DSSC)

Dye sensitized solar cells are devices which generate electricity via a photoelectrochemical reaction wherein, a light harvesting molecule gets oxidised in the presence of a semiconductor and subsequent regeneration of the dye by an electrolyte of appropriate redox potential. The first dye-sensitized solar cell was introduced in 1991, by Grätzel *et al*. with an efficiency of 7.1-7.9% (under simulated solar light) using nanocrystalline TiO_2 semiconductor coated with a trimeric Ruthenium complex as dye on a transparent conducting oxide layer along with a liquid redox electrolyte couple I^-/I_3^-.[69-79]

Dye-sensitized solar cells have attracted much attention in recent years due to their potential advantages of low cost, ease of production, flexibility, and transparency. Generally DSSC consists of a transparent conducting oxide, a mesoporous semiconductor,

photosensitizer dyes which can absorb radiations in the UV-Visible region, a redox couple electrolyte and a counter electrode. The photosensitizer dye is a key component of the DSSC since it is the one which harvests sunlight. On illumination, the dye molecule get photo-excited, whereby an electron transition occurs from its highest occupied molecular orbital (HOMO) to the lowest unoccupied molecular orbital (LUMO). This excitation energy corresponds to the energy difference between HOMO and LUMO of the dye molecule. The electron in the excited state of the dye (LUMO) is then injected into conduction band (CB) of TiO_2. It is then transported through the semiconductor layer by diffusion, to reach the conducting layer, i.e., a transparent conducting oxide (TCO), such as, Fluorine doped Tin Oxide (FTO) on glass substrate. The regeneration of the oxidized dye molecule occurs due to a redox reaction taking place in electrolyte. Typically an electrolyte containing a redox couple such as I^-/I_3^- is used. In such cases, the iodide ion donates an electron to the oxidized dye (S^+) at anode. The oxidized species of the electrolyte, i.e., the triiodide in iodide-triiodide complex, is reduced to iodide at the cathode. The above processes go in a cycle and consequently current flows through the external circuit as long as light is incident on the cell. The schematic diagram illustrating the working principle of a DSSC is given in Figure 1.6.

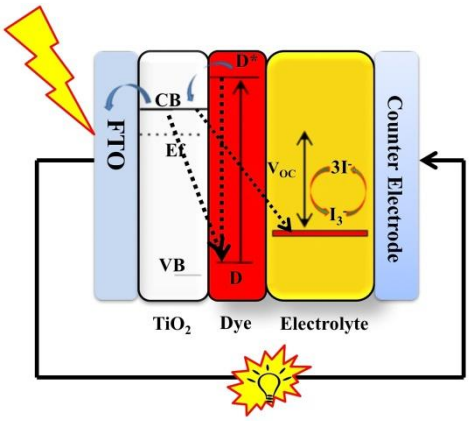

Figure 1.6.

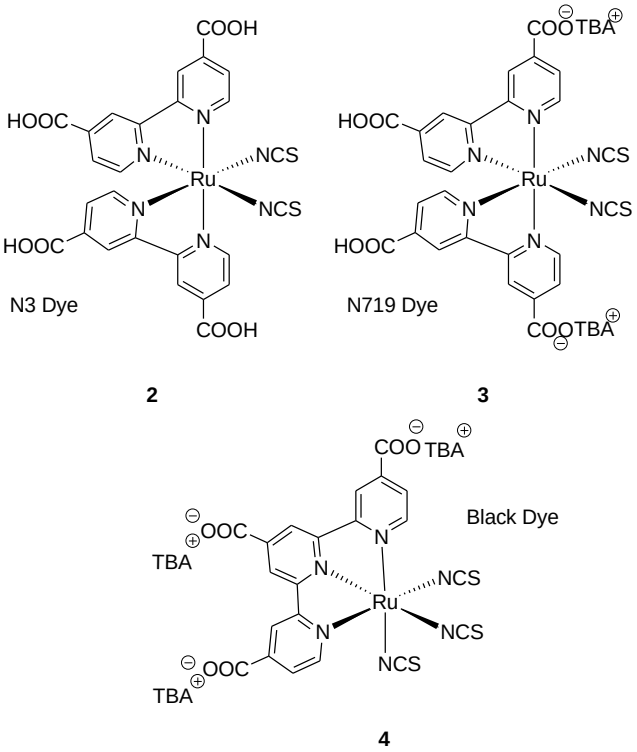

Chart 1.3. Ruthenium based photosensitizer

Many ruthenium based complexes such as, cis-dithiocyanatobis(4,4'-dicarboxy-2,2'-bipyridine)ruthenium(II) (N3 dye, **2**) and bis(tetrabutylammonium) cis-bis(thiocyanato)bis(2,2'-bipyridine-4-carboxylicacid,4'carboxylate)Ru(II) (N719, **3**) tri(cyanato)-2,2',2''-terpyridyl-4,4',4''-tricarboxylate)Ru(II) (black dye, **4**), are reported as efficient photosensitizers used in DSSCs (Chart 1.3).[80-85]

The semiconductor material of choice has been TiO_2 in the anatase form, however, many alternative wide band-gap oxides such as ZnO, SnO_2 and Nb_2O_5 have also been investigated.[86-91] Nano-sized TiO_2 powders are widely used as working electrode for dye sensitized solar cell as it offers higher surface area which results in faster electron transfer to the conducting substrate yielding higher efficiency than any other metal oxide semiconductors reported.[86]

1.2.5. Solar cell parameters: Efficiency (η), fill factor (FF), short circuit current density (J_{sc}), open circuit voltage (V_{oc})

The performance of a solar cell is studied by recording the current density-voltage curve both in the dark as well as under illumination. A typical current density-voltage curve (J-V Curve) for a functioning cell is given in Figure 1.7 where J is the current density and V is the voltage.[92]

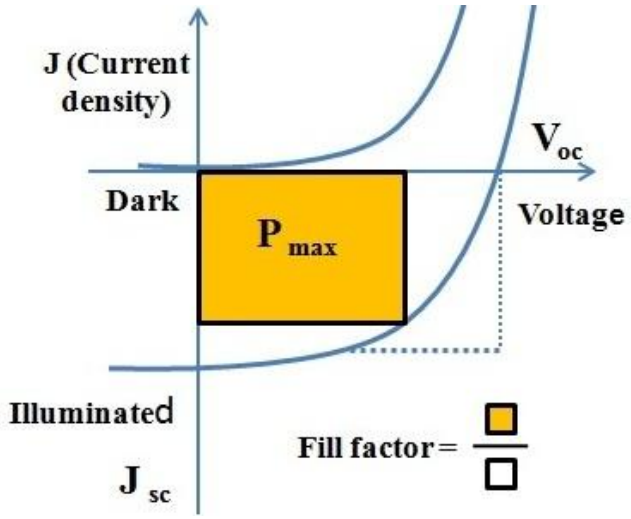

Figure 1.7. Current density-Voltage characteristics of an organic solar cell

The power conversion efficiency (η) is the key parameter to compare the performance of one solar cell with another. It depends on the solar spectrum absorbed and on the intensity of the incident sunlight as well as on other factors that vary according to the fabrication methods and materials used. Usually, for comparison purposes, cells are measured under AM 1.5 conditions at a temperature of 25^0C. The power photo conversion efficiency(η) is determined by three parameters, namely short-circuit current density (J_{SC}), open-circuit voltage (V_{OC}) and fill factor (FF).[92] The efficiency of a solar cell is determined as the fraction of incident power which is converted to electricity and is given in equation (1.1) and (1.2).[93]

$$P_{max} = V_{oc}\, J_{sc} FF \tag{1.1}$$

$$\eta = \frac{V_{oc}\, J_{sc}\, FF}{P_{in}} \tag{1.2}$$

Where,

P_{max} is the power input

P_{in} is the power maxima

V_{oc} is the open-circuit voltage

J_{sc} is the short-circuit current, FF is the fill factor

and η is the efficiency

Open circuit voltage (V_{oc})

The open-circuit voltage, V_{OC}, is the maximum voltage accessible from a solar cell, that is, when there is no current passing through the cell. The open-circuit voltage corresponds to the amount of forward bias on the solar cell owing to the bias of the solar cell junction with the light-generated current. Open-circuit voltage is a measure of the amount of recombination in the device. In DSSC it is limited by the energy difference between the redox level of the electrolyte and the Fermi level of the semiconductor.

Short circuit current (J_{sc})

The short circuit current J_{SC} corresponds to the short circuit condition when the impedance is low and is calculated when the voltage equals zero (equation (1.3)).

$$J \text{ (at } V=0) = J_{sc} \qquad (1.3)$$

J_{SC} occurs at the beginning of the forward-bias sweep and is the maximum current value in the power quadrant. For an ideal cell, the maximum current value is the total current generated in the solar cell by photon excitation.

Fill factor (FF)

The quality of the solar cell is determined by the term fill factor (FF). It is calculated by comparing the maximum power to the theoretical power (P_T).

1.2.6. Electrolytes used in DSSC

Electrolytes facilitate the ionic conduction between the electrodes in electrochemical devices.[94] In dye sensitized solar cells, the role of electrolytes is to allow the continuous passage of charge carriers between the photo anode and the counter electrode through the dye regeneration process. All the parameters which determine the efficiency of a DSSC such as, J_{sc}, V_{oc} and FF are significantly affected by the nature of the electrolytes. Electrolytes should satisfy some characteristics in order to be applicable in DSSCs. [95-97]

- It should not react with the semiconductor or with the photosensitizer.
- It should not absorb the radiation.
- It should have the ability to transport the charge carriers to the anode and cathode.
- The rate of charge diffusion should me maximum.
- It should have a slightly lower redox potential than the oxidation potential (or HOMO level) of the dye for efficient regeneration of the dye.

According to the physical state and composition, the electrolytes used in DSSC are classified into three major categories, namely, liquid,[98] quasi solid[99] and solid electrolyte.[100]

Liquid electrolytes

Liquid electrolytes are the most widely used charge transport medium in DSSCs and the maximum efficiency is obtained when liquid electrolyte is used in comparison to alternatives. The liquid electrolyte have some unique properties such as, ease of preparation, high conductivity, low viscosity and good interfacial contact with the electrodes.[101] Liquid electrolyte consists of three components namely, solvents, ionic conductor and additives. However, the major disadvantage with liquid electrolyte is the leakage of the contents of the cell. Cells with liquid electrolyte have poor long term stability as the cell gets dried up on storage. This is usually overcome by appropriate sealing techniques. This also limits the large scale deployment of DSSC for solar power generation. The common electrolyte used, the iodide/tri iodide (I^-/I_3^-) redox couple uses organic solvents. Acetonitrile was considered as the best solvent due to its low viscosity, good solubility and high stability.[102] A maximum efficiency of 13% is reported to be achieved for DSSCs with acetonitrile as the solvent.[103] Nitriles containing methoxy group is another class of solvents used for DSSC application. Methoxyacetonitrile and 3-methoxypropionitrile are also used as solvents for electrolytes by which 8% efficiency has achieved for metal free DSSCs.[104] Some esters and lactones like ethylene carbonate, propylene carbonate, γ-

butyrolactone and N-methyloxazolidinone have also been used. Often mixed solvents are used for optimum DSSC performance due to the fact that it is difficult for a single solvent to fulfil all the requirements simultaneously. For e.g., in the case of a DSSC with N3 dye, an efficiency of about 10% was reported, when the solvent used was a mixture of acetonitrile and N-methyloxazolidinone. In general, high boiling solvents such as, ethylene carbonate, propylene carbonate, γ-butyrolactone and N-methyloxazolidinone produce better results when mixed with low boiling solvents such as, acetonitrile.

Ionic liquids

Ionic liquids are salts in liquid state and are used in electrolytes as solvents due to their unique properties such as, flexible viscosity, high chemical and thermal stability, non-flammability, good ionic conductivity and above all, extremely low vapour pressure, providing evaporation free and leakage free cells.[105-107] Ionic liquids consists of organic cations such as imidazolium, tetralkylammonium or tetralkylphosphonium salts[108] and the counter anions are halides/pseudo halides, complex anions like borate or triflate derivatives, etc.[108-109] A number of reports are available in the literature, where DSSCs using ionic liquids as solvents exhibiting long term stability and high performance.[110-115] Even though ionic liquid is a promising alternative to organic solvents, they possesses few disadvantages such as, high viscosity and low ion mobility.[116]

Iodide/triiodide electrolyte and bromide/tribromide (redox couple)

Iodide/triiodide is the most common electrolyte couple used in the preparation of DSSC, especially in the Grätzel Cell where N3 or N719 dyes were used.[117] This redox couple have key role in the dye sensitized solar cells to improve the efficiency of the solar cells. Regeneration of the excited dye to its reduced state occurs with the help of redox couple. That is, the redox couple (I^-/I_3^-) provides the required electrons to the photo oxidized dye (D^+) to regenerate the dye. The electron donation from reduced electrolyte (I^-) to D^+ should be sufficiently exergonic and fast to ensure efficient dye regeneration. Similarly, the reduction of the oxidized state of the couple (I_3^-) by valence electrons of the photoanode (TiO_2) film should be slow and endergonic so as to make the dye regeneration as the sole step in completing the circuit. Therefore, the choice of the appropriate redox couple is crucial in the optimal performance of the DSSC. The I^-/I_3^- couple with a redox potential of 0.5 V *vs.* NHE satisfies energy level requirements when used with dyes having HOMO levels more positive than 0.5 V, and is the widely used redox couple in DSSC for standard dyes such as N3 or N719 and dyes with comparable oxidation potential. In addition, I^-/I_3^- couple possesses high stability, high solubility, less absorption of light and high diffusion property.

However, a major drawback of this electrolyte couple is the reduced open circuit voltage (~0.7 V). An alternative electrolyte to achieve higher V_{oc} is the bromide/tribromide electrolyte which has

a redox potential of 1.1 V *vs.* NHE. This redox couple has been recommended for dyes having an oxidation potential more positive than 1.1 V.[118-119] The drawback is often the stability of the dyes to a more aggressive bromine which is generated during the operation of the cell.

Electrolyte additives

Electrolyte additives are another important component of the liquid electrolytes which is employed for improving the overall efficiency of the device. The additives can alter the redox couple potential; conduction band edge, semiconductor surface morphology, recombination kinetics as well as the photovoltaic performance of the DSSCs. Grätzel *et al*. in 1993 reported the usage of 4-*tert*-butylpyridine (TBP) as additive in DSSC.[120] A number of N-heterocylic compounds such as pyridine, alkylaminopyridine, alkylpyridine, benzimidazole, pyrazole, quinoline, etc., have been used as additives. Besides the TBP and nitrogen heterocylic compounds, cations such as Lithium ions (Li^+), Guanidium ion [$C(NH_2)_3^+$], etc., also can be employed as additives in electrolytes to improve the efficiency of the DSSC.[121-123] In many instances the excessive dye loading and subsequent aggregation of the dye limits the efficiency of the DSSC. Addition of chenodeoxycholic acid (3α,7α-dihydroxy-5β-cholic acid) was found to reduce aggregation effects.

Quasi solid electrolyte

The drawbacks of liquid electrolytes such as, leakage and volatilisation of the solvent, photodegradation of the dye, corrosion of electrodes, desorption of the dye and sealing problems for long term stability, etc., can be addressed with using quasi solid electrolytes. In spite of the lower efficiencies of DSSCs, quasi solid electrolytes are good candidates for solving the above issues and can overcome difficulties in sealing and long term stability, simultaneously providing the advantages of the liquid electrolyte.[124-127] The quasi solid electrolytes are generally classified into four groups based on their physical states and formation mechanisms, namely, thermoplastic polymer electrolyte,[128] thermosetting polymer electrolyte,[129] composite electrolyte, quasi solid ionic liquid electrolyte.[130]

Solid state electrolyte

The long term thermodynamical stability of electrolytes cannot be fully solved even by quasi solid electrolytes. To overcome this, solid electrolytes are suggested which is useful in large scale fabrication of DSSCs. Solid state electrolytes include solid state ionic conductors,[131-134] inorganic hole transport[135-138]and organic hole transport materials.[139-142] An effective replacement of liquid electrolyte is an inorganic hole transport material, *i.e.*, p-type semiconductors.

The selection criteria for hole transporting materials are:

1. It must be able to transfer holes from the reduced dye after the electron injection to the TiO_2 to the cathode and the upper edge of the valence band of this p-type material must be located above the HOMO level of the dye enabling regeneration of the dye.[141]

2. It must be able to be deposited within the mesoporous TiO_2 films.[143-144]

3. The hole mobility of HTM should be sufficiently high.

4. It should be transparent in the visible range and cannot dissolve or degrade the sensitizer dye during the deposition process.[145]

A limited number of inorganic hole transport materials are shown to be useful. Copper based HTMs such as CuI, CuBr and CuCN are widely investigated inorganic p-type semiconductors and among these CuI have good conductivity of 10^{-2} S cm^{-1}.[146-148] CuI used DSSC were first reported in 1998 with efficiency about 2.4 % by Tennakone *et al*.[149-150]

1.2.7. Organic dyes in DSSC

Organic dyes have several advantages over metal containing photosensitizers:

(1) They have efficient light harvesting properties due to larger absorption coefficients (attributed to an intramolecular π-π transition) than metal-complex photosensitizers (MLCT absorption).

(2) The structures of organic dyes are flexible for modifications by appropriate synthesis methods and their

- Electronic properties such as HOMO and LUMO energies and absorption spectrum are tunable.

- Solubility and processability can be tuned according to the demands of the application scenario.

- Affinity to semiconductor surfaces can be tuned by introducing carboxylic acid groups or phosphoric acid groups during synthesis.

(3) Unlike inorganic complexes, they are inherently cheaper as organic dyes do not contain noble metals such as, ruthenium.

They can be made in different forms as individual molecules, as dendrimers, oligomers and as polymers. In addition to well-known dyes such as eosin Y, methylene blue etc., several donor-acceptor systems are reported as dyes for photovoltaic applications.[173] Donor-acceptor type molecules provide the opportunity to design molecules with well-defined electronic properties to suit a particular semiconductor photoanode material.

There are conjugated (D-π-A) and non-conjugated (D-A) donor acceptor systems known in the literature. Often the acceptor group itself has the functionality that favour binding to the semiconductor surface.

In a typical Donor-π-Acceptor system for DSSC a photo-induced charge transfer from the electron rich donor moiety to the electron deficient acceptor moiety occur upon light absorption. In such molecules the HOMO is mainly located at the donor part of the molecule and LUMO is located at the acceptor part of the molecule. **5** is a typical organic dye which has yielded over 10% efficiency when used in DSSC along with TiO_2 and I^-/I_3^-. Figure 8 shows the structure of compound **5** along with a comparison of the HOMO and LUMO levels with that of TiO_2 and electrolyte. The HOMO and LUMO contours were also given in the figure. The directionality of charge transfer from donor to acceptor is evident in the HOMO and LUMO contours given for the compound **5** which is a major requirement for the D-A dyes to show good photovoltaic properties.

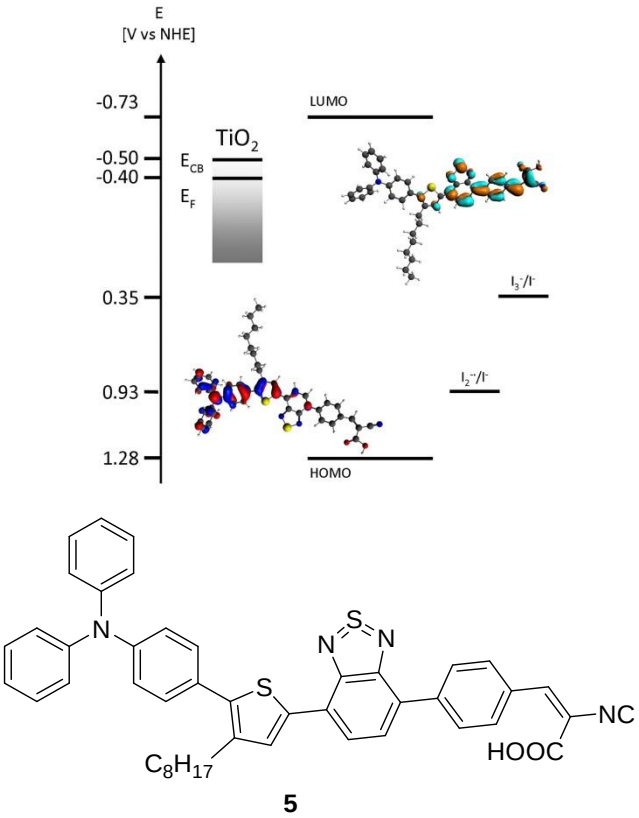

5

Figure 1.8. Frontier molecular orbitals of **5** calculated at B3LYP level of theory (Illustration from ref. 152.)

In structural modification of D-π-A system, for a given acceptor group, increase in the donor capacity reduces the HOMO-LUMO gap and make the HOMO less positive.[153-158] A similar effect is observed when length of conjugation increased in the π bridge.[158-159] When the acceptor capacity increased for a given donor group the LUMO level get lowered along with a decreased HOMO-LUMO energy gap. For an effective charge injection to the semiconductor by the dye, the dye should be anchored to the semiconductor. Several groups which show affinity to

semiconductor surface are known, for example carboxylic acids, pyridine, phosphonates, sulfonates, phenols, hydroxamates etc. These are commonly called as anchoring groups in dyes (Chart 1.4).[158] A major requirement is that along with anchoring an efficient electronic coupling between the LUMO of the dye and the conduction band of the semiconductor has to be ensured. To facilitate this, the anchoring group should be a part of the acceptor moiety in the dye so that the LUMO will have proximity to the semiconductor surface. Cyanoacetic acid is the most promising acceptor/anchoring group in this category. 1,1-dicyanoethylene, rhodanine-3-acetic acid, bisrhodanineacetic acid, benzothiazole acetic acid are some of the acceptor/anchoring groups commonly used in the dyes for DSSC (Chart 1.5).[159-160]

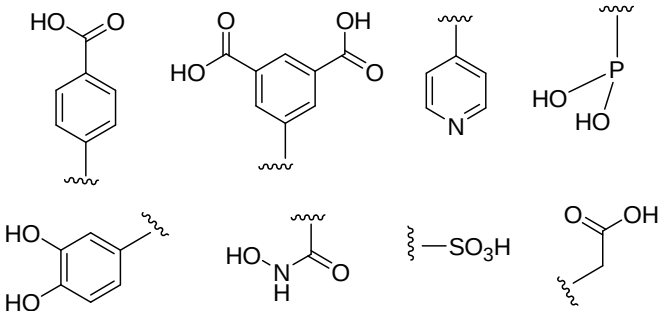

Chart 1.4. Anchoring groups

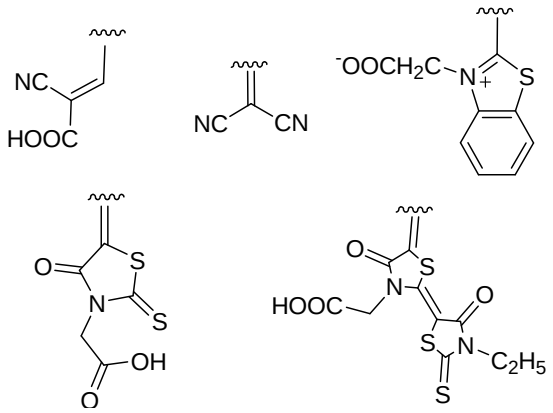

Chart 1.5. Dual function Anchoring/acceptor groups

Chart 1.6 lists some of the well-known organic donor-acceptor type dyes reported in the literature. Porphyrins are the good candidate for constructing DSSC due to the excellent absorption properties *i.e.,* it exhibit strong soret band in 450-500 nm region and moderate Q band at 550-650 nm region.[161] The LUMO orbital energy level of these dyes are well above 0.5 eV and allows for efficient electron injection in to TiO_2 and the energetics of regeneration of the dye is also favoured when I^-/I_3^- electrolyte. Cambell *et al.* reported porphyrin with conjugated dicarboxylic acid anchoring group the efficiency (η) above 7% when used with TiO_2 and I^-/I_3^- redox couple.[162] Bessho *et al.* also reported "push pull" porphyrin system with efficiency (η) about 11%[163] Grätzel's group showed Zinc-metalated porphyrines can be used with organic co-sensitizer and a Cobalt based electrolyte to achieve efficiency upto 12.3%.[164] Wang *et al.* reported a porphyrin-based DSSC without co-sensitization, gave efficiency (η) above 10 %.[165-166]

Among organic dyes, D-π-A configuration is the common architecture for sensitizers used in DSSC. These D-π-A dyes were shown to possess high electron injection efficiency and power conversion efficiency. Most widely studied systems have triphenyl amine,[167-169] carbazole[170-171] or phenothiazine as donor,[172-174] thiophene as linker and cyanoacetic acid as the anchoring group. Dyes **6**, **8**, **9** and **11** possess the simple design where the donor group is connected to the acceptor through one π–bond.[175-178] Among this phenothiazine based dye gave the maximum efficiency. Extension of conjugation proved to improve efficiency in comparison to systems with one π-bridge as is the case with **6**, **7, 9** and **10**.[179]

Another strategy used in the dye design is the use of multi-branching where either more than one donor or acceptor are used to improve current as well as efficiency. Dyes **12** to **15** are examples of this design where the results showed improvements over **11**. The results of the studies on these dyes also suggest the use of heteroaromatic π-bridges as a strategy to improve the efficiency as seen in the case of **14** and **15**.[180] More than one acceptor/anchoring group is also a strategy to improve dye binding and electron injection to the semiconductor. Dye **16** is an example of this strategy.

Another strategy that proved to be beneficial is the introduction of one acceptor moiety in a D-A-A format. In this strategy, the HOMO of the dye will be made more positive due to

the stabilization of the MO's centered on the donor moiety. This is one strategy in conjunction with an electrolyte having redox potential more than 1.1 V can yield higher V_{oc} values. Dye **9** is an example where an efficiency of over 10% is reported in an optimized DSSC configuration which involves electrolyte additives such as chenodeoxycholic acid. In this work dye aggregation was found to limit the efficiency. A strategy used in the design of the dye is to include long chain or branched alkyl groups to increase the steric bulkiness as well as the hydrophobicity. Increased hydrophobicity screens photoanode from the electrolyte ions and prevents short circuiting.

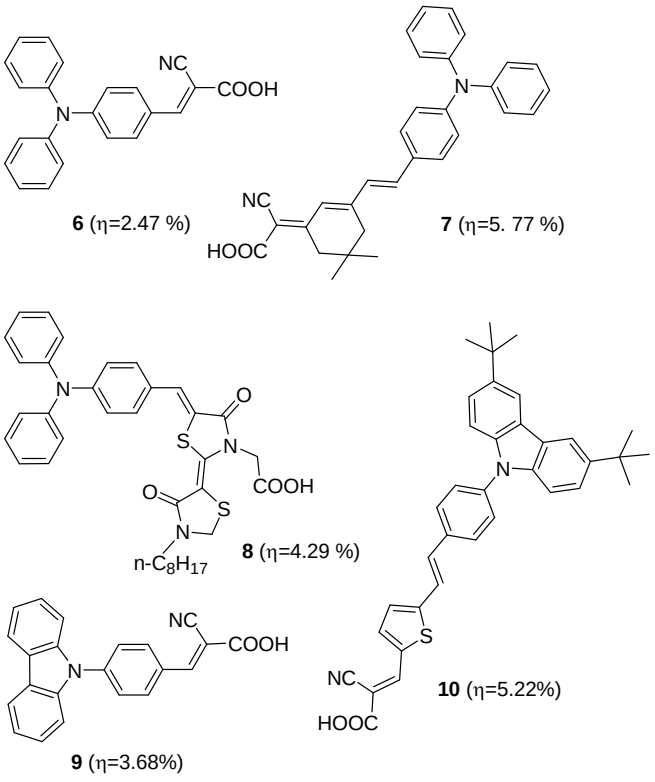

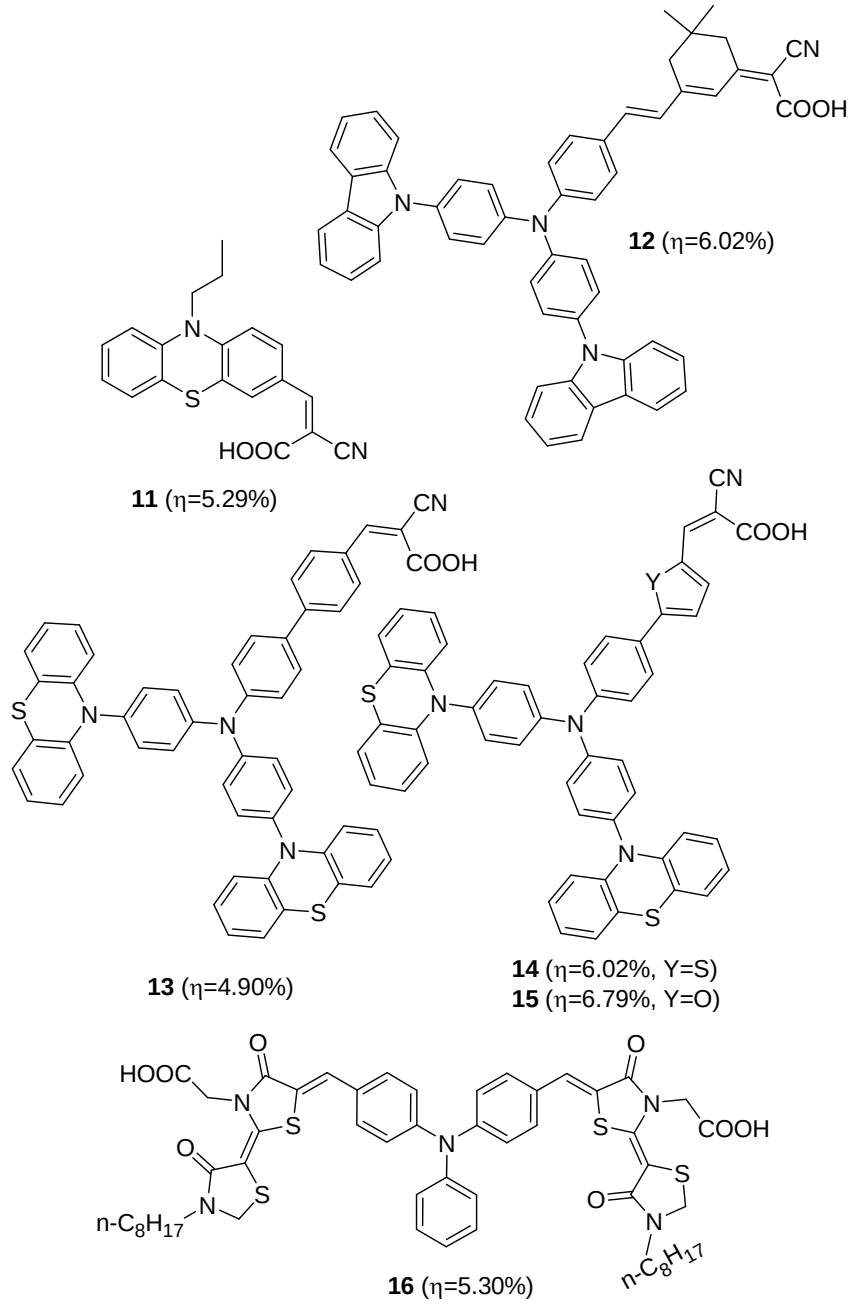

Chart 1.6. Organic donor-acceptor type dyes reported in the literature

1.3. Organic materials for nonlinear optics

The branch of Nonlinear Optics (NLO) deals with the interaction of light with matter under situations where, the principle of superposition breaks down. Principle of superposition states that for all linearly dependent systems the response caused by two or more stimuli equates to the sum of the responses obtained when each stimulus acts independently. In a nonlinear media, interaction of light and the response that it generates shows a nonlinear dependence i.e., the dielectric polarisation created in the medium respond in a nonlinear fashion with the electric field of the light. This is often manifested as harmonic generation, sum and difference frequency generation, the intensity dependence of refractive index, multiphoton absorption, etc. According to semiclassical theory, the electric polarisation vector ($\vec{P}$) caused by a light beam in a medium is defined as the sum of light field induced electric dipole moment vectors of all molecules in unit volume.[181] In the case of weak incoherent light sources (monochromatic with angular frequency ω), the $\vec{P}(\omega)$ is linearly proportional to the applied electric field ($\vec{E}$).

$$\vec{P}(\omega) = \overrightarrow{P^{(1)}}(\omega) = \varepsilon_0 \chi^{(1)}(\omega)\vec{E}(\omega \ldots) \tag{1.4}$$

where, $\overrightarrow{P^{(1)}}(\omega)$ is the first order polarisation vector, $\chi^{(1)}(\omega)$is the first order linear susceptibility of a given medium and ε_0 is the vacuum permittivity. The first order linear susceptibility $\chi^{(1)}(\omega)$ is

a complex parameter whose real part determines the refractive index of the medium and the imaginary part represents the linearly dependent light (one photon) absorption. Under the influence of a strong coherent monochromatic light of frequency ω the polarisation vector, $\vec{P}(\omega)$ can be represented as a power series expansion in the electric field, $\vec{E}(\omega)$ and the susceptibility χ. (Equation (1.5)).

$$\vec{P}(\omega) = \chi^{(1)}(\omega)\vec{E}(\omega) + \chi^{(2)}(\omega)\vec{E}^2(\omega) + \chi^{(3)}(\omega)\vec{E}^3(\omega) + \cdots \quad (1.5)$$

Where, $\chi^{(2)}, \chi^{(3)}$, etc., are the second order and third order susceptibilities, respectively. Second order susceptibility generally describes second harmonic generation and third order susceptibility describes the intensity dependent refractive index changes and third harmonic generation as well as multiphoton absorption characteristics of the medium.

The first report on the nonlinear optical property (NLO) was made by J. Kerr in 1875 as a change in refractive index of carbondisulphide (CS_2) under an electric field.[182] CS_2 has long been used as a standard for the nonlinear refractive index measurements and it show a value of 3 x 10^{-15} cm^2 W^{-1} for femtosecond laser pulses and 3.5 x 10^{-14} cm^2 W^{-1} for laser pulses of nanosecond duration. It also shows two photon absorption behaviour with a two photon absorption coefficient of 5 x 10^{-11} cm W^{-1}.[183] The NLO property of CS_2 is ascribed to both electronic and nuclear factors.[184] The electronic contribution comes from the second

hyperpolarizability of individual molecules with response time less than 1 fs. The nuclear factor is attributed to the molecular re-orientation. CS_2 being linear exhibits anisotropic polarizability and in the presence of strong electric field of the photons, a dipole is induced which results in a torque, forcing the molecules to align with the incident field.

While choosing materials for nonlinear optical properties, the major criterion to be satisfied is the high value for the nonlinear susceptibility. Moreover, the desirable qualities for the material includes, high transparency to the wavelength range required for the application, high resistance to laser damage, high chemical stability and very fast nonlinear responses. A broad classification of NLO active materials puts them into two classes: second order materials and third order materials. A non-centrosymmetric crystal that lacks an inversion centre has non-vanishing second order susceptibility. Potassium dihydrogen phosphate (KH_2PO_4) is an example for such a material, which is widely used for harmonic generation in laser sources. Many organic molecules which are asymmetric have shown to possess large hyper polarizability (β). One major requirement is the inherent asymmetry in electron density caused by the presence of an electron rich group or atom in conjugation with a relatively electron deficient group or atom. Such systems are generally termed as electron D-A systems or electron "push-pull" systems. These type of systems in the condensed phase are randomly oriented and do not yield a net effect in terms of NLO

activity. To bring about some kind of order, they are electrically poled to align the dipoles with a definite order, or use them in the crystalline form or as organised assemblies as seen in Langmuir – Blodgett films.

Third order materials find wider applicability in comparison to second order materials. They are useful for third harmonic generation, multiphoton absorption, and intensity dependent refractive materials. The intensity dependent refractive index is the key property that is required for the nonlinear optical switching devices. This phenomenon is described by the following equation.

$$n = n_0 + n_2 I \ldots \quad (1.6)$$

Where, I is the intensity of the light and n_2 the coefficient of the intensity dependent nonlinear refractive index. This is related to nonlinear susceptibility χ by,

$$n_2 = {12\pi^2 \chi^{(3)}(\omega)}\Big/{n_0^2} \ldots \quad (1.7)$$

The unit of $\chi^{(3)}$ is in esu when energy of the light source is measured in W/cm^2. A wide variety of inorganic and organic materials show third order nonlinear susceptibilities. For example, insulating materials such as Alumina (Al_2O_3) or glasses generally show $\chi^{(3)}$in the range of 10^{-13} to 10^{-14} esu. Semiconductors are also NLO active and show susceptibilities of 10^{-10} to 10^{-13} esu. This property of semiconductors largely depend on the energy of the light used and the band gap energy. Materials that show electron

redistribution upon light excitation, as seen in the semiconductors or push-pull systems, are also ideal candidates to be used as photorefractive materials (i.e., materials having nonlinear refractive index). $BaTiO_3$, GaAs etc., are some of the semiconductors that show photorefractivity. Carefully synthesised polymers from donor-acceptor type monomers and polymers with dopants are excellent candidates as photorefractive materials.[185]

Organic materials are excellent in terms of fast temporal responses such as ultrafast response time, lower dielectric constants and the possibility to design and synthesise molecularly engineered systems with defined properties. Several such systems are reported in the literature. A well-known system is the case of polydiacetylenes (**17, 18**) having donor and acceptor groups as a side chain. In this case, the $\chi^{(3)}$obtained was in the range of 10^{-10} esu.[186] In a similar work, Chen *et.al.*, reported a polyarylether having azobenzene as the side chain with a $\chi^{(3)}$of 1.15 x 10^{-11} esu (Chart 1.7).[187]

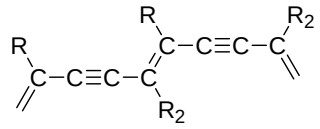

17

R = -$(CH_2)_4OCONHCH_2COOC_4H_9$

R_2 =

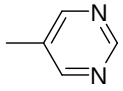

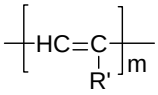

R' =

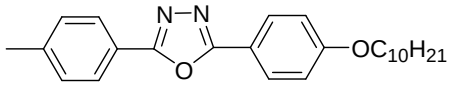

18

Chart 1.7. NLO active Polydiacetylenes and polyarylether

Phthalocyanines are yet another class of molecules that show promising properties as photorefractive materials (**19**) (Chart 1.8). They show diverse behaviour as a function of the structure and the central metal ion.[188]

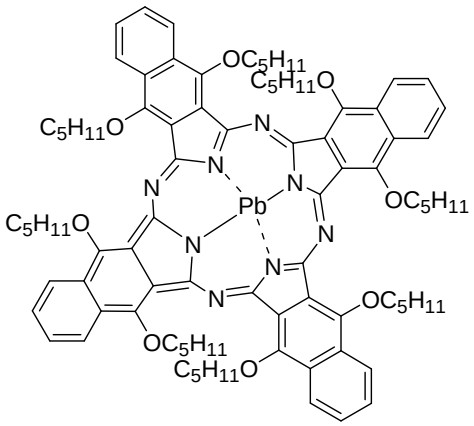

Chart 1.8. Structure of Phthalocyanine (**19**)

Liquids containing donor-acceptor molecules also show optical nonlinearities. In liquids, nonlinearity in optical properties is a result of following three situations: (1) Systems having molecular orientation time scale of 1 ps and $\chi^{(3)}$ in the range of 10^{-12} esu, (2) Systems that show electrostriction with a time scale of 1 ns and $\chi^{(3)}$ in the range of 10^{-13} esu and (3) Intramolecular charge transfer in the femtosecond time domain with $\chi^{(3)}$ in the range of 10^{-14} esu.

For example, carbondisulphide has a $\chi^{(3)}$ value of 2.2×10^{-12} esu which is much higher than CCl_4 where $\chi^{(3)}$ is only 8×10^{-14} esu. It is clear that CCl_4 being symmetric has limited electronic polarization than in the linear CS_2 molecule which is known to have anisotropic polarisation. Solutions of NLO active molecules also give such non linear susceptibilities. Kiran *et al.*, have studied a series of substituted chalcones in DMF and reported a $\chi^{(3)}$ of -2.11×10^{-13} esu.[189]

Multiphoton absorption is another third order nonlinear optical property which finds applications in optical limiters, multiphoton up conversion systems etc. In this phenomenon a molecule shows simultaneous absorption of two or more photons resulting into transition of the molecule to higher excited state other than the first excited state. These leads to nonlinear attenuation of the incident coherent light beam (optical limiting effect) or the medium can show nonlinear refractive index changes. Such molecules can undergo multiphoton excitation induced ionisation, dissociation and polymerisation reactions. Certain substances show

multiphoton induced surface photoelectric effect and enhanced conductivity as in the case semiconductors.

A schematic diagram showing multiphoton excitation is shown in Scheme 1.1.

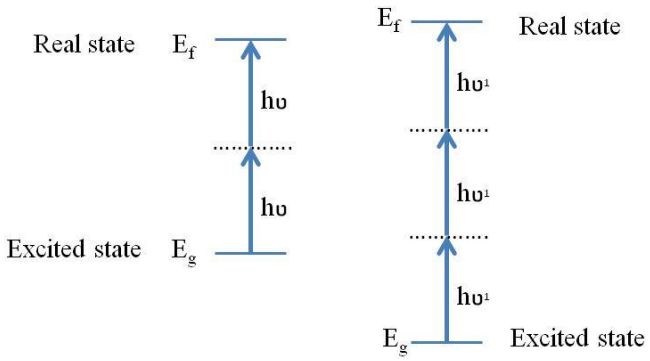

Scheme 1.1.

The attenuation of the intensity of a beam of light traversing through a medium is given by the following equation (1.8)

$$\frac{dI(z)}{dz} = -\alpha I(z) - \beta I^2(z) - \gamma I^3(z) - \eta I^4(z) \ldots \qquad (1.8)$$

Where I(z) is the intensity of light passing through the axis z and α, β, γ and η are the one, two, three and four photon absorption coefficients. When the wavelength of the incident light is not in the region of linear absorption of the molecules change in intensity can be simplified as,

$$\frac{dI(z)}{dz} = -\beta I^2(z) \ldots \qquad (1.9)$$

The solution of this equation is,

$$I(z,\lambda)= \frac{I_{0(\lambda)}}{1+\ \beta(\lambda)I_0(\lambda)z} \text{ (two photon absorption)} \qquad (1.10)$$

β, the two photon absorption coefficient is a parameter that depends on the wavelength of the incident light and the concentration of the absorbing medium. β is expressed as,

$$\beta(\lambda) = \ \sigma_2'(\lambda)N_0 = \sigma_2'(\lambda)N_A\, d_0 \times 10^{-3} \qquad (1.11)$$

$$\sigma_2(\lambda) = \sigma_2'(\lambda)\ \cdot\ h\vartheta \qquad (1.\ 12)$$

Where $\sigma_2(\lambda)$ is the two photon absorption cross section with units of cm^4 s and also expressed in GM (Göppert – Mayer) where 1 GM = $10^{-50}cm^4$ s. N_A is the Avogadro number and d_0 is the molar concentration of the absorbing medium.

An important structural requirement for organic molecules to show multiphoton activity is the presence of a strong π donor, a strong π acceptor and a polarizable π-bridge. Combinations of these structural motifs can lead to dipolar, quadrupolar and octupolar structures that show multiphoton absorption. Some of the typical acceptor groups that have been used are nitro groups, cyano groups, malononitrile, triflyl etc., Many heterocyclic systems have been used as acceptor groups. For example, pyridyl and pyridinium ions, benzothiazole, triazole, oxadiazole and organoboron compounds have been reported as acceptor groups in molecular systems that show multiphoton absorption. Examples of typical donor chromophores are dialkyl or diaryl amino groups, N-susbtituted carbazoles, thiazines, pyrroles etc. The π-conjugate bridges used were mainly phenylene, vinylene and its homologues, 2,7-fluorenyl

bridges, dihydrophenanthrene, phenanthroline, anthracene etc. Some of the typical two or multiphoton absorbing molecular systems is given in Chart 1.10. The two photon absorption coefficient (β) and the two photon absorption cross section (σ_2) of the compounds listed in Chart 1.9 (**20**-**27**) are given in Table 1.1.

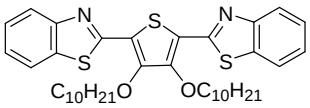

20

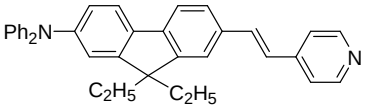

21

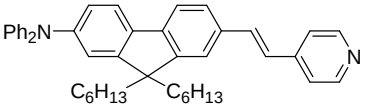

22

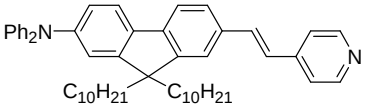

23

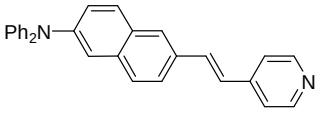

24

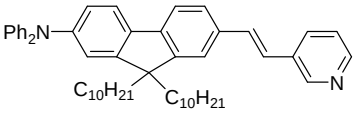

25

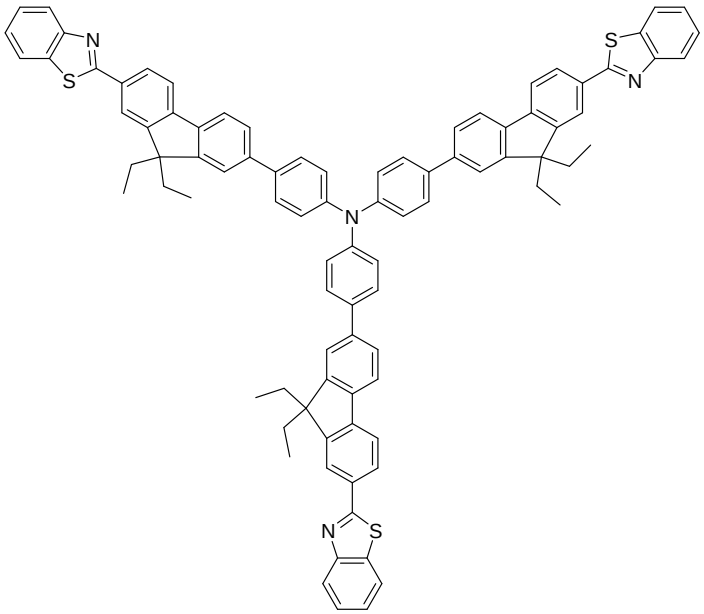

26

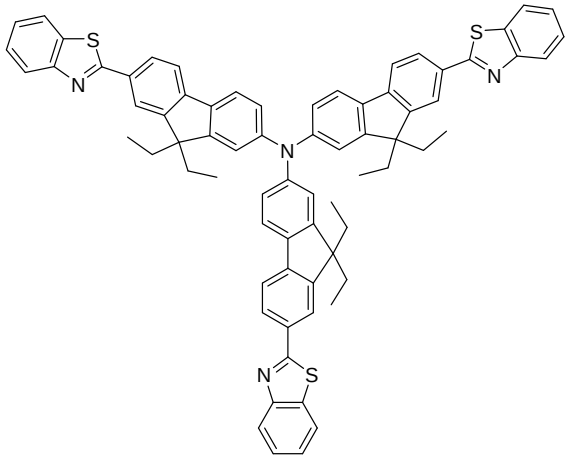

27

Chart 1.9. Typical two or multiphoton absorbing molecular systems

Table 1.1. The two photon absorption coefficient (β) and the two photon absorption cross section (σ_2) of the compounds listed in Chart 1.9

Compound	β, cm/ GW	σ_2, GM
20	0.2	490
21	4.7	9700
22	5.1	10610
23	5.6	11560
24	3.3	6840
25	5.6	11560
26	13.5	23800
27	12.0	22800

1.4. *s*-Triazine based D-A systems for OLED, NLO and photovoltaic applications

1,3,5-Triazine (**28**) and its derivatives have been recognized as synthons for the preparation of many pharmaceutical products, pesticides, dyestuffs, optical brightners, explosives and surface active agents. For example, 2,4,6-trichloro-1,3,5-triazine (Chart 1.10) has been used as an anchoring unit in reactive dyeing of textiles.[190] Triazine derivatives such as, amitole, atrazine, cyanazine, simazine, trietazine are used as herbicides. The advantages of using triazine based herbicides are that, they hydrolyze rather fast under acidic or alkaline conditions, but remain stable at neutral pH. They get disintegrated by microbial action or photochemical de-halogenation.[191] In biomedical applications

triazine based scaffolds are used due to their antitubercular and antimicrobial activity.[192-195] Several drug molecules having triazine structural units are used in antimalarial, antiviral, anticancer and estrogen receptor modulators.[196-200] They have also been used as a bioselector in enantioselective chromatography of biological molecules.[201] Another important material which contains triazine is melamine formaldehyde resin, a thermosetting resin used in the manufacture of surface coatings, laminates such as Formica and kitchen utensils.[202]

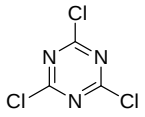

28

Chart 1.10. 2,4,6-trichloro 1,3,5-triazine

Recently, Peter Strohriegl and coworkers reported symmetrical triazine based blue fluorescent molecules (**29-38**) as host material for organic light emitting Diodes (Chart 1.11).[203-206]

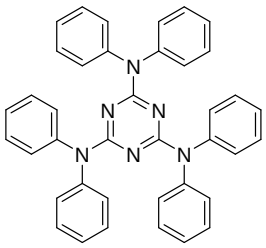

29

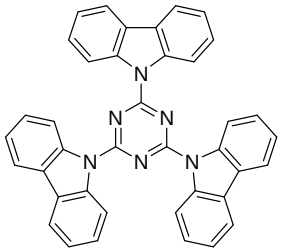

30

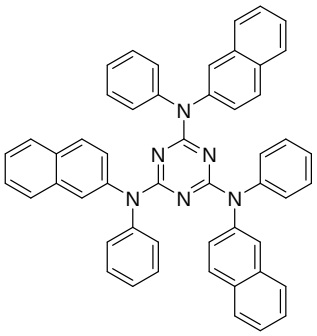

31

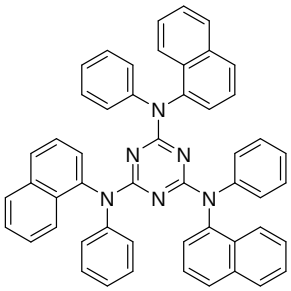

32

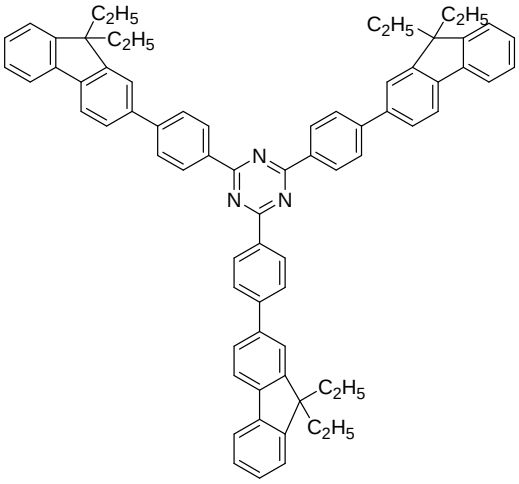

33

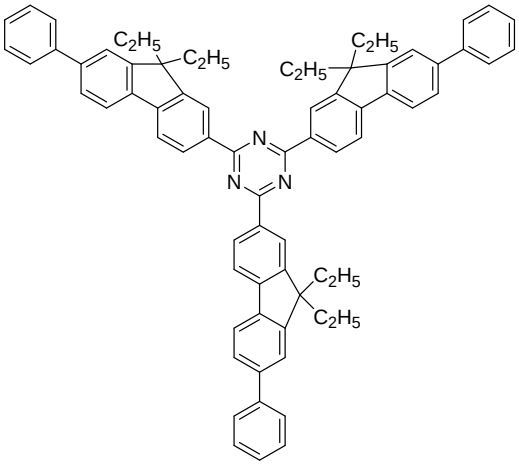

34

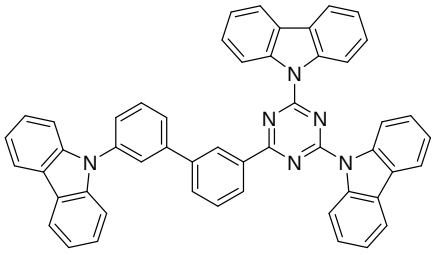

35

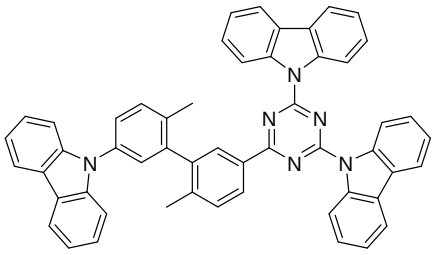

36

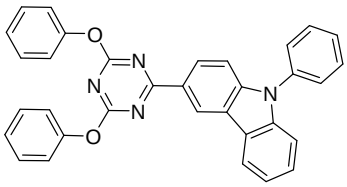

37

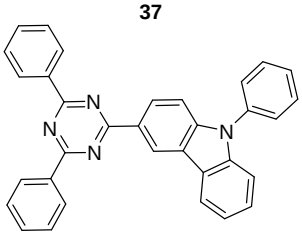

38

Chart 1.11. Symmetrical triazine based blue fluorescent molecules Organic Light Emitting Diodes

Molecules with an asymmetric polarization are useful as nonlinear optical materials. Such molecules with high nonlinearity optical transparency and photochemical and thermal stability are the major requirements for NLO applications. Azobenzene and

stilbene dyes having conjugated Donor and Acceptor groups are widely studied nonlinear optical materials.[207-208] Yoting *et. al.*, have prepared a Zn complex with *s*-triazine derivative (**39**) which showed third order NLO properties in DMF solutions. The molecule is shown to possess a nonlinear refractive index of 1.25 x 10^{-13} cm^2 W^{-1} and a $\chi^{(3)}$ value of 3.03 x 10^{-11} esu (Chart 1.12)

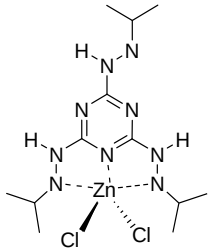

39

Chart 1.12. Zn complex with *s*-triazine based ligand

D-π-A systems with triazine as the acceptor have been reported to have two photon absorption properties. For example compounds **40** to **42** have σ_2 values 488, 1345 and 2523 respectively. Tan *et. al.*, reported a multi-branched donor substituted symmetrical triazine derivative (**43-45**) as a two photon absorbing material. The β and the σ_2 values reported for these compounds are one order higher than the values reported for typical D-A systems (Chart 1.13).

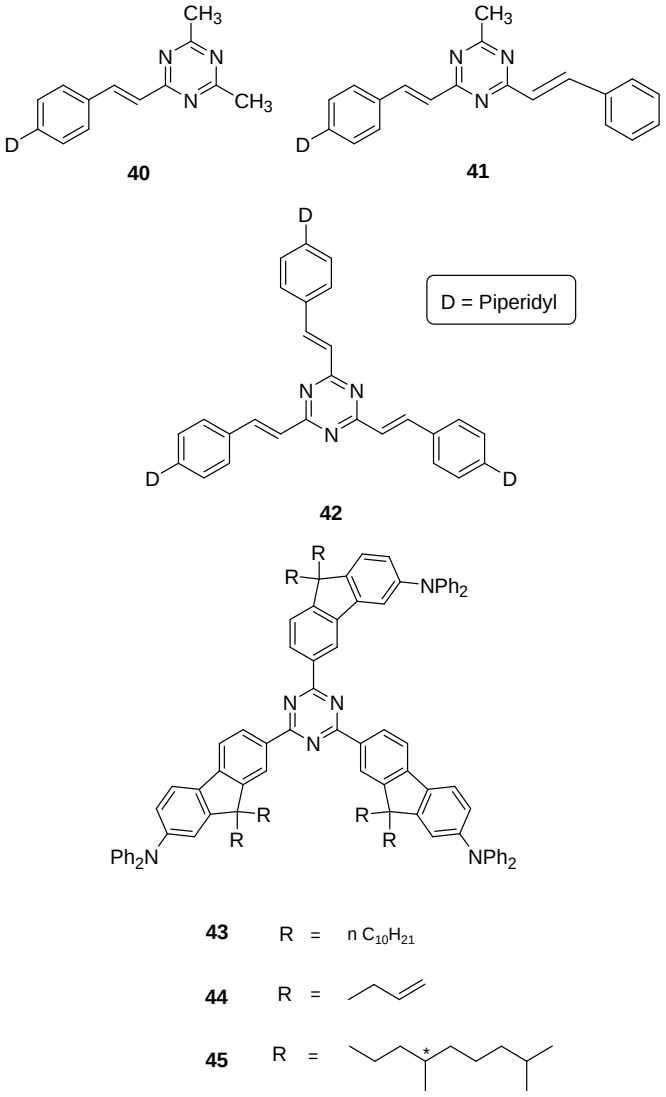

Chart 1.13. Molecular structure of two photon absorbing symmetrically substituted multi-branched triazine derivative

s-Triazines having unsymmetrical substitution pattern are promising structural unit for the synthesis of Donor-Acceptor systems. The unique structure of *s*-triazine do not permit direct coupling between the donor and acceptor moieties and this has

been used as an effective tool for tuning HOMO and LUMO energy levels of such donor-acceptor molecules. Athanassios G. Coutsolelos and coworkers reported a triazine based D-A system having porphyrin as a donor and *s*-triazine as the acceptor moiety having glycine anchoring unit for DSSC (Chart 1.14) and reported power conversion efficiency of 3.61% and 4.46% respectively,[209] for compounds **46** and **47**. In another report, triphenylamine coupled to triazine *via* direct arylation has been used in conjunction with rhodanine-3-acetic acid as the acceptor as well as the anchoring unit (**48, 49**). DSSC devices fabricated with this design philosophy yielded efficiencies in the range of 0.35-1.81%. The same group in 2013 reported another series of novel D-A organic sensitizers with improved conjugation length (**50-56**) for photovoltaic applications with power conversion efficiency about 2.70 - 3.69 % (Chart 1.14).[210]

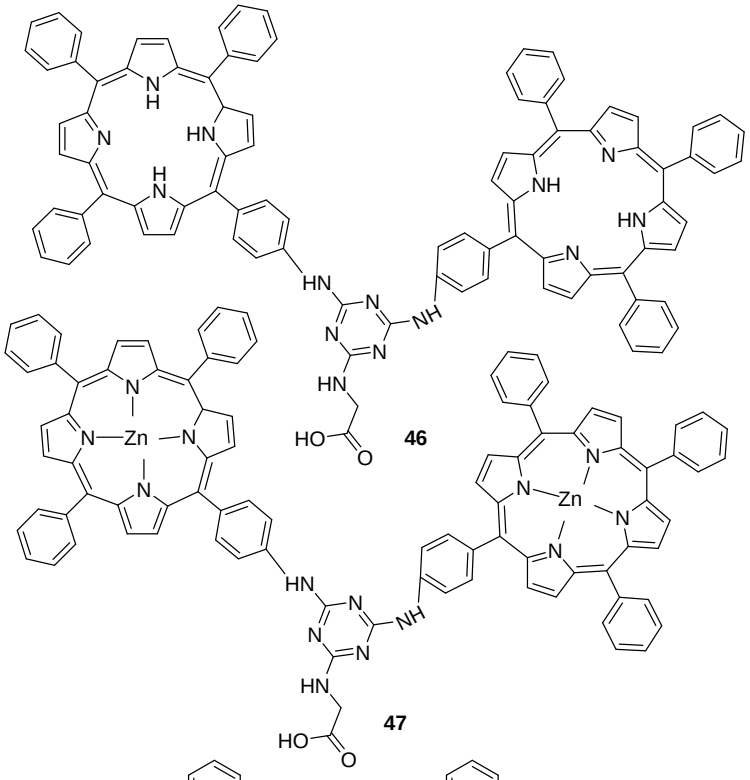

46

47

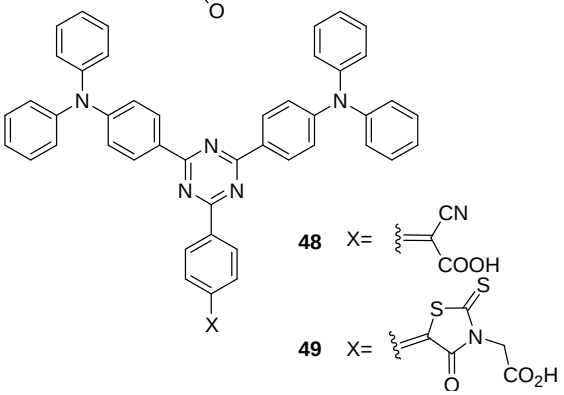

48 X=

49 X=

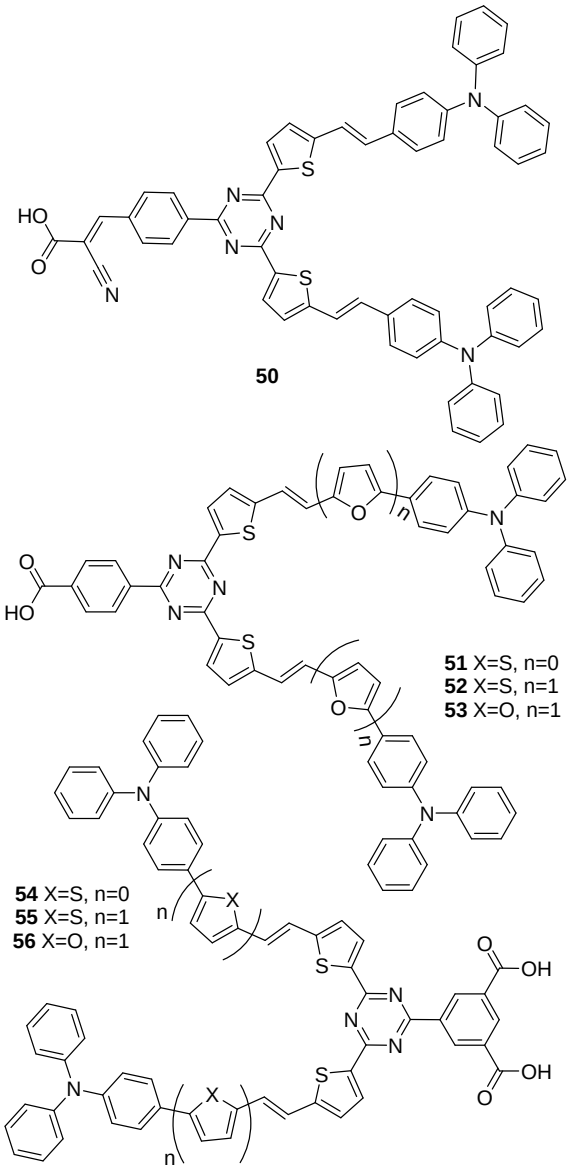

Chart 1.14. Triazine based photosensitizers

Some of the most efficient dyes reported for DSSC applications are based on inorganic complexes of Ruthenium and they are very

expensive. In this respect triazine based dyes offer the cost advantage as the starting material used for their synthesis is 2,4,6-trichloro-1,3,5-triazine (Chart 1.10) which is a cheap synthon. This molecule can undergo facile aromatic nucleophilic substitution, as well as Suzuki coupling reactions which offers the possibility of making symmetrically and unsymmetrically substituted triazine derivatives. Based on this design philosophy, we designed 1,3,5-triazine derivatives with diphenylamine as the donor and a series of heterocyclic cyclic amides as acceptors. The acceptor/anchoring groups were rhodanine-3-acetic acid, barbituric acid and thiobarbituric acid along with cyanoacetic acid for comparison (Chart 1.15). We expected a strong binding interaction with TiO_2 surface as these cyclic amides are also strong acids which can deprotonate and bind as observed in dyes with cyanoacetic acid as the anchoring unit.

Though triazine derivatives have been used as materials for NLO applications, molecules with the D-A-A configuration have not been studied for NLO applications. We, for the first time report the third order nonlinear optical properties of the proposed multibranched D-A-A systems with triazine as the core.

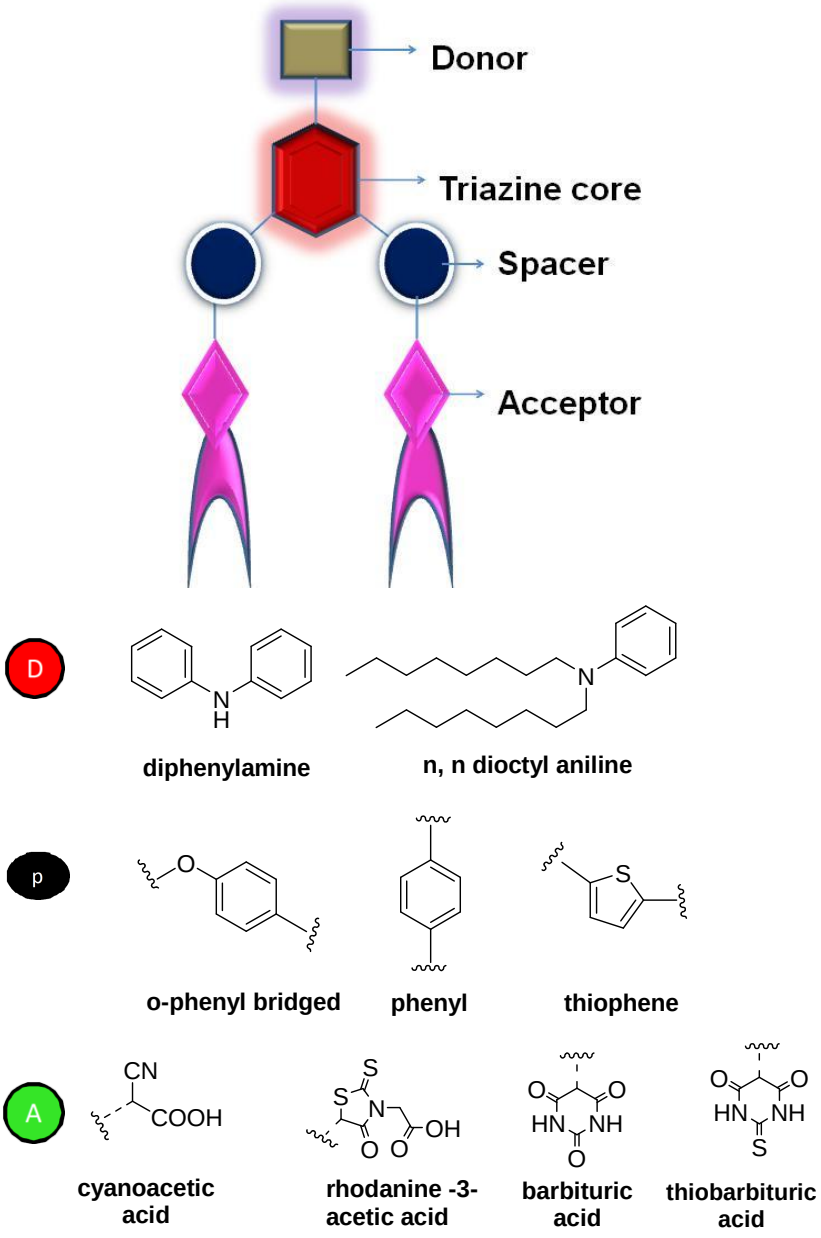

Chart 1.15. Our design for the molecule

1.5. Objectives of the thesis

The major objectives of the present thesis are:

1. Synthesis and characterization of multibranched D–A–A systems incorporating triazine as the internal spacer and cyclic amides as the acceptor.
2. Study of the photovoltaic properties of the synthesized compounds.
3. Study of the nonlinear optical properties of the synthesized compounds.

1.6. References

1. Kivala, M.; Diederich, F., *Acc. Chem. Res*. **2009**, *42*, 235.
2. Kato, S.; Diederich, F., *Chem. Commun*. **2010**, *46*, 1994.
3. Meier, H., *Angew. Chem., Int. Ed*. **2005**, *44*, 2482.
4. Kivala, M.; Diederich, F., *Pure Appl. Chem.* **2008**, *80*, 411.
5. Burland, D.; *Chem. Rev*. **1994**, *94*, 1.
6. He, G. S.; Tan, L.-S.; Zheng.; Q. Prasad, P. N., *Chem. Rev.* **2008**, *108*, 1245.
7. Kawabe, Y.; Ikeda, H.; Sakai, T.; Kawasaki, K., *J. Mater. Chem*. **1992**, *2*, 1025.
8. Marder, S. R.; Perry, J. W., *Adv. Mater*. **1993**, *5*, 804.
9. Coe, B. J., *Chem. - Eur. J*. **1999**, *5*, 2464.
10. Asselberghs, I.; Clays, K.; Persoons, A.; Ward, M. D.; McCleverty, J., *J. Mater. Chem*. **2004**, *14*, 2831.
11. Sullivan, P. A.; Dalton, L. R., *Acc. Chem. Res.* **2010**, *43*, 10.
12. Stahelin, M.; Zysset, B.; Ahlheim, M.; Marder, S. R.; Bedworth, P. V.; Runser, C.; Barzoukas, M.; Fort, A., *J. Opt. Soc. Am. B*. **1996**, *13*, 2401.
13. Chen, F.; Zhang, J.; Wan, X., *Chem. - Eur. J.* **2012**, *18*, 4558.
14. Raymo, F. M.; Tomasulo, M., *Chem. Eur. J.* **2006**, *12*, 3186.
15. Reichardt, C.; *Solvents and solvent effects in organic chemistry*, *Wiley-VCH*, Weinheim, **2004,** *3rd ed.*
16. Bureˇs, F.; Pytela, O.; Kivala M.; Diederich, F., *J. Phys. Org. Chem*. **2011**, *24*, 274.
17. Bureˇs, F.; Pytela, O.; Diederich, F., *J. Phys. Org. Chem*. **2009**, *22*, 155.
18. Forrest, S. R.; Thompson, M. E., *Chem. Rev*, **2007**, *107*, 923.
19. Miller, R. D.; Chandross, E. A., *Chem. Rev*. **2010**, *110*, 1.
20. Mayor, M., *Chimia*, **2010**, *64*, 348.
21. Batail, P., *Chem. Rev*, **2004**, *104*, 4887.
22. Bredas, J. L.; Durrant, J. R., *Acc. Chem. Res*, **2009**. *42*, 1689.
23. Lin, Y.; Li, Y.; Zhan, X., *Chem. Soc. Rev.* **2012**, *41*, 4245.
24. Nozik, A. J.; Miller, J. R., *Chem. Rev*. **2010**, *110*, 6443.
25. Wu, Y.; Zhu, W., *Chem. Soc. Rev*. **2013**, *42*, 2039.

26. Clifford, J. N.; Mart´ınez-Ferrero, E.; Viterisi, A.; Palomares, E., *Chem. Soc. Rev*. **2011**, *40*, 1635.
27. Duan, C.; Zhang, K.; Zhong, C.; Huang, F.; Cao, Y., *Chem. Soc. Rev*. **2013**, *42*, 9071.
28. Liang, M.; Chen, J., *Chem. Soc. Rev*. **2013**, *42*, 3453.
29. Achelle, S.; Baudequin, C.; Pl´e, N. *Dyes Pigm*. **2013**, *98*, 575.
30. Achelle, S.; Pl´e, N.; Turck, A., *RSC Adv*. **2011**, *1*, 364.
31. Achelle, S.; Pl´e, N., *Curr. Org. Synth*. **2012**, *9*, 163.
32. Hrob´arik, P.; Hrob´arikov´a, V.; Sigmundov´a, I.; Zahradn´ık, P.; Fakis, M.; Polyzos, I.; Persephonis, P., *J. Org. Chem*. **2011**, *76*, 8726.
33. Hrob´arikov´a, V.; Hrob´arik, P.; Gajdoˇs, P.; Fitilis, I.; Fakis, M.; Persephonis, P.; Zahradn´ık, P., *J. Org. Chem*. **2010**, *75*, 3053.
34. Handbook of thiophene-based materials, applications in organic electronics and photonics, ed. I. F. Perepichka and D. F. Perepichka, Wiley, Chicester, **2009**, vol. 1 and 2.
35. Andreu, R.; Carrasquer, L.; Franco, S.; Gar´ın, J.; Orduna, J.; de Baroja, N. M.; Alicante, R.; Villacampa, B.; Allain, M., *J. Org. Chem*. **2009**, *74*, 6647.
36. Andreu, R.; Gal´an, E.; Gar´ın, J.; Herrero, V.; Lacarra, E.; Orduna, J.; Alicante, R.; Villacampa, B., *J. Org. Chem*. **2010**, *75*, 1684.
37. Faux, N.; Caro, B.; Robin-Le Guen, F.; Le Poul, P.; Nakatani, K.; Ishow, E., *J. Organomet. Chem*. **2005**, *690*, 4982.
38. Gauthier, S.; Vologdin, N.; Achelle, S.; Barsella, A.; Caro, B.; Robin-Le Guen, F.; *Tetrahedron* **2013**, *69*, 8392.
39. Long, N. J., *Angew. Chem., Int. Ed. Engl*. **1995**, *34*, 21.
40. Nalwa, H. S., *Appl. Organomet. Chem*. **1991**, *5*, 349.
41. Kulh´anek, J.; Bureˇs, F.; Kuznik, W.; Kityk, I. V.; Mikysek, T.; R uzicka, A., *Chem. Asian J*. **2013**, *8*, 465.

42. Barlow, S.; Bunting, H. E.; Ringham, C.; Green, J. C.; Bublitz, G. U.; Boxer, S. G.; Perry, J. W.; Marder, S. R., *J. Am. Chem. Soc*. **1999**, *121*, 3715.
43. Salman, S.; Br´edas, J.-L.; Marder, S. R.; Coropceanu V.; Barlow, S., *Organometallics* **2013**, *32*, 6061.
44. Kinnibrugh, T. L.; Salman, S.; Getmanenko, Y. A.; Coropceanu, V.; Porter III, W. W.; Timofeeva, T. V.; Matzger, A. J.; Br´edas, J.-L.; Marder, S. R.; Barlow, S., *Organometallics* **2009**, *28*, 1350.
45. Reichardt, C., *Chem. Rev.* **1994,** *94*, 2319.
46. Nazeeruddin, M. K.; Kay, A.; Rodicio, I.; Humphry-Baker, R.; Muller, E.; Liska, P.; Vlachopoulos, N.; Gr.atzel, M., *J. Am. Chem. Soc.* **1993**, *115*, 6382.
47. Smith, W., *Nature* **1873**, *7*, 303.
48. Pochettino, A., *Acad. Lincei Rend.* **1906**, *15*, 355.
49. Hoegel, H., *Phys. Chem.* **1965,** *69*, 755.
50. Stork, M.; Gaylord, B. S.; Heeger, A. J.; Bazan, G. C., *Adv. Mater*. **2002**, *14*, 361.
51. Thomas, S. W., III.; Joly, G.; Swager, T. M., *Chem. Rev*. **2007**, *107*, 1339.
52. Chapin, D. M.; Fuller, C. S.; Pearson. G. L., *J. Appl. Phys.* **1954,** *25*, 676.
53. Sarah, K.; Keith, E., National Renewable Energy Laboratory (NREL), Golden, CO, February 2016, https://en.wikipedia.org/wiki/Solar_cell.
54. Andersen, T. R.; Dam, H. F.; Hosel, M.; Helgesen, M.; Carle, J. E.; Larsen-Olsen, T. T.; Gevorgyan, S. A.; Andreasen, J. W.; Adams, J.; Li, N.; Machui, F.; Spyropoulos, G. D.; Ameri, T.; Lemaitre, N.; Legros, M.; Scheel, A.; Gaiser, D.; Kreul, K.; Berny, S.; Lozman, O. R.; Nordman, S.; Valimaki, M.; Vilkman, M.; Sondergaard, R. R.; Jorgensen, M.; Brabec, C. J.; Krebs, F. C., *Energy Environ. Sci.* **2014,** *9*, 2925.

55. Morel, D. L.; Gosh, A. K.; Feng, T.; Stogryn, E. L.; Purwin, P. E.; Shaw, R. F.; Fishman, C., *Appl. Phys. Lett.* **1978**, *32*, 495.
56. Ramanathan, K.; Contreras, M. A.; Perkins, C. L.; Asher, S.; Hasoon, F. S.; Keane, J.; Young, D.; Romero, M.; Metzer, W.; Noufi, R.; Ward, J.; Duda, A., *Prog. Photovolt. Res. Appl.* **2003**, *11*, 225.
57. Tang, C.W., *Appl. Phys. Lett*. **1986,** *48*, 183.
58. Nguyen, B. P.; Kim, T.; Park, C. R., *J Nanomater.* **2014,** 1.
59. Hiramoto, M.; Fujiwara, H.; Yokoyama, M., *J. Appl. Phys*. **1992**, *72*, 3781.
60. Taima, T.; Chikamatsu, M.; Yoshida, Y.; Saito, K.; Yase, K., *Appl. Phys. Lett*. **2004**, *85*, 6412.
61. Xue, J.; Rand, B. P.; Uchida, S.; Forrest, S. R., *J. Appl. Phys*. **2005**, *98*, 124903.
62. Kong, F. T.; Dai S.Y.; Wang, K. J., *Adv. Opto Electron.* **2007**, *1*.
63. Hara, K., *Sol. Energy Mater. Sol. Cells*. **2003**, *103*, 7789.
64. Regan, B. O'; Grätzel, M., *Nature* **1991**, *353*, 737.
65. Sarah, K.; Keith E., National Renewable Energy Laboratory (NREL), Golden, CO, February 2016, https://en.wikipedia.org/wiki/Solar_cell.
66. Sun, K.; Li, P.; Xia, Y.; Chang, J.; Ouyang, J., *ACS Appl. Mater. Interfaces.* **2015,** *7*, 15314.
67. Kim, H. S.; Lee, C. R.; Im, J. H.; Lee, K. B.; Moehl, T.; Marchioro, A.; Moon, S. J.; Humphry-Baker, R.; Yum, J. H.; Moser, J. E.; Grätzel, M.; Park, N. G., *Sci. Rep.* **2012**, *2*, 591.
68. Tanaka, K.; Takahashi, T.; Ban, T.; Kondo, T.; Uchida, K.; Miura, N., *Solid State Commun*. **2003**, *127*, 619.
69. Qing, J., *Org. Electron.* **2015,** *27*, 12.
70. Tang, C. W.; VanSlyke, S. A., *Appl. Phys. Lett.* **1987**, *51*, 913.
71. Walzer, K.; Maennig, B.; Pfeiffer, M.; Leo, K., *Chem. Rev*. **2007**, *107*, 1233.
72. Burn, P. L.; Lo, S.-C.; Samuel, I. D. W., *Adv. Mater*. **2007**, *19*, 1675.

73. Forrest, S. R.; Thompson, M. E., *Chem. Rev.* **2007**, *107*, 923.
74. Burroughes, J. H.; Bradley, D. C.; Brown, A. R.; Marks, R. N.; MacKay, K.; Friend, R. H.; Burn, P. L.; Holmes, A. B., *Nature* **1990**, *347*, 539.
75. Gustafsson, G.; Cao, Y.; Treacy, G. M.; Klavetter, F.; Colaneri, N.; Heeger, A. J., *Nature* **1992**, *357*, 477.
76. Grimsdale, A. C.; Chan, K. L.; Martin, R. E.; Jokisz, P. G.; Holmes, A. B., *Chem. Rev.* **2009**, *109*, 897.
77. Grimsdale, A. C.; Mullen, K., *Adv. Polym. Sci.* **2006**, *199*, 1.
78. Bernius, M. T.; Inbasekaran, M.; O'Brien, J.; Wu, W. S., *Adv. Mater*. **2000**, *12*, 1737.
79. Tsumura, A.; Koezuka, H.; Ando, T., *Appl. Phys. Lett*. **1986**, *49*, 1210.
80. Nazeeruddin, M. K.; Pechy, P.; Grätzel, M. *Chem. Commun*. **1997**, 1705.
81. Gerischer, H.; Tributsch, H.; *Ber. Bunsen-Ges., Phys. Chem.* **1968**, *72*, 437.
82. Nazeeruddin M. K.,; Pechy, P.; Renouard, T.; Zakeeruddin, S. M.; Humphry-Baker, R.; Comte, P.; Liska, P.; Cevey, L.; Costa, E.; Shklover, V.; Spiccia, L.; Deacon, G. B.; Bignozzi, C. A.; Grätzel, M., *J. Am. Chem. Soc.* **2001**, *123*, 1613.
83. Nazeeruddin, M. K.; Zakeeruddin, S.M.; Humphry-Baker, R.; Jirousek, M.; Liska, P.; Vlachopoulos, N.; Shklover, V.; Fischer, C.-H; Sugihara, H.; Singh, L.P.; Sayama, K.; Arakawa, H.;. Nazeeruddin, Md. K.; Grätzel, M. *Chem. Lett*. **1998**, *10*, 1005.
84. Hara, K.; Sugihara, H.; Tachibana, Y.; Islam, A.; Yanagida, M.; Sayama, K.; Arakawa, H.; Fujihashi, G.; Horiguchi, T.; Kinoshita, T. *Langmuir* **2001**, *17*, 5992.
85. Smestad, G.; Bignozzi, C.; Argazzi, R. *Sol. Energy Mater. Sol. Cells* **1994**, *32*, 259.
86. Zi, M.; Zhu, M.; Chen, L.; Wei, H.; Yang, X.; Cao, B., *Ceram. Int*. **2014**, *40*, 7965.

87. Zhu, S.; Tian, X.; Chen, J.; Shan, L.; Xu, X.; Zhou, Z., *J. Phys. Chem. C*. **2014,** *118*, 16401.
88. Lee, K.; Lee, E. S.; Yoo, B.; Shin, D. H., *Elect. Acta*. **2013,** *109*, 181.
89. Rani, R. A.; Zoolfakar, A. S.; Subbiah, J.; Ou, J. Z.; Kalantar-Zadeh, K., *Ele. Com.* **2013**, *40*, 20
90. Rani, R. A; Zoolfakar, A. S.; Subbiah, J., Ou, J. Z.; Kadir, R. A.; Nili, H.; Latham, K., *Chem. Commun.* **2013**, *49*, 6349.
91. Jeong B. Y.; Jung, E. H., *Met. Mater. Int*. **2013,** 19, 617.
92. Yang, J. H.; Bark, C. W.; Kim, K. H.; Choi, H. W., *Materials* **2014,** *7*, 3532.
93. Grätzel, M., *Acc. Chem.* Res. **2009**, *42*, 1788.
94. Winter, M.; Brodd, R., *Chem. Rev*. **2004**, *104*, 4245.
95. Xu, K., *Chem. Rev*. **2004**, *104*, 4303.
96. Wu, J.; Lan, Z.; Hao, S.; Li, P.; Lin, J.; Huang, M.; Fang, L.; Huang, Y., *Pure Appl. Chem.* **2008**, *80*, 2241.
97. Ardo, S.; Meyer, G. J., *Chem. Soc. Rev*. **2009**, *38*, 115.
98. Yu, Z.; Vlachopoulos, N.; Gorlov, M.; Kloo, L., *Dalton Trans.* **2011**, *40*, 10289.
99. Freitas, J.; Nogueira, A.; De Paoli, M., *J. Mater. Chem*. **2009**, *19*, 5279.
100. Zhang, W.; Cheng, Y.; Yin, X.; Liu, B., *Macromol. Chem. Phys*. **2011**, *212*, 15.
101. Yu, Z.; Vlachopoulos, N.; Gorlov, M.; Kloo, L., *Dalton Trans*. **2011**, *40*, 10289.
102. Hagfeldt, A.; Grätzel, M., *Acc. Chem. Res.* **2000**, *33*, 269.
103. Mathew, S.; Yella, A.; Gao, P.; Humphry Baker, R.; Curchod, B.; Ashari-Astani, N.; Tavernelli, I.; Rothlisberger, U.; Nazeeruddin, M.; Grätzel, M., *Nat. Chem*. **2014**, *6*, 242.
104. Hagfeldt, A.; Boschloo, G.; Sun, L.; Kloo, L.; Pettersson, H., *Chem. Rev*. **2010**, *110*, 6595.
105. Mecerreyes, D., *Prog. Polym. Sci.* **2011**, *36*, 1629.
106. Weingartner, H., *Angew. Chem. Int. Ed*, **2008**, *47*, 654.

107. Li, F.; Jennings, J.; Wang, X.; Fan, L.; Koh, Z.; Yu, H.; Yan, L.; Wang, Q., *J. Phys. Chem. C.* **2014**, *118*, 17153.
108. Krossing, I.; Reisinger, A., *Coord. Chem. Rev*. **2006**, *250*, 2721.
109. Papageorgiou, N.; Athanassov, Y.; Armand, M.; Bonhote, P.;Pettersson, H.; Azam, A.; Grätzel, M., *J. Electrochem. Soc*. **1996**, *143*, 3099.
110. Wang, P.; Zakeeruddin, S.; Moser, J.; Baker, R.; Grätzel, M., *J. Am. Chem. Soc*. **2004**, *126*, 7164.
111. Bai, Y.; Cao, Y.; Zhang, J.; Wang, M.; Li, R.; Wang, P.;Zakeeruddin, S.; Grätzel, M., *Nat. Mater*. **2008**, *7*, 626.
112. Paulsson, H.; Hagfeldt, A.; Kloo, L., *J. Phys. Chem. B*. **2003**, *107*, 13665.
113. Ramirez, R.; Sanchez, E., *Sol. Energy Mater. Sol. Cells* **2006**, *90*, 2384.
114. Santa-Nokki, H.; Busi, S.; Kallioinen, J.; Lahtinen, M.; Korppi-Tommola, J., *J. Photochem. Photobiol*. A. **2007**, *186*, 29.
115. Xi, C.; Cao, Y.; Cheng, Y.; Wang, M.; Jing, X.; Zakeeruddin, S.; Ito, S.; Nazeeruddin, M.; Liska, P.; Comte, P.; Charvet, R.; Pechy, P.; Jirousek, M.; Kay, A.; Zakeeruddin, M.; Grätzel, M., *Prog. Photovoltaics Res. Appl*. **2006**, *14*, 589.
116. Zakeeruddin, S.; Gratzel, M. *Adv. Funct. Mater.***2009**, *19*, 2187.
117. Boschloo, G.; Hagfeldt, A., *Acc. Chem. Res*. **2009**, *42*, 1819.
118. Wang, Z.; Sayama, K.; Sugihara, H., *J. Phys. Chem. B*. **2005**, *47*, 22449.
119. Teng, C.; Yang, X.; Yuan, C.; Li, C.; Chen, R.; Tian, H.; Li, S.; Hagfeldt, A.; Sun, L., *Org. Lett.*, **2009,** *11*, 5542.
120. Nazeeruddin, K.; Kay, A.; Rodicio, I.; Humphry-Baker, R.; Mueller, E.; Liska, P.; Vlachopoulos, N.; Grätzel, M., *J. Am. Chem. Soc*. **1993**, *115*, 6382.
121. Watson, D.; Meyer, G., *Coord. Chem. Rev*. **2004,** *248*, 1391.

122. Zhang, C.; Huang, Y.; Huo, Z.; Chen, S.; Dai, S., *J. Phys. Chem. C*. **2009**, *113*, 21779.
123. Grätzel, M., *J. Photochem. Photobiol*, A. **2004**, *164*, 3.
124. Hagfeldt, A.; Boschloo, G.; Sun, L.; Kloo, L.; Pettersson, H., *Chem. Rev*. **2010**, *110*, 6595.
125. Wu, J.; Lan, Z.; Hao, S.; Li, P.; Lin, J.; Huang, M.; Fang, L.; Huang, Y., *Pure Appl. Chem*. **2008**, *80*, 2241.
126. Nogueira, A.; Longo, C.; De Paoli, M., *Coord. Chem. Rev*. **2004**, *248*, 1455.
127. Freitas, J.; Nogueira, A.; De Paoli, M., *J. Mater. Chem*. **2009**, *19*, 527.
128. Wu, J.; Hao, S.; Lan, Z.; Lin, J.; Huang, M.; Huang, Y.; Fang,L.; Yin, S.; Sato, T., *Adv. Funct. Mater.* **2007**, *17*, 2645.
129. Wu, J.; Lan, Z.; Lin, J.; Huang, M.; Hao, S.; Sato, T.; Yin, S., *Adv. Mater*. **2007**, *19*, 4006.
130. *Gorlov, M.; Kloo, L.Dalton Trans.2008, 2655*
131. Li, D.; Qin, D.; Deng, M.; Luo, Y.; Meng, Q., *Energy Environ. Sci*. **2009**, *2*, 283.
132. Stathatos, E.; Lianos, P.; Lavrencic-Stangar, U.; Orel, B., *Adv. Mater*. **2002**, *14*, 354.
133. Nogueira, A. F.; Durrant, J. R.; DePaoli, M. A., *Adv. Mater*. **2001**, *13*, 826.
134. Wu, J.; Hao, S.; Lan, Z.; Lin, J.; Huang, M.; Huang, Y.; Li, P.; Yin, S.; Sato, T., *J. Am. Chem. Soc.*, **2008,** *130*, 11568.
135. Lowman, G. M.; Hammond, P. T., *Small*, **2005,** *1*, 1070.
136. Meng, Q.; Takahashi, K.; Zhang, X.; Sutanto, I.; Rao, T.; Satom, O.; Fujishima, A., *Langmuir* **2003**, *19*, 3572.
137. Saito, Y.; Azechi, T.; Kitamura, T.; Hasegawa, Y.; Wada, Y.; Yanagida, S., *Coord. Chem. Rev*. **2004**, *248*, 1469.
138. Li, B.; Wang, L.; Kang, B.; Wang, P.; Qiu, Y., *Sol. Energy Mater. Sol. Cells* **2006**, *90*, 549.
139. Chung, I.; Lee, B.; He, J.; Chang, R.; Kanatzidis, M., *Nature* **2012**, *485*, 486.

140. Bach, U.; Lupo, D.; Comte, P.; Moser, J. E.; Weissortel, F.; Salbeck, J.; Spreitzer, H.; Grätzel, M., *Nature* **1998**, *395*, 583.
141. Zhang, W.; Cheng, Y.; Yin, X.; Liu, B., *Macromol. Chem. Phys*. **2011**, *212*, 15.
142. Snaith, H.; Moule, A.; Klein, C.; Meerholz, K.; Friend, R.; Grätzel, M., *Nano Lett.* **2007**, *7*, 3372.
143. Kroeze, J.; Hirata, N.; Schmidt-Mende, L.; Orizu, C.; Ogier, S.; Carr, K.; Grätzel, M.; Durrant, J., *Adv. Funct. Mater*. **2006**, *16*, 1832.
144. Schmidt-Mende, L.; Grätzel, M., *Thin Solid Films*. **2006**, *500*, 296.
145. Smestad, G.; Spiekermann, S.; Kowalik, J.; Grant, C.; Schwartzberg, A.; Zhang, J.; Tolbert, L.; Moons, E. , *Sol. Energy Mater. Sol. Cells* **2003**, *76*, 85.
146. Tennakone, K.; Kumara, G.; Kumarasinghe, A.; Wijayantha, K.; Sirimanne, P. M., *Semicond. Sci. Technol*. **1995**, *10*, 1689.
147. Kumara, G.; Konno, A.; Senadeera, G.; Jayaweera, P.; De Silva, Tennakone, K.; Senadeera, G.; De Silva, D.; Kottegoda, I., *Appl.Phys. Lett*. **2000**, *77*, 2367.
148. O'Regan, B.; Schwartz, D., *Chem. Mater*. **1998**, *10*, 1501.
149. Tennakone, K.; Kumara, G.; Kottegoda, I.; Wijayantha, K.; Perrera, V., *J. Phys. D: Appl. Phys.* **1998**, *31*, 1492.
150. Tennakone, K.; Perera, V.; Kottegoda, I.; Kumara, G., *J. Phys. D*. **1999**, *32*, 374.
151. Taher, M. El-Agez.; Sopyan, A. T.; Kamal S. E.; Monzir S. Abdel- Latif, *Optica Applicata*. **2014**, *44*, 345.
152. Joly, D.; Pellejà, L.; Narbey, S.; Oswald, F.; Chiron, J.; Clifford, J.N.; Palomares, E.; Demadrille, R., *Sci. Rep*. **2014**, *4*, 4033. doi:10.1038/srep04033
153. Clifford, J. N.; Martınez-Ferrero, E.; Viterisi, Palomares, E., *Chem. Soc. Rev*. **2011**, *40*, 1635.
154. Duan, C.; Zhang, K.; Zhong, C.; Huang, F.; Cao, Y., *Chem. Soc. Rev*. **2013**, *42*, 9071.

155. Liang, M.; Chen, J., Chem. *Soc. Rev.* **2013**, *42*, 3453.
156. Zhang, J.; Yang, L.; Zhang, M.; Wang, P., *RSC Adv*. **2013**, *3*, 6030.
157. Bureš, F., *RSC Adv*. **2014**, *4*, 58826.
158. Zhao, Y.; Zhang, C.; Chin, K. F.; Pytela, O.;Wei, G.; Liu, H.; Bureˇs, F.; Jiang, Z., *RSC Adv*. **2014**, *4*, 30062.
159. Grätzel, M., *Inorg. Chem*. **2005**, *44*, 6841.
160. Zhang, L.; Cole, J. M., *ACS Appl. Mater. Interfaces* **2015,** *7*, 3427.
161. Gouterman, M., *J. Mol. Spectrosc*. **1961**, *6*, 138.
162. Campbell, W. M.; Jolley, K. W.; Wagner, P.; Wagner, K.; Walsh, P. J.; Gordon, K. C.; Schmidt-Mende, L.; Nazeeruddin, M. K.; Wang, Q.; Grä tzel, M.; Officer, D. L., *J. Phys. Chem. C*. **2007**, *111*, 11760.
163. Wang, C.-L.; Chang, Y.-C.; Lan, C.-M.; Lo, C.-F.; Diau, E. W.-G.; Lin, C.-Y., *Energy Environ. Sci.* **2011**, *4*, 1788.
164. Yella, A.; Lee, H. W.; Tsao, H. N.; Yi, C.; Chandiran, A. K.; Nazeeruddin, M. K.; Diau, E. W. G.; Yeh, C. Y.; Zakeeruddin, S. M.; Grätzel, M. , *Science.* **2011**, *334*, 629.
165. Bessho, T.; Zakeeruddin, S. M.; Yeh, C.-Y.; Diau, E. W.-G.; Grätzel, M., *Angew. Chem., Int. Ed*. **2010**, *49*, 6646.
166. Wang, C.-L.; Lan, C.-M.; Hong, S.-H.; Wang, Y. F.; Pan, T.-Y.; Chang, C. W.; Kuo, H. H.; Kuo, M. Y.; Diau, E. W.-G.; Lin, C. Y., *Energy Environ. Sci*. **2012**, *5*, 6933.
167. Satoh, N.; Cho, J. S.; Higuchi, M.; Yamamoto, K., *J. Am. Chem. Soc*. **2003**, *125*, 8104.
168. Satoh, N.; Nakashima, T.; Yamamoto, K., *J. Am. Chem. Soc*. **2005**, *127*, 13030.
169. Wang, Q.; Zakeeruddin, S. M.; Cremer, J.; Ba ¨uerle, P.; Humphry-Baker, R.; Grätzel, M., *J. Am. Chem. Soc*. **2005**, *127*, 5706.
170. Koumura, N.; Wang, Z.-S.; Mori, S.; Miyashita, M.; Suzuki, E.; Hara, K., *J. Am. Chem. Soc*. **2006**, *128*, 14256.

171. Wang, Z.-S.; Koumura, N.; Cui, Y.; Miyashita, M.; Mori, S.; Hara, K., *Chem. Mater*. **2009**, *21*, 2810.
172. Tian, H.; Yang, X.; Chen, R.; Pan, Y.; Li, L.; Hagfeldt, A.; Sun, L., *Chem. Commun*. **2007**, *36*, 3741.
173. Chen, C.; Liao, J.-Y.; Chi, Z.; Xu, B.; Zhang, X.; Kuang, D.-B.; Zhang, Y.; Liu, S.; Xu, J., *J. Mater. Chem*. **2012**, *22*, 8994.
174. Cao, D.; Peng, J.; Hong, Y.; Fang, X.; Wang, L.; Meier, H., *Org. Lett*. **2011**, *13*, 1610.
175. Xu, W., Peng, B., Chen, J., Liang, M., Cai, F. *J. Phys. Chem. C.* **2008**, *112*, 874.
176. Wu, G.; Kong, F.; Zhang, Y.; Zhang, X.; Li, J.; Chen, W.; Liu, W.; Ding, Y.; Zhang, C.; Zhang, B.; Yao, J.; Dai, S., *J. Phys. Chem. C.* **2014,** *118*, 8756.
177. Teng, C.; Yang, X.; Yuan, C.; Li, C.; Chen, R.; Tian, H.; Li, S.; Hagfeldt, A.; Sun, L., *Org. Lett.* **2009,** *11*, 5545.
178. Kim, S. H.; Kim, H. W.; Sakong C.; Namgoong, J.; Park, S. W.; Ko, M., J. L.; Choong, H. L., Wan, I.; Kim, J. P., *Org. Lett*. **2011**, *13*, 5784.
179. Ning, Z.; Zhang, Q.; Wu, W.; Pei, H.; Liu, B.; Tian, H., *J. Org. Chem.* **2008,** *73*, 3791.
180. Wan, Z.; Jia, C.; Duan, Y.; Zhou, L.; Lin, Y.; Shi, Y., *J. Mater. Chem.* **2012,** *22*, 25140.
181. He, G. S.; Tan, L. S.; Zheng, Q.; Prasad, P. N., *Chem. Rev.* **2008,** *108* ,1245.
182. Reichert, M.; Hu, H.; Ferdinandus, M. R.; Seidel, M.; Zhao, P.; Ensley, T. R.; Peceli, D.; Reed, J. M.; Fishman, D. A.; Webster, S.; Hagan, D. J.; Van Stryland, E. W., *Optica* **2014,** *1*, 436.
183. Ganeev, R. A.; Ryasnyanski, A. I.; Kuroda, H., *Opt. Spectrosc.* **2006,** *100*, 108.
184. R. W. Boyd., *Nonlinear Optics*, 2008, Academic /Elsevier, 3rd ed.
185. P. Yeh., Introduction to Photorefractive Nonlinear Optics, Wiley, New York, **1993**.

186. Kim, W. H.; Kodali, N. B; Kumar, J.; Tripathi, S. K., *Macromolecules* **1994**, *27*, 1819.
187. Chen, X., *Dyes Pigm*. **2008**, *77*, 223.
188. Shirk, J. S.; Lindle, J. R.; Bartoli, F. J.; Boyle, M. E., *J. Phys. Chem*. **1992**, *96*, 5847.
189. John Kiran, A.; Chandrasekharan, K.; Nooji, S. R.; Shashikala, H. D.; Umesh, G.; Kalluraya, B., *Chem. Phys.* **2006**, *324*, 699.
190. Horst, T.; Walter, H.; Peter, M.; Karl, R.; Uwe, R.; Werner, R.; Ludwig, S.; Petra, V., Wiley-VCH, Weinheim, **2000.**
191. Penuela, G. A.; Barcelo, D., Trac-Trend. *Anal. Chem.* **1998**, *10*, 605.
192. Comins, D. L.; O′ 'Connor; Katritzky, A. R., *Adv. Heterocycl. Chem.;* Ed.; Academic: New York, NY, **1988**, *44*, 243.
193. Giacomelli, G.; Porcheddu, A.; De Luca, L., *Curr. Org. Chem*. **2004**, *8*, 1497.
194. LeBaron, H. M.; McFarland J. E.; Burnside, O. C., *The Triazine Herbicides*; Elsevier, San Diego, USA, **2008.**
195. Amit B. Patel; Rahul V. Patel; Premlata Kumari; Dhanji P. Rajani; Kishor H. Chikhalia; *Med. Chem. Res.* **2013,** *22*, 367.
196. Melato, S.; Prosperi, D.; Coghi, P.; Basilico, B.; Monti, D., *Chem. Med. Chem*. **2008**, *3*, 873.
197. Pandey, V. K.; Tusi, S.; Tusi, Z.; Joshi, M.; Bajpai, S., *Acta. Pharm*. **2004**, *54*, 1.
198. Mayumi, O.; Kawahara, N.; Santo, Y., *Cancer Res*. **1996**, *56*, 1512.
199. Menicagli, R.; Samaritani, S.; Signore, G.; Vaglini, F.; Via, L. D., *J. Med. Chem*. **2004**, *47*, 4649.
200. Henke, B. R.; Consler, T. G.; Go, N.; Hohman, R.; Jones, S. A.; Lu, A. T.; Moore, L. B.; Moore, J. T.; Miller, L. A. O.; Robinett, R. G.; Shearin, J.; Spearing, P. K.; Stewart, L.; Turnball, P. S.; Wearver, S. L.; Willams, S. P.; Wisely, G. B.; Lambart, M. H., *J. Med. Chem*. **2002**, *45*, 5492.

201. Lecci, C.; Iuliano, A., *Biomed. Chromatogr.* **2005,** *19*, 439.
202. Deim, H.; Matthias, G.; Wagner, R. A., *Ullmann's Encyclopedia of Industrial Chemistry*. **2012**, Wiley-VCH, Weinheim.
203. Tsai, M. H.; Lin, H. W.; Su, H. C.; Ke, T. H.; Wu, C. C.; Fang, F. C.; Liao, Y. L.; Wong K. T.; Wu, C. I., *Adv. Mater*. **2006**, *18*, 1216.
204. Li, J. Y.; Liu, D.; Li, Y. Q.; Lee, C. S.; Kwong H. L.; Lee, S. T.; *Chem. Mater.* **2005**, *17*, 1208.
205. Nomata, I. H.; Goushi, K.; Masuko, T.; Konno, T.; Imai, T.; Sasabe, H.; Brown, J. J.; Adachi, C., *Chem. Mater*. **2004**, *16*, 1285.
206. Liu, X. K.; Zheng, C. J.; Xiao, J.; Liu, J. L.; Wang, S-D.; Zhaoe, W-M.; Zhang, X-H., *Phys. Chem. Chem. Phys*. **2012**, *14*, 14255.
207. De la Torre, G.; Vazquez, P.; Agullo-Lopez, F.; Torres, T., *J. Mater. Chem.* **1998,** *8*, 1671.
208. Senge, M. O.; Fazekas, M.; Notaras, E. G. A.; Blau, W. J.; Zawadzka, M.; Locos, O. B.; Mhuircheartaigh, E. M. N., *Adv. Mater.* **2007,** *19*, 2737.
209. Galateia, E. Z.; Mahesh, S. R.; Manas, K. P.; Panagiotis, A. A.; Emmanouel, C.; Ganesh, D. S.; Athanassios, G. C., *Inorg. Chem*. **2013**, *52*, 9813.
210. Liu, J.; Kai; Feng, X.; Zekun, T.; Wei, Z.; Jiyuan, Z.; Chenghui Li; Tao, Y.; Xiaozeng, Y., *Tetrahedron Lett.* **2011**, *52*, 6492.

Chapter 2

Synthesis, characterization, photovoltaic and nonlinear optical studies of a series of O-phenyl bridged diphenylamine-*s*-triazine based Donor-Acceptor triads with different π-Acceptor groups

Contents

Abstract

Novel Donor-Acceptor systems of starburst D-A-A type incorporating electron deficient triazine moiety as a non-conjugating π-spacer/acceptor with rhodanine-3-acetic acid (DTOP-RHA), barbituric acid (DTOP-BA) or thiobarbituric acid (DTOP-TBA) as anchoring/acceptor groups have been synthesized. diphenylamine is used as the donor moiety and the role of the anchoring group and the π-spacer are studied. These dyes are tested as sensitizers in the dye sensitized solar cells. The efficiencies obtained were low compared to the standard dye N719 under identical experimental conditions. This is attributed to less coverage of the absorption spectrum of the dyes in the visible

region of the solar spectrum as well as the large energy gap between the LUMO of the dyes and the TiO_2 conduction band. Z-scan measurements show that all compounds are NLO active with high nonlinear susceptibility and good two photon absorption properties. DTOP-BA possess the highest two photon absorption coefficient among the three compounds studied.

2.1. Introduction

In recent years dye sensitized solar cells (DSSCs) have engrossed much interest due to their potential advantages like cost effective, flexible and straight forward device fabrication.[1-7] DSSCs based on coordination complexes with heavy metal ions are considered as the most efficient devices, but cannot be used for large scale applications due to the limited resources and high cost.[8-11] The challenge is open to develop new systems using cost effective materials with promising photoconversion efficiencies. Use of organic D-π-A dyes is one such option which led to encouraging results. Most widely studied D-π-A systems include triphenylamine as the donor and cyanoacetic acid moiety as the acceptor.[12-15] Different π-spacers with planar geometry effectively improve the electron transportation from donor units to acceptor units and results in significant change in the overall photovoltaic performances[16-18]. Electron deficient heterocyclic structural units such as thiazole, triazine, cyano- and fluoro-substituted phenyl groups etc., have been used as the core in a starburst design to get triads of D-A-A systems. They exhibit several advantages over the straight D-π-A systems, with significant changes in the molecular

energy levels, absorption characteristics and finally the overall photovoltaic performance.[19-20] 1,3,5-triazine have been used as a building block for the synthesis of starburst D-A-A systems as dyes in DSSC.[21-22] In recent literature triphenylamine or porphyrins have also been used in a similar solar cell design with cyanoacetic acid as the acceptor unit as well as the anchoring group.[23] Here we report a series of dyes where diphenylamine as the donor unit and rhodanine-3-acetic acid, barbituric acid or thiobarbituric acid linked to 1,3,5-triazine core in a single donor two acceptor/anchoring group in a bipodal design.

In simple valence bond terms when there are two substituents on a benzene ring which are *meta* to each other the possibility of conjugation of π-orbitals of one with the other is not possible due to the absence of resonance form of the benzene ring supporting such conjugation with these substituents. This gives us the possibility of designing dyes having intra-molecular charge transfer states in which Donor and Acceptor moieties are separated in space and thus increase the length of the charge separation in comparison to directly coupled D-π-A systems. But such charge separation is useful only when the life time of such intra-molecular charge separated state is long enough to permit subsequent electron transfer cascade when they are used as dyes and light harvesting systems in photovoltaic or photoelectrochemical systems. The lifetime of the ICT excited state depends on the free energy of the back electron transfer regenerating the ground state.[24-25]

Keeping these ideas in mind we have designed dye molecules of starburst D-A-A type triads with 1,3,5-triazine as the first acceptor and as the core bridging π-unit. Donor moiety chosen was diphenylamine. Phenylydene derivatives of rhodanine-3-acetic acid, barbituric acid and thiobarbituric acid were chosen as the second acceptors bridged to triazine through an O-phenyl ether linkage with varying electron affinity and binding ability to TiO_2 surface. In the current chapter we report the synthesis, photo physical and photoelectrochemical properties of these three starburst D-A-A triads (Chart 2.1).

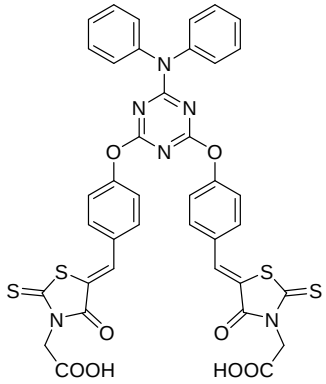

DTOP-RHA (1a)

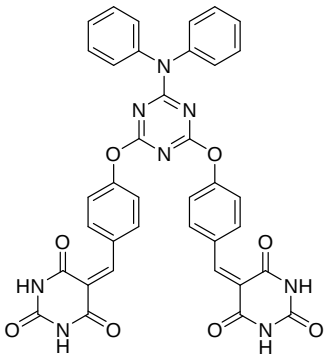

DTOP-BA (1b)

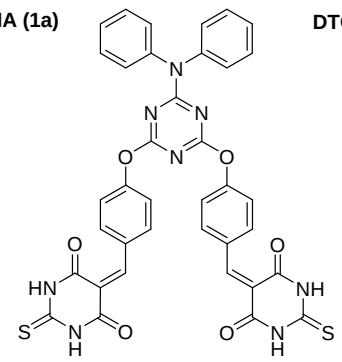

DTOP-TBA (1c)

Chart 2.1.

2.2. Results and discussion

2.2.1. Design and synthesis

We have made use of the ability of cyanuric chloride to undergo nucleophilic substitution reactions with amines and alcohols. All the chlorine atoms of cyanuric chloride can be substituted by primary amines or alcohols at room temperature or at slightly elevated temperatures. However, mono-substitution by nucleophiles requires low temperatures and in the present synthesis mono-substitution by diphenylamine was ensured by carrying out the reaction at -10 $^{\circ}$C using $NaHCO_3$ as the base. The remaining chlorine atoms were substituted successfully at room temperature by the *in situ* generated phenoxide anion of 4-hydroxybenzaldehyde with 10% NaOH in dichloromethane in the presence of a phase transfer catalyst tetrabutylammonium bromide (TBAB). The dialdehyde was made to react with two equivalents of rhodanine-3-acetic acid, barbituric acid or thiobarbituric acid to produce the corresponding starburst D-A-A type triads (Scheme 2.1). All these were soluble in DMF and DMSO. Moderate solubility was observed in methanol and in acetonitrile. DMF was used as the solvent for photophysical as well as electrochemical studies.

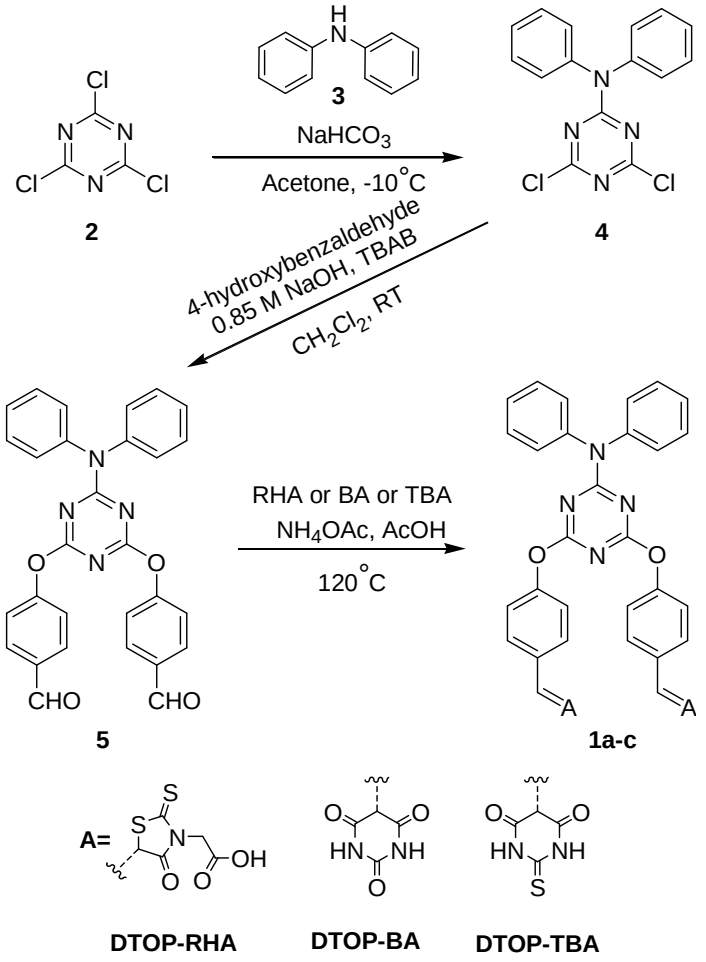

Scheme 2.1.

2.2.2. Photophysical studies

Absorption spectra of all dyes show characteristic charge transfer absorption bands around 370 nm, with onset of absorption extending to 450 nm. The diffuse reflectance spectra of all the compounds in the powder form however show broad absorption spectra peaking at 400 nm and the onset of absorption extending to

500 nm (Figure 2.1). This red shift could be due to the stacking arrangement that facilitate intramolecular charge transfer.[26]

The ability of these dyes in binding with TiO_2 thin films was probed by diffuse reflectance spectroscopy. TiO_2 thin films were made from a paste of TiO_2 by doctor blading followed by annealing at 450 $^{\circ}$C in air. These films were immersed in respective dye solutions (~2 x 10^{-2} M) in DMF for 24 h for coating the dyes. Dye coated thin films showed light yellow for the DTOP-RHA, dark yellow for DTOP-BA and light orange for DTOP-TBA. The diffuse reflectance spectra obtained for these dye coated films were presented in Figure 2.2. Upon binding the dye DTOP-RHA showed red shift of 10 nm in the absorption maximum and the spectrum was broadened compared to that obtained in DMF. In the case of DTOP-BA and DTOP-TBA the spectrum obtained showed new bands at 486 nm and 523 nm respectively. The singlet excited state energy ($E_{0\text{-}0}$) of these compounds was estimated from onset of the normalized absorption using the following equation (2.1). Photophysical properties of all the compounds are summarized in Table 2.1.

$$\text{HOMO} = \frac{1242}{\lambda_{\text{onset}}}\ \text{eV} \qquad (2.1)$$

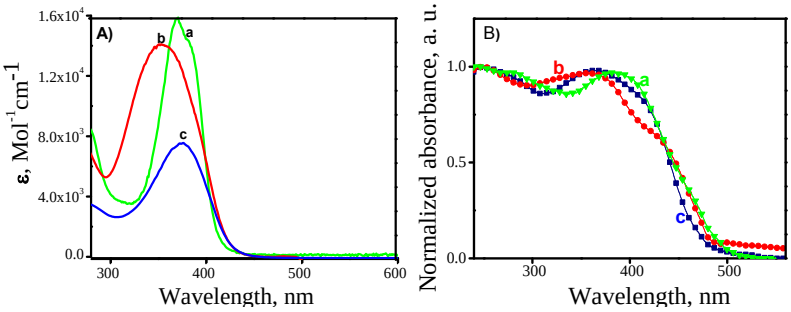

Figure 2.1. Normalized absorption spectra of DTOP-RHA (a) DTOP-BA (b) and DTOP-TBA (c) A) DMF solution B) powder form

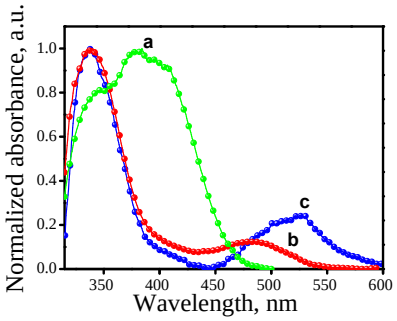

Figure 2.2. Diffuse reflectance spectrum of DTOP-RHA (a) DTOP-BA (b) and DTOP-TBA (c) adsorbed on TiO_2 thin films

Table 2.1. Photophysical properties of DTOP-RHA, DTOP-BA and DTOP-TBA

Dyes	λ_{max} (Abs), nm	ε_{max}, mol^{-1} cm^{-1}	λ_{onset}, nm	$E_{0\text{-}0}$, eV
DTOP-RHA	370 390*	1.6 x 10^4	412	3.04
DTOP-BA	357 375*	1.4 x 10^4	421	3.01
DTOP-TBA	375 380*	8.0 x 10^3	425	2.92

*for the powder form

2.2.3. Tautomerism in DTOP-BA

Interestingly, DTOP-BA showed sensitivity to the presence of water in the DMF solutions. Figure 2.3 is the spectrum of DTOP-BA obtained in ordinary DMF (blue trace) and dry DMF (black trace). The spectrum obtained in the dry DMF is characterised by a single absorption band at 350 nm. The spectrum obtained in ordinary DMF containing moisture has two bands one at 384 nm and a more red shifted band at 468 nm. Moreover, the ^{1}H NMR also showed 3 types of proton resonances for the amide protons of the barbituric acid moiety. This observation prompted us to explore this in detail. We recorded ^{1}H NMR spectrum in the presence of D_2O, which led to the disappearance of amide protons suggesting the presence of easily exchangeable protons from the amide or the enol forms of a mixture involving keto-imido tautomeric forms (Figure 2.4). The observation of the band at 468 nm in moist DMF may be due to a deprotonated form as showed in Scheme 2.2 involving tautomeric and zwitterionic forms. The spectrum recorded in the presence of triethylamine (TEA) show a single red shifted band with maximum at 468 nm (red trace in Figure 2.3). IUPAC commission on electroanalytical chemistry in their report discusses the nature of dry DMF and its properties in the presence of water.[27] In the presence of water DMF hydrolyses slowly generating formic acid and dimethylamine, which ionises and leads to a buffered solution containing formate anion and dimethylammonium cation with a basic character. Thus, the form of DTOP-BA responsible for the red shifted absorption maximum is the doubly deprotonated form.

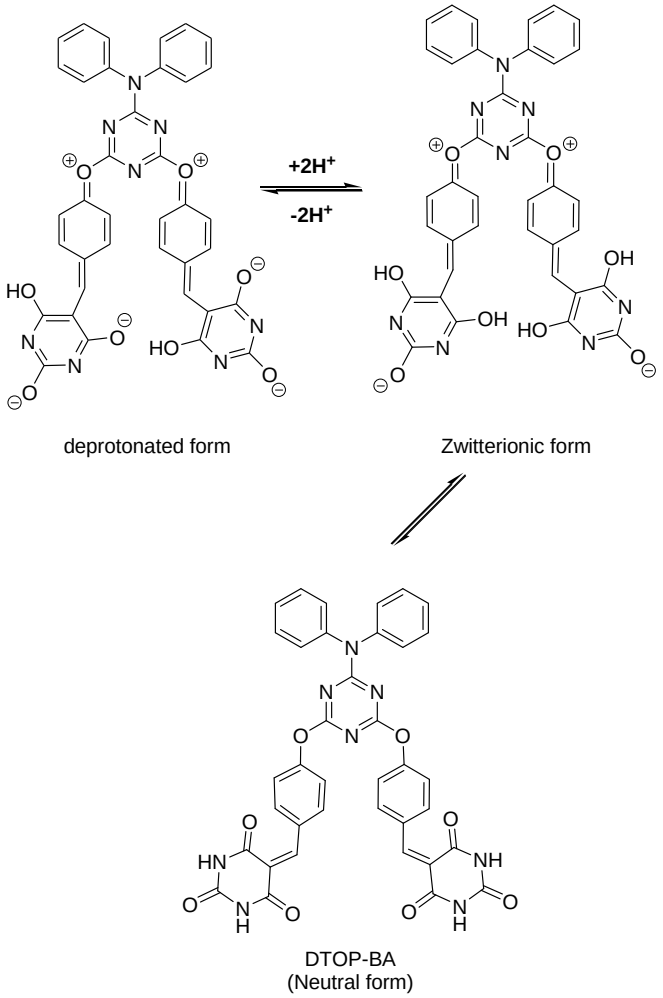
+2H+
-2H+
deprotonated form
Zwitterionic form
DTOP-BA
(Neutral form)

Scheme 2.2.

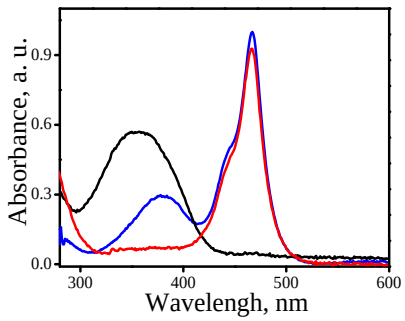

Figure 2.3. UV-Visible spectrum of DTOP-BA in dry DMF (black), in the presence of 10 µL of TEA (red) and in normal DMF (blue)

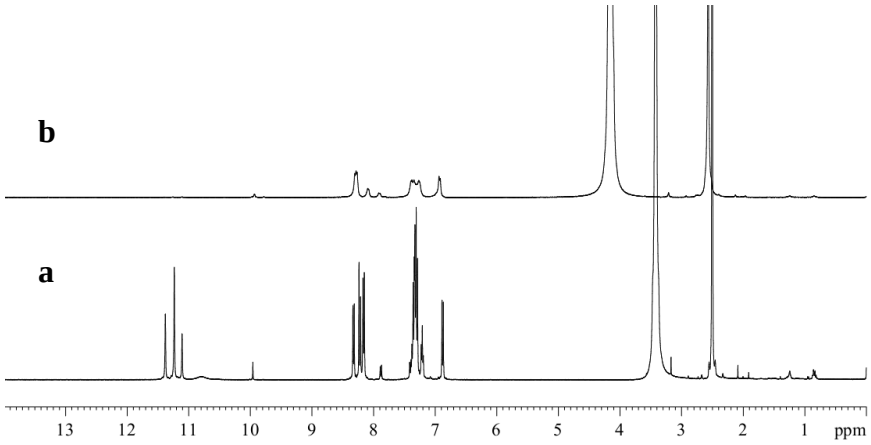

Figure 2.4. ^{1}H NMR spectrum of DTOP-BA in a) DMSO and b) D_2O

2.2.4. Electrochemical properties

The oxidation potentials of these dyes were determined from the square wave voltammograms. They exhibit characteristic oxidation potentials at 1.26 V DTOP-RHA and DTO-BA and 1.22 V respectively *vs.* NHE. The results are summarized in Table 2.2. These values are lower than the redox potential of redox couples I^-/I_3^- and Br^-/Br_3^- the common redox couples used in the construction of DSSCs. The energy gap between the redox couple and oxidation potential of the dye is significant in determining the current as well

as the fill factor in DSSC. For the dyes used in the present study the energy gap obtained is very large for I^-/I_3^- (0.53 V *vs.* NHE) is 0.73 V in comparison to Br^-/Br_3^- (1.09 V *vs.* NHE) which is 0.17 V which makes the regeneration of the oxidized dye thermodynamically favourable during the operation of the cell. The HOMO and the LUMO energies of these dyes referenced to NHE were calculated from the oxidation potentials of these dyes and their respective singlet energy. Estimations of HOMO and LUMO energies against vacuum continuum were also been made and all the values are presented in Table 2.2. The energy gap (E_{gap}) between the LUMO of the dye and the conduction band of the TiO_2 is also estimated .This value decides the exergonicity of electron injection from excited dye to the conduction band of the TiO_2. The obtained energy gap shows that, the electron injection is facile and energetically favourable.

Table 2.2. Electrochemical properties of dyes in DMF[28-31]

Compounds	E_{onset}/ V in DMF	E_{onset} (ox) *vs.* E_{FOC}/V	$E_{(S+/S)}$ *vs.* NHE/ V	LUMO *vs.* NHE/V	E_{gap}/ V
DTOP-RHA	1.17	1.06	1.26	-1.74	1.24
DTOP-BA	1.17	1.06	1.26	-1.74	1.24
DTOP-TBA	1.13	1.02	1.22	-1.68	1.18

E_{FOC} = –0.11 V *vs.* Ag/AgCl the ground-state oxidation potentials $E_{(S+/S)}$ (HOMO) were measured in DMF containing 0.1 M tetrabutylammonium hexafluorophosphate as supporting electrolyte using a glassy carbon working electrode, a Pt counter electrode and a Ag/AgCl reference electrode; E_{gap} is the energy gap between LUMO of the dye and the conduction band level of TiO_2 (−0.5 V *vs.* NHE); ionization potential: IP (eV) = -4.8-(E_{onset} (ox)-E_{FOC}); electron affinity: EA = IP + E_{0-0}

2.2.5. Theoretical study

The optimized geometry of the dyes as well as the frontier orbitals and their energies are computed by density functional theory (DFT) with B3LYP exchange-correlation functional [32- 33] and 6-31G+(d) basis set. The stationary points are characterized by frequency calculation. To include the effects of solvation the polarization continuum model (PCM) for DMF has been used in the calculations. All calculations were performed with the GAUSSIAN 09 quantum chemistry package. The optimized geometry along with the frontier orbital representation and their respective energies against vacuum continuum is given in Figure 2.6 along with the respective energy levels of the semiconductor TiO_2 and redox couple. Contrary to our expectation the orbital coefficients of the HOMO for all compounds were found to be delocalized over the triazine core which is one of the acceptor units in the D-A-A triad. This delocalization extends over the terminal rhodanine-3-acetic acid acceptor unit in the case of the dye DTOP-RHA. Delocalization of HOMO over the triazine has a profound effect in lowering of the HOMO energies as well as on the observed more positive oxidation potential. A similar dye without the triazine linker having cyanoacetic acid as the acceptor has a HOMO of 1.04 V *vs.* NHE which is high lying than that is observed for the HOMO of the dyes reported in the present chapter (~1.2 V *vs.* NHE).[34] Thus it is clear that the introduction of triazine has a profound effect in lowering the HOMO of these dyes. This lowering is beneficial to obtain higher V_{oc} values when DSSC were

constructed using redox electrolyte such as Br^-/Br_3^- whose redox level is 1.0 V. Both electrochemical and theoretical data suggest that they are difficult to oxidize in comparison to oxidation of diphenylamine. This also explains the higher excitation energy and thus lower coverage of the solar spectrum in the visible region. The dyes DTOP-BA and DTOP-TBA show better directionality of charge transfer as the HOMO and LUMO are localized on different regions of the molecule. This effect is evident in the more red shifted absorption spectrum obtained for these dyes. The theoretically calculated energy levels are also found to be matching with the experimental values obtained from electrochemical measurements (Table 2.3).

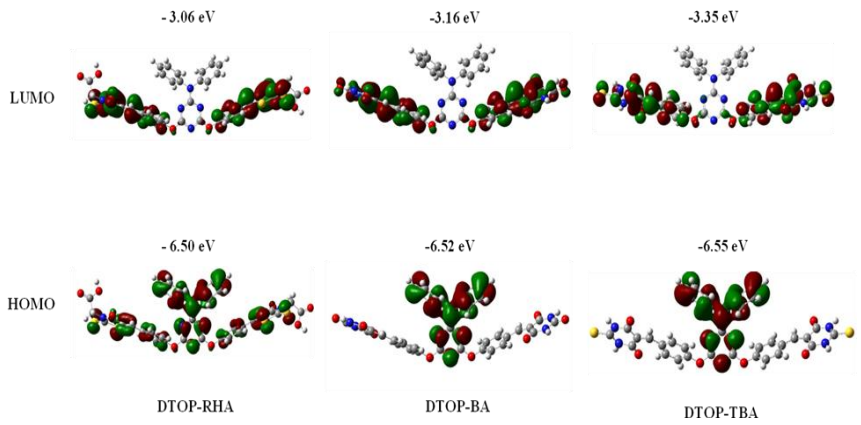

Figure 2.6. Optimized geometries of the dyes computed using DFT theory at the B3LYP/6-31G + (d) level

Table 2.3. Comparison of experimental and theoretical frontier orbital energies of DTOP-RHA, DTOP-BA and DTOP-TBA

Compounds	Experimental		Theoretical	
	HOMO, eV[a]	LUMO, eV[b]	HOMO, eV	LUMO, eV
DTOP-RHA	-6.64	-3.05	-6.50	-3.06
DTOP-BA	-6.63	-3.53	-6.52	-3.16
DTOP-TBA	-6.50	-3.64	-6.55	-3.35

[a]Ionization potential: IP = – 4.8 – (E_{onset} (ox)– E_{FOC}); [b]electron affinity: EA − $E_{0\text{-}0}$ = IP

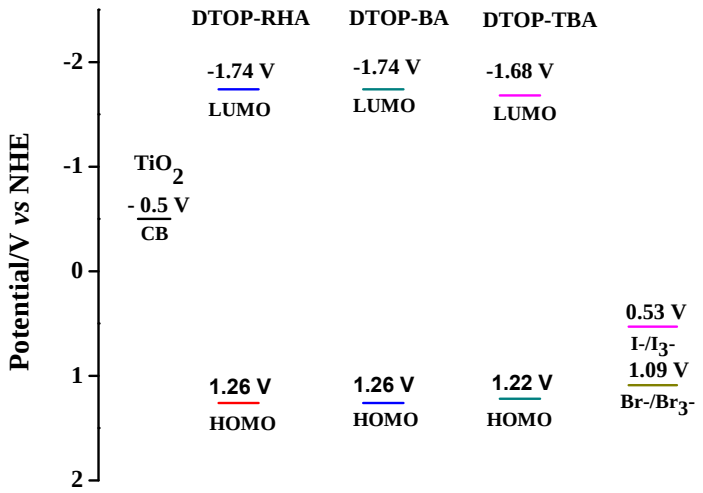

Figure 2.7. Schematic energy level diagram for compounds DTOP-RHA, DTOP-BA and DTOP-TBA along with the conduction band of TiO_2 and the respective redox levels of electrolytes

2.2.6. Photoelectrochemical properties

Under illumination by an AM 1.5 light source all the cells constructed gave Current *vs.* Voltage (I-V) characteristics typical for photodiodes. A few representative Current density *vs.* Voltage

(J-V) curves obtained for dyes DTOP-RHA, DTOP-BA and DTOP-TBA when Br^-/Br_3^- was used as the electrolyte are given in Figure 2.8. The solar cell parameters obtained from the photocurrent measurements were summarized in Table 2.4. The solar energy to electrical energy conversion efficiency (η) was calculated from open circuit voltage (V_{oc}), short circuit current (J_{sc}), fill factor (FF) and the incident photon flux (P_{in}) by using equation,

$$\eta(\%) = \frac{J_{SC} V_{OC} FF}{P_{in}} \qquad (2.2)$$

Under our experimental conditions an efficiency of 3 % was obtained for the N719 dye when I^-/I_3^- was used as the electrolyte. The results show that the observed conversion efficiency are lower and are in the range of 0.01-0.06 % where the cell made from the dye DTOP-TBA with Br^-/Br_3^- was found to be the most efficient in the series. The data obtained for the cells with I^-/I_3^- as the electrolyte were very low in comparison to the data obtained for Br^-/Br_3^- in terms of V_{oc} and η. This is due to the low potential difference between the Fermi level and the high lying redox potential of I^-/I_3^- in comparison to Br^-/Br_3^-. The poor efficiency data observed could be due to a combined effect of lower coverage of the solar spectrum by the dyes as well as lower binding coefficients. Relatively better performance of DTOP-TBA may be the result of the high lying HOMO making regeneration of the dye efficient in comparison to other dyes and very large energy gap between the dye and conduction band of TiO_2. Based on a similar

design strategy better performing dye sensitizers can be synthesized by incorporating better donor groups and groups that enhance conjugation at the acceptor site.

Table 2.4. DSSC Performance data obtained for DTOP-RHA, DTOP-BA and DTOP-TBA

Dyes	J_{sc}, mA cm^{-2}	V_{oc}, mV	FF, %	η, %
DTOP-RHA	-0.160[a*](±0.001)	0.273[a](±0.001)	45[a]	0.02[a]
	-0.078[b*](±0.006)	0.477[b](±0.007)	79[b]	0.03[b]
DTOP-BA	-0.094[a](±0.001)	0.210[a](±0.002)	50[a]	0.01[a]
	-0.124[b](±0.005)	0.580[b](±0.004)	62[b]	0.04[b]
DTOP-TBA	-0.129[a](±0.005)	0.182[a](±0.008)	42[a]	0.01[a]
	-0.215[b](±0.00)	0.475[b](±0.004)	58[b]	0.06[b]

a* I^-/I_3^- electrolyte. b* Br^-/Br_3^-elctrolyte

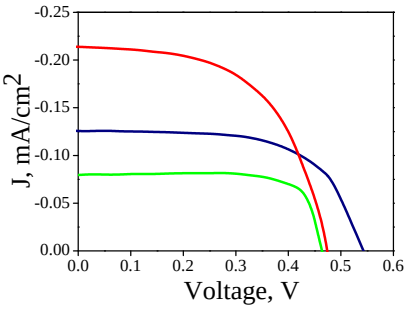

Figure 2.8. Photocurrent density–voltage curves obtained for the compounds DTOP-RHA (—), DTOP-BA (—) and DTOP-TBA (—) using Br^-/Br_3^- electrolyte

2.2.7. Nonlinear optical properties

Recent years has seen a spurt in the research directed to the development of new materials for photonic applications. Organic molecules generally show large third order nonlinear optical properties such as nonlinear refractive index and multiphoton absorption. All the compounds reported in this chapter show asymmetry in the electron density due to the basic donor-acceptor nature of the structure. This is further confirmed by the DFT calculations. Figure 2.9 show the HOMO and LUMO orbitals of these compounds. In DTOP-RHA the HOMO is delocalised over the entire molecule whereas in the other two the HOMO is centered on the diphenylamine and the triazine core. In all the compounds the LUMO is centred on the O-phenyl bridge and both the acceptor moieties. These molecules were surveyed for their Nonlinear optical behaviour by Z-scan technique using 532 nm second harmonic of an Nd-YAG laser with a pulse width of 7 ns. A DMF solution of ~1 mM concentration was used for the experiment.[31] No appreciable optical damages were observed after the Z-scan measurements. This is for the first time that a triazine based D-A systems without centre of symmetry has been studied for their nonlinear optical properties. All the triazine based donor-acceptor systems possess excellent nonlinear refractive property as well as two photon absorption coefficient and very high non linear absorption cross section.[36] Experimentally the nonlinear behaviour is manifested in the observation of reverse saturable absorption (RSA), two photon absorption (TPA) and saturable absorption (SA)

depending on the variation (increase or decrease) in transmission of the sample with the intensity of the laser. For a molecule, decreased transmittance or increase in the light absorption for a given laser light due to an enhanced light absorption property of the excited state in comparison to the ground state is the result of TPA and RSA with increasing laser intensity.[37] DTOP-RHA and DTOP-BA showed SA at lower fluences i.e., away from the focus and it switched over to RSA near the focus. Since the excitation wavelength 532 nm was at the edge of the ground state absorption of these molecules at lower fluences the molecules gets excited and may not have sufficient time to relax to the ground state leading to an increased transmittance. Such behaviour is common to many substances. At higher laser intensity i.e., closer to the focus, the excited state absorption becomes dominant and SA behaviour switches to RSA behaviour. DTOP-TBA however, showed RSA behaviour away from the focus and switched over to SA behaviour at the focus. This is due to the saturation of the excited state absorption which is responsible for the switching of RSA behaviour to SA behaviour. As evident from the solid lines in the Figures 2.9a-c, theoretical fit to the two photon absorption theory showed very good correlation. This shows that TPA is the main mechanism involved in the nonlinear absorption process for all these molecules. The nonlinear absorption coefficient (β) was determined by fitting the data obtained from the open aperture measurements to the equation (2.3). The results are tabulated in

Table 2.5. The β value obtained for DTOP-BA is high compared to that of the other two compounds.

$$T_Z = \frac{C}{q_0\sqrt{\pi}} \int_{-\infty}^{\infty} In(1 + q_0\, e^{-r^2})dt \qquad (2.3)$$

Where q_0 (z, r, t) = $bI_0(t)$ L_{eff} and L_{eff} = $(1+e^{-\alpha I})/\alpha$ is the effective thickness of linear absorption coefficient α, I_0 is the irradiance at focus.

The nonlinear refractive index and nonlinear susceptibility of NLO active materials at high laser fluences can be measured in the Z-scan technique. Here, the transmittance is measured by varying the laser spot size at the plane of a finite aperture detector combination and is called the closed aperture method. The NLO active material will act as a thin lens with varying focal length as it moves along the optical axis of the Z-scan set-up. The transmission data obtained in the open aperture Z-scan is sensitive to nonlinear absorption only and the closed aperture scan involves both nonlinear refraction and absorption effects. In order to exclude the nonlinear absorption effects, the closed aperture data obtained were divided by the corresponding open aperture data. Figure 2.10a to 2.10c show the normalized transmission data obtained for DTOP-RHA, DTOP-BA and DTOP-TBA, respectively in the closed aperture scan. The nonlinear transmittance T(z) is related to on-axis nonlinear phase shift ($\Delta\phi_0$) and the ratio z/z_0. This relation is given by equation (2.4).[38]

$$T(z) = 1 - \frac{4x\Delta\emptyset_0}{(x^2 + 9)(x^2 + 1)} \quad (2.4)$$

Typical peak valley pattern due to nonlinear refraction was observed for all the compounds and indicative of a negative nonlinear refractive (NLR) index due to self-defocusing (Figures 2.10a-2.10c). The data were fitted to equation (2.4) and the nonlinear phase shift ($\Delta\phi_0$) is determined. The nonlinear refractive index (n_2), the real (Re χ^3) and the imaginary part (Im χ^3) and thus the nonlinear susceptibility χ^3 were determined by using the following set of equations (2.5)– (2.10).

$$\chi^{(3)} = Re\,\chi^{(3)} + iIm\chi^{(3)} \quad (2.5)$$

$$Im\chi^{(3)} = n_0^2 c^2\, \beta / 240\omega\pi^2 \quad (2.6)$$

$$\Delta n_0 = \frac{\Delta\emptyset_0}{KL_{eff}} \quad (2.7)$$

$$\gamma = \frac{\Delta n_0}{I_o} \quad (2.8)$$

$$n_{2\,(esu)} = \frac{cn_0}{40\pi}\,\gamma \quad (2.9)$$

$$Re\,\chi^{(3)} = \frac{n_0 n_2}{3\pi}\ \text{(esu)} \quad (2.10)$$

Where γ, the molecular cubic hyperpolarizability of polymer and k is the wave vector. The calculated values of nonlinear absorption coefficient (β), the nonlinear refractive index

(n_2), the third order susceptibility (χ^3) and molecular cubic hyperpolarizability (γ) are listed in Table 2.5. Among the three donor-acceptor systems studied, DTOP-BA shows the highest NLO activity.

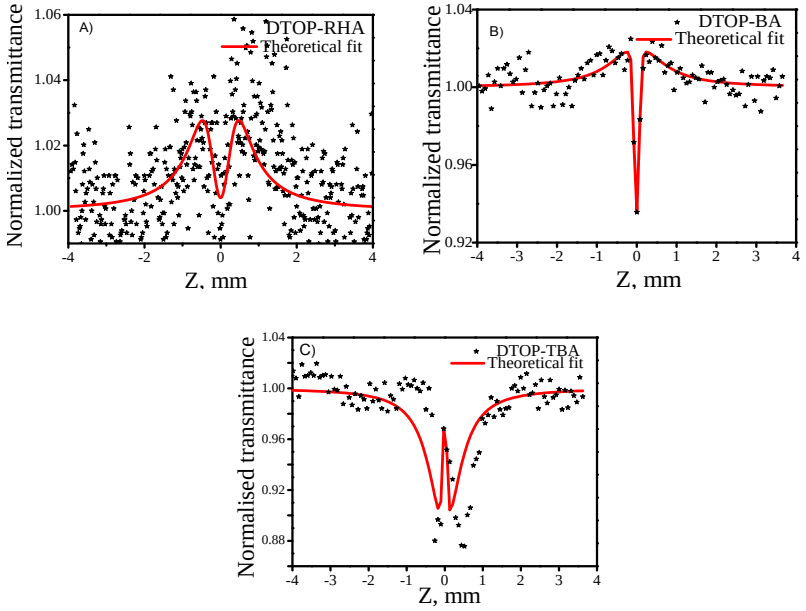

Figure 2.9. Open aperture Z-scan profile of DTOP-RHA (A), DTOP-BA (B) and DTOP-TBA (C) in DMF

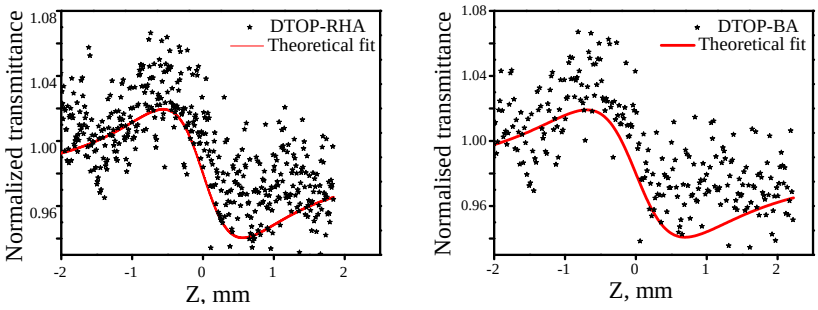

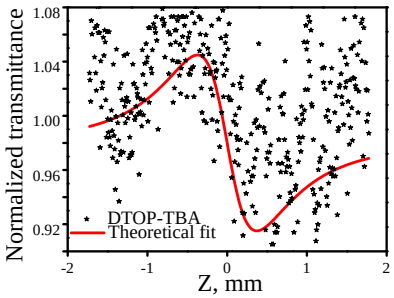

Figure 2.10. Closed aperture Z-scan profile of DTOP-RHA, DTOP-BA and DTOP-TBA in DMF

2.2.8. Optical limiting property

The decrease in the transmittance of a material with higher light intensities is termed as the optical limiting property.[35] Optical limiting property is due a combination of multi-photon absorption, excited state absorption, self-focussing, self-defocusing, etc., A major contributor to optical limiting is the nonlinear absorption. Among the three donor-acceptor systems studied, DTOP-BA showed the best optical limiting behaviour. Optical limiting behaviour was absent in DTOP-TBA due to the switching of RSA to SA at higher laser fluences.

Table 2.5. NLO properties of the compounds DTOP-RHA, DTOP-BA and DTOP-TBA

Compounds	Nonlinear absorption coefficient (β, mW^{-1})	Nonlinear refractive index (n_2, esu)	Imaginary part of nonlinear susceptibility (Im $\chi^{(3)}$, esu)	Real part of nonlinear susceptibility (Re $\chi^{(3)}$, esu)	Nonlinear susceptibility ($\chi^{(3)}$, esu)	σ_2 (GM)
DTOP-RHA	-0.12×10^{-9}	-2.5×10^{-11}	0.27×10^{-11}	-3.77×10^{-12}	0.37×10^{-11}	7762
DTOP-BA	-2.5×10^{-9}	-2.5×10^{-11}	5.4×10^{-11}	-3.77×10^{-12}	0.66×10^{-11}	157029
DTOP-TBA	0.04×10^{-9}	-4.3×10^{-11}	0.23×10^{-11}	-6.48×10^{-12}	0.65×10^{-11}	5745

2.3. Conclusion

We have designed and synthesized three novel starburst D-A-A systems with triazine core as the non-conjugating spacer/acceptor with rhodanine-3-acetic acid (DTOP-RHA), barbituric acid (DTOP-BA) or thiobarbituric acid (DTOP-TBA) as anchoring/acceptor groups. Electrochemical, photophysical and theoretical studies show that they have properties suitable for use as dyes in dye sensitized solar cells. The applicability of these dyes for the DSSC was tested by constructing the sandwich model cell. However, the observed efficiency was lower than that obtained for N719 dye under similar experimental conditions. This is attributed to the low coverage of the solar spectrum, inability of the dyes to binding with TiO_2 and large energy gap between the LUMO of the

dyes and the conduction band of the TiO_2. The results suggest tuning of the LUMO energy by incorporating additional conjugating groups in the acceptor side of the design. The preceding chapter addresses this issue with design, synthesis and study of appropriate dye. All compounds are NLO active with nonlinear refractive index of $\sim 10^{11}$ esu. Among the three compounds studied DTOP-BA showed the highest nonlinear absorption coefficient value.

2.4. Experimental

2.4.1. Electrochemical measurements

The electrochemical properties of the dyes were investigated by cyclic voltammetric (CV) and square wave voltametry on a BAS 50W electrochemical workstation using a three-electrode configuration. A glassy carbon electrode was used as the working electrode, platinum wire was used as the counter electrode, and Ag/AgCl was used as the reference electrode. A 0.1 M DMF solution of *n*-Bu_4NPF_6 was used as the electrolyte. The sample solutions were saturated with argon prior to measurements. Ferrocene was used as the reference to standardize the measurements and the corrected values are reported against standard hydrogen electrode (SHE).

2.4.2. DSSC fabrication and characterization

The photoelectrochemical properties of these dyes were studied by constructing photoelectrochemical cells using dye

adsorbed TiO_2 as the photoanode, Pt coated Fluorine doped ITO as the cathode. The electrolyte used was either I^-/I_3^- containing LiI (0.4 M) and I_2 (0.04 M) in anhydrous CH_3CN or Br^-/Br_3^- containing LiBr (0.4 M) and Br_2 (0.04 M) in anhydrous CH_3CN. The preparation of the photoelectrodes and the fabrication of the DSSCs were carried out based on methods reported earlier. The rectangular shaped thin film TiO_2 photoanode was made by doctor blade technique using a TiO_2 paste (Ti-Nanoxide, Solaronix SA, Aubonne, Switzerland) followed by annealing in a muffle furnace for 30 min at 450 $^{\circ}C$. The TiO_2 thin films were exposed to dye solution for 24 h and washed successively with DMF, water and ethanol. Prior to cell assembly, the dye coated thin films were dried under vacuum in vacuum desiccators at room temperature. Pt coated FTO having drilled holes (1 mm) for injecting appropriate electrolyte was used as the cathode. The dye coated electrode and the Pt counter electrode were assembled in a sealed sandwich model cell using meltonix as the binder/spacer. The active area of the cell was 0.16 cm^2 and the remaining area was masked with a black tape prior to cell characterization. Dark and illuminated I-V characteristics of the cell were measured using a Keithley (2420C) Source Measure Unit. The cell was illuminated using a Photoemission tech AM 1.5 solar simulator.

2.4.3. Measurement of nonlinear optical properties by Z-scan technique

NLO properties were measured by the single beam Z-scan technique using a Q-switched Nd:YAG laser system (Spectra

Physics LAB-1760) with a pulse width of 7 ns at 10 Hz repetition rate and 532 nm wavelength. Scheme 2.3 show an illustration of the experimental setup used.

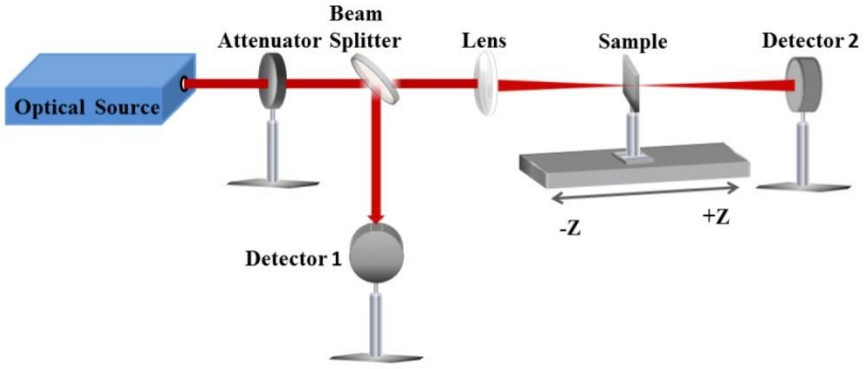

Scheme 2.3.

A lens of focal length 200 mm was used to focus the laser beam. The sample was kept in the optical axis of the lens on a motorised sample stage. During measurements, the sample moved along the optical axis keeping focal point as the origin. The radius of the beam used is measured as 42.56 μm. The Rayleigh length $Z_0 = \pi\omega_0^2/\lambda$, was calculated to be 10.69 mm, which was greater than the thickness of the sample cuvette (1 mm), an essential requirement for Z-scan experiments. The Z-scan setup was standardised using CS_2 as the reference. The intensity ratio of the transmitted and the reference beam were measured in the form of energy by Joule meter (REJ 7620, Laser Probe Corp.) having two identical pyroelectric heads (RJP 735). The effect of fluctuations of laser beam is eliminated by the measurement of ratio of energies at the transmitted and reference detector. The data obtained were analyzed by the procedure described by Bahae *et al.*[39] In this

method the nonlinear coefficients were obtained by fitting routine of the experimental Z-scan plot with a simulated plot obtained based on the theory. The experiments were repeated at least thrice prior to analysis for obtaining the nonlinear optical coefficients from the best fits. Two modes of experiments can be performed. One in which an aperture is placed before the detector that receives the transmitted light to prevent a part of light and only allows the core part of the beam. This method, known as closed aperture method where the data obtained is used for determining the nonlinear refractive index of the nonlinear optical material. In the open aperture method, no apertures are used and the entire transmitted light beam is received by the detector. The data obtained is used for determining the nonlinear absorption coefficient of the multiphoton absorbing nonlinear optical material.

2.4.4. Synthesis and characterization

2.4.4.1. Synthesis of 4,6-dichloro-N,N-diphenyl-1,3,5-triazine-2-amine (3)

A solution of cyanuric chloride (**2**, 100 mmol) in acetone (10 mL) was added slowly to an aqueous solution of $NaHCO_3$ (100 mmol) at -10 $^{\circ}$C followed by diphenylamine (**3**, 100 mmol) in acetone (10 mL) and stirred for 2 h. The white precipitate obtained was filtered and washed with cold water to remove unreacted cyanuric chloride and dried in vacuum. Column chromatography of the dried precipitate over silica gel using hexane and ethyl acetate (4:1) and drying under vacuum gave colorless crystals of **4** in 63% yield. mp 145 ^{0}C. FT-IR (cm^{-1}): 3049, 1489, 1333, 1240. ^{1}H NMR

(400 MHz, $CDCl_3$ δ ppm): 7.42-7.38 (m, 2H), 7.33-7.28 (m, 1H), 7.27-7.24 (m, 2H); ^{13}C NMR (100 MHz, $CDCl_3$, δ ppm): 170, 165, 141, 129, 127, 124. ESI (m/z): 316.2 (M-1) Anal. Calcd. for $C_{15}H_{10}Cl_2N_4$ (MW = 316. 17) C, 56.80; H, 3.18; Cl, 22.36; N, 17. 66. Found C, 56.70; H, 3.10; N, 17.60.

2.4.4.2. Synthesis of 4,4'-(6-(diphenylamino)-1,3,5-triazine-2,4-diyl)bis(oxy)dibenzaldehyde (5)

A solution of 4-hydroxybenzaldehyde (20 mmol) in 10 mL of dichloromethane was treated with aqueous NaOH (50 mL, 0.85 M) at room temperature followed by a solution of compound **4** (100 mmol) in dichloromethane (50 mL) and tetrabutylammonium bromide (TBAB) (20 mol %) was added slowly during 30 minutes. The mixture was stirred for 24 h and the organic layer was separated and washed well with 10% NaOH, followed by distilled water. The resulting solution was dried with anhydrous Na_2SO_4 and the solvent was removed under vacuum and recrystallization from ethyl acetate to yield **5** as a colorless solid (Yield 63%). mp. 169 $^{\circ}C$. FT-IR (cm^{-1}): 1697, 1582, 1375, 1261. ^1H NMR (400 MHz, $CDCl_3$, δ ppm): 9.95(s, 1H), 7.80-7.77 (d, 2H), 7.28-7.24 (m, 4H), 7.19-7.16 (m, 3H) .^{13}C NMR (100 MHz, $CDCl_3$, δ ppm): 190, 171, 167, 156, 142, 133, 130,129, 127, 126. ESI (m/z): 487.17 (M-1), Anal. Calcd. for $C_{29}H_{20}N_4O_4$ (MW= 488.49); C, 71.30; H, 4.13; N, 11.47, Found: C, 71.20; H, 4.10; N, 11.37.

2.4.4.3. General procedure for DTOP-RHA (1a), DTOP-BA (1b) and DTOP-TBA (1c)

A mixture of aldehyde **5** (1 mmol) and of rhodanine-3-acetic acid/ barbituric acid/thiobarbituric acid (22 mmol) and ammonium acetate (19 mmol) were dissolved in 0.5 M glacial acetic acid heated 120 $^{\circ}$C for 12 h. After cooling, the precipitated target product was washed with chloroform and methanol to remove the unreacted reagents and starting materials.

DTOP-RHA (1a); Yellow powder. Yield 58%. mp. 250 $^{\circ}$C (decomp.), FT-IR (cm^{-1}): 3330, 1707, 1598, 1501, 1323, 1289. ^{1}H NMR (400 MHz, DMSO, δ ppm): 7.81 (s, 1H) 7.62-7.60 (d, 2H), 7.38-7.31 (m, 6H), 7.22 (m, 2H), 4.58 (s, 2H). ^{13}C NMR (100 MHz, DMSO, δ ppm): 185, 171, 131, 128, 127, 122. Anal. Calcd for $C_{39}H_{26}N_6O_8S_4$ (MW= 834.92). C, 56.10; H, 3.14; N, 10.07; S, 15.36, Found: C, 56.05; H, 3.10; N, 9.97; S, 15.30.

DTOP-BA (1b); Yellow powder. Yield 68%, mp. 245 $^{\circ}$C (decomp.) FT-IR (cm^{-1}): 3325, 1603, 1390, 1115. ^{1}H NMR (400 MHz, DMSO, δ ppm): 11.23 (s, 1H), 11.10 (s, 1H), 10.79 (s, 1H), 8.30-8.21 (m, 4H), 7.31-6.88 (m, 5H). ^{13}C NMR (100 MHz, DMSO, δ ppm): 163.0, 153.1, 150.1, 136.5, 132.6, 129.1, 127.7, 127.4. Anal. Calcd. for $C_{37}H_{24}N_8O_8$ (MW =740.77). C, 62.71; H, 3.41; N, 15.81; Found C, 62.65; H, 3.31; N, 15.75.

DTOP-TBA (1c); Yellow powder. Yield 66%. mp. 225 $^{\circ}$C (decomp.) FT-IR (cm^{-1}): 3460, 1655, 1546, 1364, 1209, 1152. ^{1}H NMR (400 MHz, DMSO, δ ppm): 12.36 (s, 1H), 12.25 (s, 1H),

8.16 (s, 1H), 8.13-8.11 (d, 2H) 7.29-7.22 (m, 6H), 7.14-7.10 (m, 1H). ^{13}C NMR (100 MHz, DMSO, δ ppm): 178, 170, 159, 154, 142, 135, 130, 128, 127, 122, 121, 118. Anal. Calcd. for $C_{37}H_{24}N_8O_6S_2$ (MW =708.64) C, 59.99; H, 3.27; N, 15.13; S, 8.66, Found: C, 59.89; H, 3.20; N, 15.05; S, 8.60.

2.5. References

1. Hagfeldt, A.; Grätzel, M., *Chem. Rev.* **1995**, *95*, 49.
2. Do, K.; Choi, H.; Lim, K.; Jo, H.; Cho, J. W.; Nazeeruddin, M. K.; Ko, J., *Chem. Commun*. **2014**, *50*, 10971.
3. Liu, J.; Wang, K.; Zhang, X.; Li, C.; You, X., *Tetrahedron* **2013**, *69*, 190.
4. Ning, Z.; Tian, H., *Chem. Commun*. **2009**, 5483.
5. Ooyama, Y.; Harima, Y., *Eu. J. Org. Chem.* **2009**, 2903.
6. Sharma, G. D.; Angaridis, P. A.; Pipou, S.; Zervaki, G. E.; Nikolaou, V.; Misra, R.; Coutsolelos, A. G., *Org. Electron.* **2015**, *25*, 295.
7. Zervaki, G. E.; Roy, M. S.; Panda, M. K.; Angaridis, P. A.; Chrissos, E.; Sharma, G. D.; Coutsolelos, A. G., *Inorg. Chem.* **2013**, *52*, 9813.
8. Bella, F.; Gerbaldi, C.; Barolo, C.; Grätzel, M., *Chem. Soc. Rev.* **2015**, *44*, 3431.
9. Grätzel, M., *Nature* **2001**, *414*, 338.
10. Nazeeruddin, M. K.; Pechy, P.; Renouard, T.; Zakeeruddin, S. M.; Humphry-Baker, R.; Comte, P.; Liska, P.; Cevey, L.; Costa, E.; Shklover, V.; Spiccia, L.; Deacon, G. B.; Bignozzi, C. A.; Grätzel, M., *J. Am. Chem. Soc.* **2001**, *123*, 1613.
11. Nazeeruddin, M. K.; Zakeeruddin, S. M.; Humphry-Baker, R.; Jirousek, M.; Liska, P.; Vlachopoulos, N.; Shklover, V.; Fischer, C. H.; Grätzel, M., *Inorg. Chem.* **1999**, *38*, 6298.
12. Hwang, S.; Lee, J. H.; Park, C.; Lee, H.; Kim, C.; Park, C.; Lee, M.-H.; Lee, W.; Park, J.; Kim, K.; Park, N. G.; Kim, C.,

Chem. Commun. **2007**, 4887.
13. Xu, M.; Li, R.; Pootrakulchote, N.; Shi, D.; Guo, J.; Yi, Z.; Zakeeruddin, S. M.; Graetzel, M.; Wang, P., *J. Phys. Chem. C*. **2008**, *112*, 19770.
14. Sayama, K.; Hara, K.; Mori, N.; Satsuki, M.; Suga, S.; Tsukagoshi, S.; Abe, Y.; Sugihara, H.; Arakawa, H., *Chem. Commun*. **2000**, 1173.
15. Hara, K.; Sayama, K.; Ohga, Y.; Shinpo, A.; Suga, S.; Arakawa, H., *Chem. Commun*. **2001**, 569.
16. Horiuchi, T.; Miura, H.; Sumioka, K.; Uchida, S., *J. Am. Chem. Soc*. **2004**, *126*, 12218.
17. Wang, Z.-S.; Koumura, N.; Cui, Y.; Takahashi, M.; Sekiguchi, H.; Mori, A.; Kubo, T.; Furube, A.; Hara, K., *Chem. Mater*. **2008**, *20*, 3993.
18. Song, J.-L.; Amaladass, P.; Wen, S.-H.; Pasunooti, K. K.; Li, A.; Yu, Y.-L.; Wang, X.; Deng, W.-Q.; Liu, X. W., *New J. Chem*. **2011**, *35*, 127.
19. Wu, Y.; Zhu, W., *Chem. Soc. Rev*. **2013**, *42*, 2039.
20. Zhong, H.; Xu, E.; Zeng, D.; Du, J.; Sun, J.; Ren, S.; Jiang, B.; Fang, Q., *Org. Lett*. **2008**, *10*, 709.
21. Liang, M.; Xu, W.; Cai, F.; Chen, P.; Peng, B.; Chen, J.; Li, Z., *J. Phys. Chem. C*. **2007,** *111*, 4465.
22. Liu, J.; Wang, K.; Zhang, X.; Li, C.; You, X., *Tetrahedron* **2013,** *69*, 190.
23. Sharma, G. D.; Angaridis, P. A.; Pipou, S.; Zervaki, G. E.; Nikolaou, V.; Misra, R.; Coutsolelos, A. G., *Org. Electron*. **2015,** *25*, 295.
24. Suneesh, C. V.; Vinayak, M. V.; Gopidas, K. R., *J. Phys. Chem. C*. **2010**, *114*, 18736.
25. Suneesh, C. V.; Gopidas, K. R., *J. Phys. Chem. C*. **2010**, *114*, 18725.
26. Zhong, H.; Lai, H.; Fang, Q., *J. Phys. Chem. C*. **2011**, *115*, 2423.
27. Juillard, J., *Pure & Appl. Chem*. **1977**, *49*, 885.
28. Neil, G.; William, E. G., *Chem. Rev*. **1996**, *96*, 877.

29. Wang, Z. S.; Sayama, K.; Sugihara, H., *J. Phys. Chem. B.* **2005**, *109*, 22449.
30. Xie, Q. J.; Kuwabata, S.; Yoneyama, H., *J. Electroanal. Chem.* **1997**, *420*, 219.
31. Fermin, D. J.; Teuel, H.; Scharaifker, B. R., *J. Electroanal. Chem*. **1996**, *401*, 207.
32. Xu, W.; Peng, B.; Chen, J.; Liang, M.; Cai, F., *J. Phys. Chem. C*. **2008**, *112*, 874.
33. Lee, C.; Yang, W.; Parr, R. G., *Phys. Rev. B*. **1988**, *37*, 785.
34. Becke, A. D., *J. Chem. Phys*. **1993**, *98*, 5648.
35. Yaoting, F. *J. Mol. Struct*. **2004**, *693*, 217.
36. Wang, J.; Gu, B.; Wang, H. T.; X.W.Ni., *Opt. Commun.* **2010,** *283*, 3525.
37. Sona, N.; Sreejesh, P. R.; Aby C. P.; Sebastian M., Sreekumar, K.; Sudha, K.; Rani, J., *New J. Chem*. **2015**, *39*, 2795.
38. Prem Kiran, P.; Naga Srinivas, N.K.M., Raghunath Reddy, D.; Maiya, B. G. Dharmadhikari, A. Sandhu, A. S. Ravindra Kumar, G; Narayana Rao, D., *Opt. Commun.* **2002**, *202*, 347.
39. Bahae, M. S.; Said, A. A.; Van Stryland, E. W., *Opt. Lett*. **1989**, *14*, 955.

Chapter 3

Synthesis, characterization and studies on the photovoltaic and nonlinear optical properties of a series of phenyl bridged diphenylamine-*s*-triazine based Donor-Acceptor triads with different π -Acceptor groups

Contents

Abstract

Novel Donor-Acceptor triads of starburst D-A-A type incorporating electron deficient triazine moiety as a non-conjugating π-spacer/acceptor with two acceptor/anchoring arms comprising of cyanoacetic acid (DTP-CYA), rhodanine-3-acetic acid (DTP-RHA), barbituric acid (DTP-BA) or thiobarbituric acid (DTP-TBA) linked to triazine core via a phenyl bridge have been synthesized. Diphenylamine is used as the donor moiety and the role of the π-spacer on the absorption spectra and other electronic properties were studied. These compounds are tested as sensitizers in the compound sensitized solar cells. The efficiencies obtained

showed improvement compared to the compounds reported in the previous chapter under identical experimental conditions. The low efficiency obtained in comparison to standard dye N719 is attributed to the poor absorption coverage of the solar spectrum and to the larger energy gap between the LUMO of the dyes and the TiO_2 conduction band. All the compounds were tested for their nonlinear optical properties and determined the nonlinear absorption coefficient (β) and nonlinear refractive index (n_2) in DMF solutions.

3.1. Introduction

Compounds in the DTOP series reported in the previous chapter feature an O-phenyl flexibile linkage of the acceptor/anchoring group on to the diphenylamine-triazine conjugate. This flexibility may lead to a less rigid geometry for the molecule where, the small average donor-acceptor distance of separation may lead to increased through space interaction between the donor and the acceptor moieties. The theoreticaly calculated optimal geometry for these compounds reveal a smaller distance of separation in these series of compounds. The less rigid structure makes increased non-radiative deactivation of the excited state thus reducing the excited state lifetime and reduced probability of electron transfer between the semiconductor and the dye. The relative orientation and disposition of HOMO and LUMO orbitals also play significant role in the rate of charge separation as well as

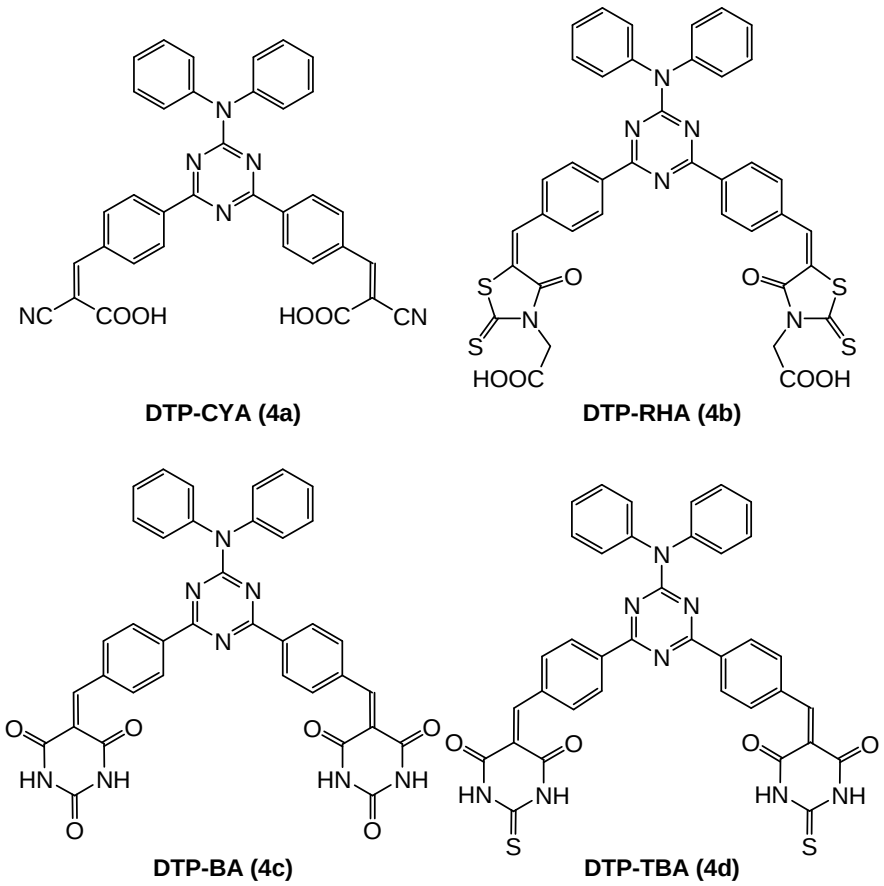

Chart 3.1.

the rate of back electron transfer within the D-A-A triad under study.[1] This orientation dependence on electron transfer has been studied in detail by R. A. Marcus and coworkers.[2-6] Nature adopts proper orientation as a means to effectively reduce the importance of back electron transfer in natural photosynthetic systems.[7-9] Similar results have been reported for synthetic systems where

carefully designed sytems with reduced back electron transfer has been reported by Chang.[10-13]

In order to bring better control on the orientation of Donor and Acceptor groups, a series of new moleucles are designed where the bridging O-phenyl group was replaced by a phenyl group via direct coupling of phenyl and triazine units. Chart 3.1 lists the moleucles which are designed, synthesised and studied in this chapter. The present design is expected to improve through bond coupling between the donor and the terminal acceptor parts of the molecules resulting into a low energy intramolecular charge transfer absorption with high molar extinction coefficient.

3.2. Results and discussion

3.2.1. Synthesis and characterization of Donor-π-Acceptor systems

Synthesis of the diphenylamine substituted triazine derivative **1** was carried out using previously reported procedure. The dialdehyde **3** was synthesized by a modified Suzuki coupling strategy for arylation of aromatic compounds. The dialdehyde (**3**) was subjected to knoevenagel condensation with cyanoacetic acid, rhodanine-3-acetic acid, barbituric acid or thiobarbituric acid respectively, in the presence of ammonium acetate in glacial acetic acid at 120 $^{\circ}$C (Scheme 3.1). The product DTP-CYA, DTP-RHA, DTP-BA and DTP-TBA (**4a-d**) were obtained in 50-60% yield. All

the compounds were characterized by using ^{1}H NMR, ^{13}C NMR and FT-IR spectroscopy and elemental analysis.

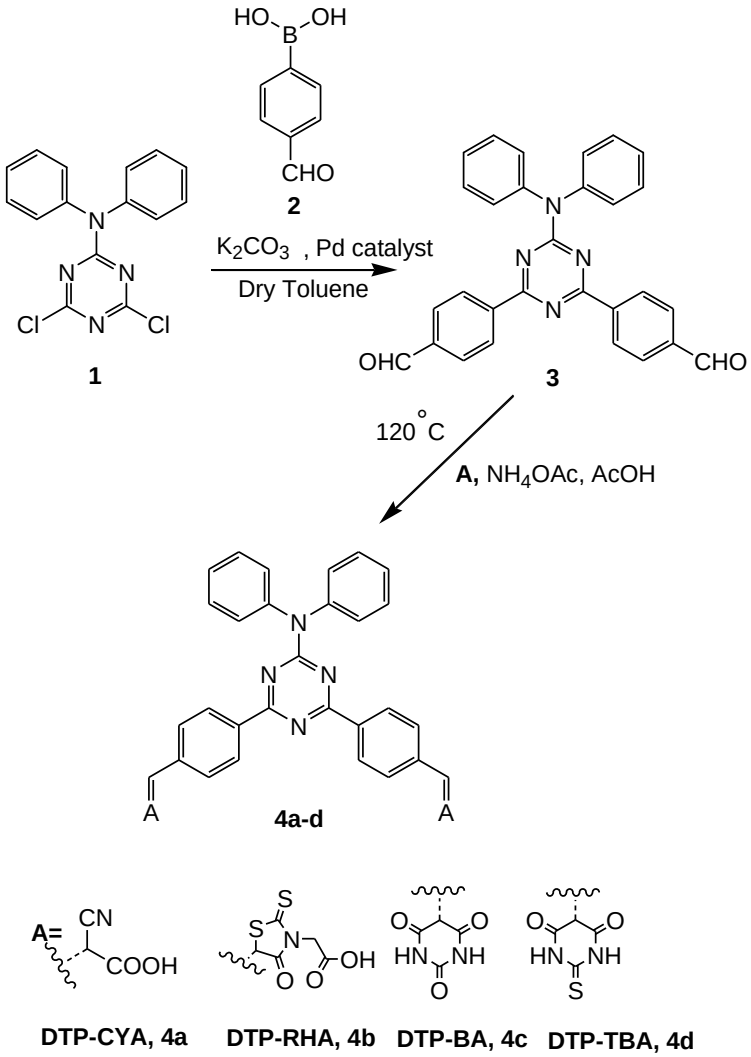

Scheme 3.1.

3.2.2. Photophysical properties

All compounds show very poor solubility in methanol, chloroform and acetonitrile and good solubility in DMF and DMSO. Absorption spectra of DTP-CYA, DTP-RHA, DTP-BA

and DTP-TBA were recorded in DMF and show characteristic intramolecular charge transfer (ICT) absorption band at 322 nm, 388 nm, 345 nm and 380 nm, respectively. The onset of absorption for these compounds extends upto 450 nm except for DTP-CYA which ends at 400 nm (Figure 3.1). The diffuse reflectance spectra of all the compounds in the powder form showed broad absorption maximum peaking at 400 nm and the onset of absorption extending to 500 nm for DTP-CYA, 600 nm for DTP-RHA and DTP-BA. In the case of DTP-TBA, this absorption extends upto 650 nm (Figure 3.2). This red shift could be due to the stacking arrangement that facilitate intramolecular charge transfer.[14] Nano-crystalline TiO_2 thin films were made from a paste of TiO_2, purchased from Solaronix SA, by doctor blading and annealing at 500 $^{\circ}$C for 30 minutes in a muffle furnace. The dye coated TiO_2 thin films were prepared by immersing these thin films in respective dye solutions in DMF for 24 h followed by washing successively with fresh DMF, water and ethanol. The air dried dye coated thin films showed light yellow to light orange color and diffuse reflectance spectra obtained were presented in Figure 3.3. DTP-RHA showed a red shifted and broad absorption spectrum and DTP-BA and DTP-TBA showed an additional weak band at 415 nm and 520 nm, respectively. The singlet excited state energy ($E_{0\text{-}0}$) of these compounds was calculated from onset absorption using the following equation (3.1).[15]

$$\text{HOMO} = \frac{1242}{\lambda_{\text{onset}}} \qquad (3.1)$$

The absorption spectral properties of all the compounds were summarized in Table 3.1. In comparison to the O-phenyl bridged compounds described in the previous chapter, DTP-RHA showed a red shift of 26 nm and DTP-TBA showed a red shift of 5 nm. This shows that direct coupling of phenyl bridge between the triazine and acceptor moieties led enhanced electronic coupling between the donor and acceptor groups. Whereas, DTP-BA showed a blue shift of 9 nm in comparison to O-phenyl bridged dye (vide supra).

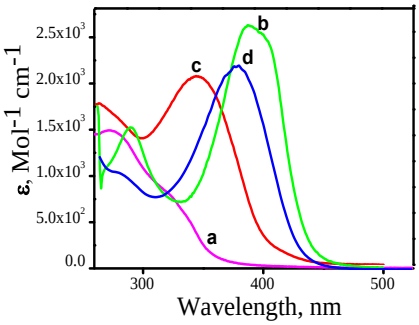

Figure 3.1. Absorption spectra of DTP-CYA (a) DTP-RHA (b) DTP-BA (c) and DTP-TBA (d) in DMF

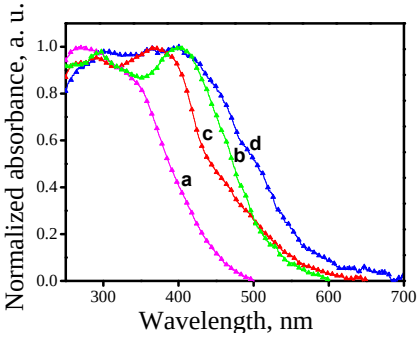

Figure 3.2. Diffuse reflectance spectra of DTP-CYA (a) DTP-RHA (b) DTP-BA (c) and DTP-TBA (d) in Powder form

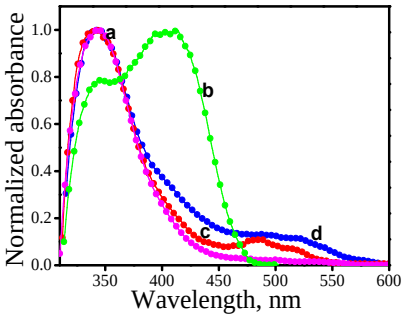

Figure 3.3. Diffuse reflectance spectra of DTP-CYA (a) DTP-RHA (b) DTP-BA (c) and DTP-TBA (d) adsorbed on TiO_2 thin film

Table 3.1. Photophysical properties of DTP-CYA, DTP-RHA, DTP-BA and DTP-TBA in DMF

Compound	**$\lambda_{max\ (Abs),}$ nm**	**$\lambda_{onset,}$ nm**	**$\varepsilon_{max\ ,}$ $mol^{-1}cm^{-1}$**	**$E_{0\text{-}0,}$ eV**
DTP-CYA	276, 322 (sh)	372	2.8×10^4 1.5×10^4	3.45
DTP-RHA	388	465	1.6×10^4	2.85
DTP-BA	345	439	6.9×10^3	3.07
DTP-TBA	380	456	2.3×10^4	2.87

3.2.3. Electrochemical properties

The oxidation potentials of these compounds were determined from the square wave voltammograms (Figure 3.4). They exhibit characteristic oxidation potentials at 1.25, 1.26, 1.13 and 1.23 V respectively *vs.* NHE. The results are summarized in Table 3.2. These values lie at a higher potential than the redox potential of electrolytes I^-/I_3^- and Br^-/Br_3^-, the common redox couples used in the construction of DSSC's. The energy gap between the redox couple and oxidation potential of the compound

is significant in determining the current as well as the fill factor. For the compounds used in the present study, this energy gap is very large for I^-/I_3^- electrolyte whereas, for the electrolyte Br^-/Br_3^- this gap is 0.16, 0.17, 0.04 and 0.14 V respectively, for DTP-CYA, DTP-RHA, DTP-BA and DTP-TBA. This energy gap makes the regeneration of the oxidized form of the compound thermodynamically favorable during the operation of the cell (Figure 3.5).[17] Too high an energy gap may also be detrimental to efficient functioning of the cell as inverted region effect can reduce the rate of regeneration of the dye.[18-20] The values of HOMO energy levels of these compounds referenced to NHE were calculated from the oxidation potentials of these compounds. The values are comparable to that observed for the O-phenayl bridged compounds except for DTP-BA. In this case the oxidation potential is less positive. The LUMO energy level was determined by adding the respective singlet state energies obtained from the onset of absorption spectra of respective compounds. Estimations of HOMO and LUMO energies against vacuum continuum were also been made and the calculated values are presented in Table 3.3.

Table 3.2. Electrochemical properties of DTP-CYA, DTP-RHA, DTP-BA and DTP-TBA in DMF[16]

Compound	E_{onset} [a]/V in DMF	E_{onset} (ox) *vs.* E^{b}_{FOC}/V	$E^{c}_{(S+/S)}$ *vs* NHE/V	LUMO *vs.* NHE/V	[d]E_{gap}/ V
DTP-CYA	1.16	1.05	1.25	-2.2	-1.70
DTP-RHA	1.17	1.06	1.26	-1.59	-1.15
DTP-BA	1.04	0.93	1.13	-1.94	-1.44
DTP-TBA	1.14	1.03	1.23	-1.64	-1.03

[a] Observed reduction potentioan in DMF, [b]E_{FOC} = –0.11 V *vs*. Ag/AgCl. [c]The ground-state oxidation potentials $E_{(S+/S)}$ (HOMO) were measured in DMF containing 0.1M tetrabutylammonium hexafluorophosphate as supporting electrolyte using a glassy carbon working electrode, a Pt counter electrode and a Ag/AgCl reference electrode.[d]E gap is the energy gap between LUMO of the compound and the conduction band level of TiO_2 (−0.5 V *vs*. NHE).

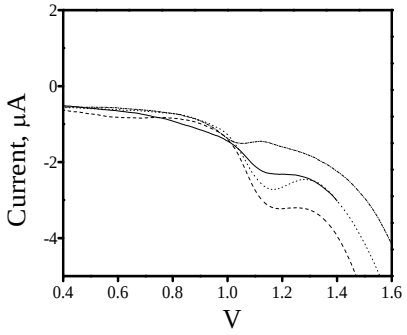

Figure 3.4. Square wave voltamograms obtained for compounds DTP-CYA (⋯), DTP-RHA (----), DTP-BA (-·-·-) and DTP-TBA (—) in DMF

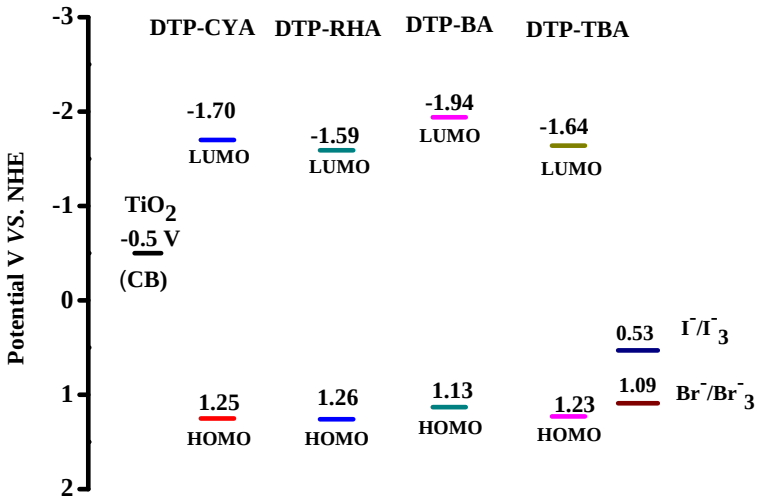

Figure 3.5. Schematic energy level diagram for a DSSC based on dyes coated nanocrystalline TiO_2 film on conducting FTO

3.2.4. Theoretical study

The optimized geometry of the compounds as well as the frontier orbitals and their energies are computed by density functional theory (DFT) with B3LYP exchange-correlation functional[23-24] and 6-31+G(d) basis set. The stationary points are characterized by frequency calculation. To include the effects of solvation, the polarization continuum model (PCM) for DMF has been used in the calculations. All calculations were performed with the GAUSSIAN 09 quantum chemistry package. The optimized geometry along with the frontier orbital representation and their respective energies against vacuum continuum is given in Figure 6. Contrary to our expectation, the orbital coefficients of the HOMO

for all compounds were found to be delocalized over the triazine core which is one of the acceptor units. Similar result was obtained in the case of O-phenyl bridged compounds. Delocalization of HOMO over the triazine has a profound effect in the lowering of HOMO energies as well as on the observed oxidation potential of all the compounds in comparison to the HOMO of Diphenylamine (-5.8 eV or 1 V *vs.* NHE). Both electrochemical and theoretical data suggests that they are difficult to oxidize in comparison to diphenylamine.The LUMO calculated for these series of compouds show extensive delocalisation over two arms of the compounds bearing acceptor groups. This extended delocalization has lead to the stabilization of the respective LUMOs in the case of DTP-RHA and DTP-TBA. All the compounds show better directionality of charge transfer on electronic excitation as the HOMO and LUMO are localized on different regions of the molecule. For DTP-RHA and DTP-TBA the theoretically calculated energy levels are in good agreement with the experimental values obtained from electrochemical measurements.

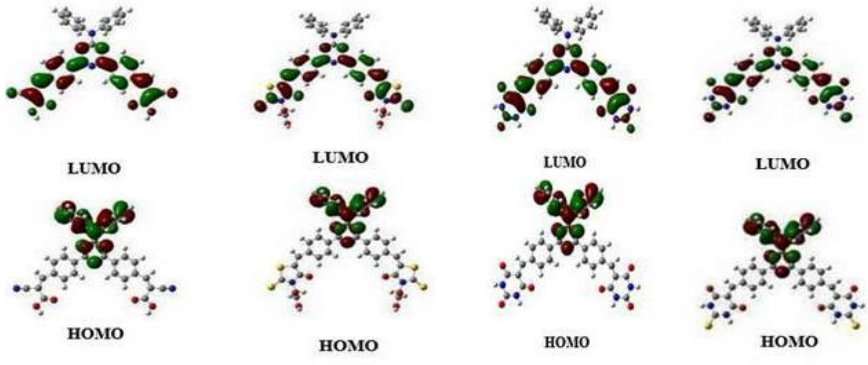

Figure 3.6. Optimized geometries of the computed using DFT theory at the B3LYP/6-31G + (d) level

Table 3.3. Comparison of theoretical and experimental orbital energies of DTP-CYA, DTP-RHA, DTP-BA and DTP-TBA [21-22]

Compounds	Experimental		Theoretical	
	[a]HOMO (IP), eV	[b]LUMO (EA), eV	HOMO, eV	LUMO, eV
DTP-CYA	-6.05	-2.61	-6.29	-3.30
DTP-RHA	-6.06	-3.21	-6.30	-3.56
DTP-BA	-5.93	-2.86	-6.29	-3.43
DTP-TBA	-6.03	-3.16	-6.24	-3.28

[a]Ionization potential: IP = – 4.8 – (E_{onset} (ox)– E_{FOC}); [b]electron affinity: EA − $E_{0\text{-}0}$ = IP

3.2.5. Photoelectrochemical properties

Under illumination by an AM 1.5 light source all the dye sensitised solar cells constructed using the dyes gave current-voltage (I-V) characteristics for typical photodiodes. A few representative current density-voltage (J-V) curves obtained for DTP-CYA, DTP-RHA, DTP-BA and DTP-TBA when Br^-/Br_3^- were used as the electrolyte[25] are given in Figure 3.7. The solar cell parameters obtained from the photocurrent measurements were summarized in Table 4. The solar energy to electrical energy conversion efficiency (η) was calculated from open circuit voltage (V_{oc}), short-circuited current (J_{sc}), fill factor (FF) and the incident photon flux (P_{in}) by using equation (3.2).[26]

$$\eta(\%) = \frac{J_{SC} V_{OC} FF}{P_{in}} \qquad (3.2)$$

Under our experimental conditions an efficiency of 6.6 % was obtained for the N719 compound when I^-/I_3^- was used as the electrolyte and 3% for Br^-/Br_3^-. The results show that the observed light conversion efficiency are lower and are in the range of 0.04-0.1. Among these the cell made from the compound DTP-TBA with Br^-/Br_3^- as the electrolyte was found to be the most efficient. Low values of V_{OC} were obtained for cells with I^-/I_3^- as the electrolyte in comparison to the data obtained for Br^-/Br_3^-. This could be due to the low potential difference between the Fermi level and the high lying redox potential of I^-/I_3^- in comparison to Br^-/Br_3^-. The poor efficiency data observed could be due to a combined effect of lower absorption coverage of the solar spectrum by the compounds as well as due to the larger energy gap between the TiO_2 conduction band and the LUMO of the dyes. Relatively better performance of DTP-TBA may be the result of the suitable energy levels for electron injection and regeneration of the dye.

Table 3.4. DSSC Performance data obtained for compounds DTP-CYA, DTP-RHA, DTP-BA and DTP-TBA

Compounds	J_{sc}, mA cm $^{-2}$	V_{oc}, mV	FF, %	η, %
DTP-CYA	0.1586[a*] (±0.001)	0.3388[a*] (±0.002)	48	0.02
	0.1853[b*] (±0.005)	0.4995[b*] (±0.005)	43	0.04
DTP-RHA	0.1612[a*] (±0.001)	0.3761[a*] (±0.002)	41	0.02
	0.1057[b*] (±0.005)	0.4332[b*] (±0.003)	43	0.02
DTP-BA	0.1599[a*] (±0.001)	0.2776[a*] (±0.003)	56	0.02
	0.2127[b*] (±0.006)	0.6012[ba*] (±0.006)	47	0.06
DTP-TBA	0.1374[a*] (0.001)	0.4469[a*] (0.002)	48	0.03
	0.3196[b*] (0.006)	0.7033[b*] (0.005)	44	0.10

[a*] I^-/I_3^- electrolyte [b*] Br^-/Br_3^- electrolyte

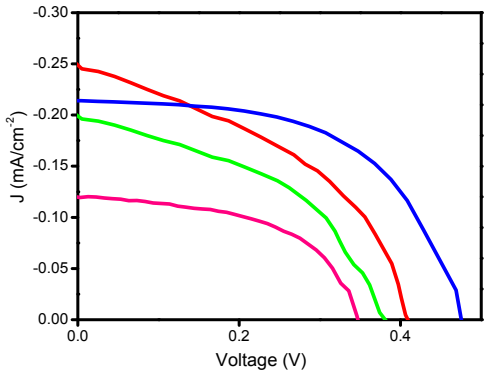

Figure 3.7. Photocurrent density–voltage curves of the compounds DTP-CYA (—), DTP-RHA (—), DTP-BA (—) and DTP-TBA (—) using Br^-/Br_3^- electrolyte

3.2.6. Nonlinear optical properties

Similar to the compounds reported in the previous chapter, all compounds show asymmetry in the electron density due to the basic donor-acceptor nature of the structure. This is further confirmed by the DFT calculations. One important difference between the DTOP series and the present compounds is in the geometry of the molecule where the phenyl π-bridge and the triazine unit are coplanar with the arylidne acceptor unit. Moreover the molecule is more rigid and the difference in the electron distribution between the HOMO and LUMO is not as pronounced as it is seen in the DTOP series. Figure 3.6 show the HOMO and LUMO orbitals of these compounds. In all the compounds the HOMO is centered on the diphenylamine and the triazine core. The LUMO is delocalized over the phenyl bridge and two acceptor moieties. These molecules were tested for their Nonlinear optical behaviour by Z-scan technique using 532 nm second harmonic of

an Nd-YAG laser with a pulse width of 7 ns. A ~1 mM solution in DMF was used for the experiment.[26] No appreciable optical damages were observed after the Z-scan measurements.

Experimentally the nonlinear behaviour is manifested in the observation of reverse saturable absorption (RSA), two photon absorption (TPA) and saturable absorption (SA) depending on the variation (increase or decrease) in transmission of the sample as a function of intensity of the laser. For a molecule, decreased transmittance or increase in the light absorption for a given laser light due to an enhanced light absorption property of the excited state in comparison to the ground state is the result of TPA and RSA with increasing laser intensity.[27] DTP-RHA and DTP-BA showed RSA closer to the focus i.e., decreased transmittance as the excited state absorption become dominant. DTP-TBA however, showed SA behaviour, i.e., increased tranmittance closer to the focus. This is because, the excitation wavelength 532 nm was at the edge of the ground state absorption by these molecules at lower fluences the molecules gets excited and may not have sufficient time to relax to the ground state leading to an increased transmittance. Such behaviour is common to many substances. As evident from the solid lines in the Figures 3.8a-c theoretical fit to the two photon absorption theory showed very good correlation. This shows that TPA is the main mechanism involved in the nonlinear absorption process for all these molecules. The nonlinear absorption coefficient (β) was determined by fitting the data obtained from the open aperture measurements to the equation (3.3)

. The results are tabulated in Table 3.5. The β value obtained for DTP-BA is high compared to other two compounds.

$$T_Z = \frac{C}{q_{0\sqrt{\pi}}} \int_{-\infty}^{\infty} In(1 + q_0\, e^{-r^2}) dt \qquad (3.3)$$

Where $q_0(z,r,t) = bI_0(t)\, L_{eff}$ and $L_{eff} = (1+e^{-\alpha I})/\alpha$ is the effective thickness of linear absorption coefficient α, I_0 is the irradiance at focus. The nonlinear refractive index and nonlinear susceptibility of NLO active materials at high laser fluences can also be measured by the Z-scan technique. Here, the transmittance is measured by varying the laser spot size at the plane of a finite aperture detector combination and is called the closed aperture method. The NLO active material will act as a thin lens with varying focal length as it moves along the optical axis of the Z-scan set-up. The transmission data obtained in the open aperture Z-scan is sensitive to nonlinear absorption only and the closed aperture scan involves both nonlinear refraction and absorption effects. In order to exclude the nonlinear absorption effects the closed aperture data obtained were divided by the corresponding open aperture data. Figure 3.9a to 3.9c show the normalized transmission data obtained for DTP-RHA, DTP-BA and DTP-TBA respectively in the closed aperture scan. The Nonlinear transmittance T(z) is related to on-axis nonlinear phase shift ($\Delta\phi_0$) and the ratio z/z_0. This relation is given by equation (3.4).[28]

$$T(z) = 1 - \frac{4x\Delta\emptyset_0}{(x^2 + 9)(x^2 + 1)} \qquad (3.4)$$

Typical peak valley pattern due to nonlinear refraction was observed for all the compounds and indicative of a negative NLR index due to self - defocusing (Figures 3.9a–3.9c). The data were fitted to equation (3.5) and the nonlinear phase shift ($\Delta\phi_0$) is determined. The nonlinear refractive index (n2), the real (Re χ^3) and the imaginary part (Im χ^3) and thus the nonlinear susceptibility χ^3 were determined by using the following set of equations 3.5 – 3.10.

$$\chi^{(3)} = Re\,\chi^{(3)} + iIm\chi^{(3)} \tag{3.5}$$

$$Im\chi^{(3)} = n_0^2 c^2\, {}^{\beta}/_{240\omega\pi^2} \tag{3.6}$$

$$\Delta n_0 = \frac{\Delta\emptyset_0}{KL_{eff}} \tag{3.7}$$

$$\gamma = \frac{\Delta n_0}{I_o} \tag{3.8}$$

$$n_{2\,(esu)} = \frac{cn_0}{40\pi}\,\gamma \tag{3.9}$$

$$Re\,\chi^{(3)} = \frac{n_0 n_2}{3\pi}\;(esu) \tag{3.10}$$

where γ, the molecular cubic hyperpolarizability of the compounds and k is the wave vector. The calculated values of nonlinear absorption coefficient (β), the Nonlinear refraction index (n_2), the third order susceptibility (χ^3), molecular cubic hyperpolarizability

(σ_2), are listed in Table 3.5. Among the three donor-acceptor systems studied, DTP-BA shows the highest NLO activity but an order less than the DTOP-BA. This may be due to the lesser asymmetry in the electron density of the excited state in this category of molecules.

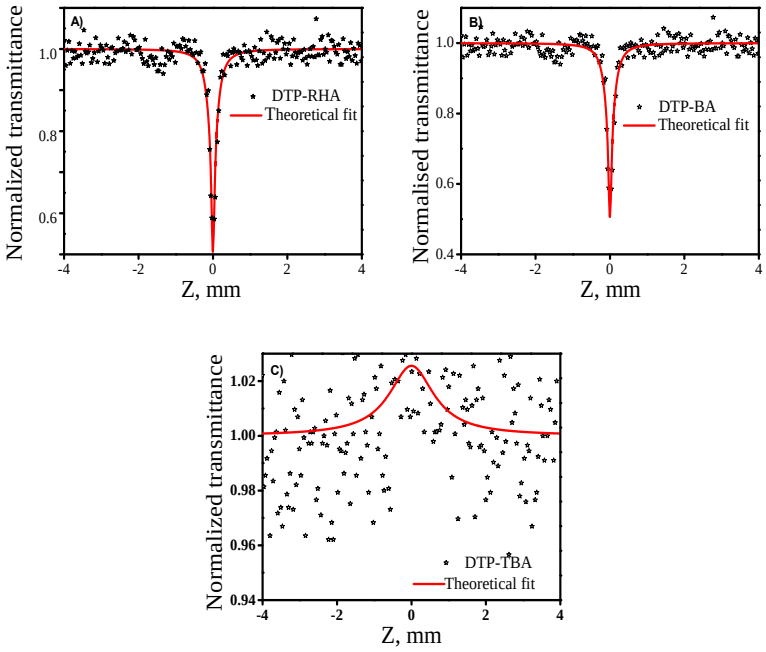

Figure 3.8. Open aperture profile of the DTP-RHA (A), DTP-BA (B) and DTP-TBA (C) in DMF (~4 x 10^{-4} M).

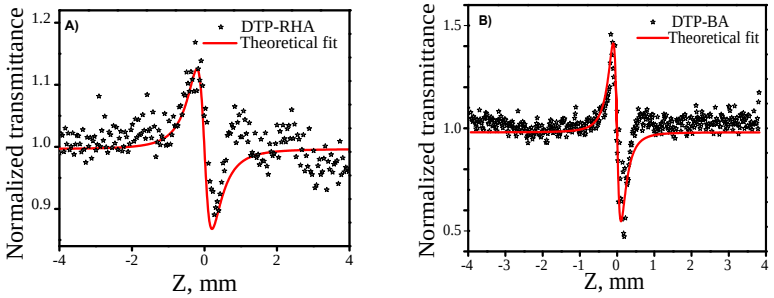

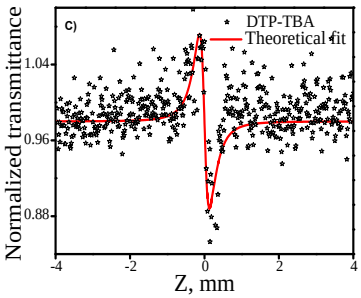

Figure 3.9. Closed aperture Z-scan profile of the DTP-RHA (A), DTP-BA (B) and DTP-TBA (C) DMF (~4 x 10^{-4} M)

3.2.7. Optical limiting property

Since all the studied molecules show third order nonlinear optical properties, these are suitable systems for optical limiting applications. The transmittance of a material with higher light intensities is termed as the optical limiting property.[29] Among the three donor-acceptor systems studied, DTP-RHA showed the best optical limiting behaviour. A plot of normalised transmittance against the input intensity is given in Figure 3.10. The optical limiting threshold of DTP-BA is estimated as 1.7G W/cm^2.

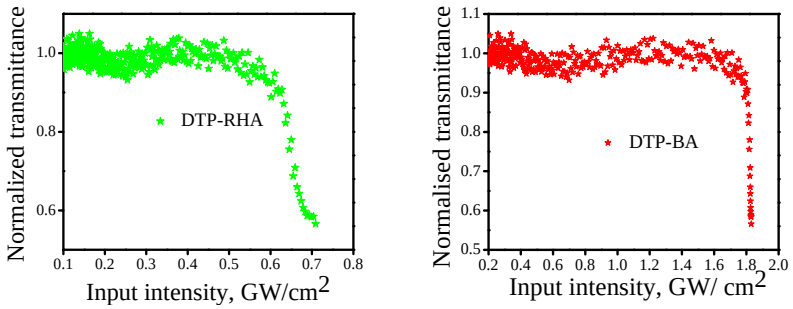

Figure 3.10. Optical limiting profile of DTP-RHA and DTP-BA

Table 3.5. Nonlinear optical properties of the DTP-CYA, DTP-RHA, DTP-BA and DTP-TBA

Compounds	Nonlinear absorption Coefficient (β, mW^{-1})	σ_2 (GW)	Nonlinear refractive index (n_2, esu)	Imaginary part of nonlinear susceptibility (Im $\chi^{(3)}$, esu)	Real part of nonlinear susceptibility (Re $\chi^{(3)}$, esu)	Nonlinear susceptibility ($\chi^{(3)}$, esu)	Optical limiting threshold (GW/cm^2)
DTP-RHA	$0.8x10^{-10}$	4026	$-0.73x10^{-10}$	$0.17x10^{-11}$	$-1.09x10^{-11}$	$1.10x10^{-11}$	0.6
DTP-BA	$7.6x10^{-10}$	45581	$-2.78x10^{-10}$	$1.64x10^{-11}$	$-4.10x10^{-11}$	$4.35x10^{-11}$	1.7
DTP-TBA	$0.3x10^{-10}$	2618	$-0.60x10^{-10}$	$0.06x10^{-11}$	$-0.92x10^{-11}$	$0.92x10^{-11}$	-

3.3. Conclusion

We have designed and synthesised three tripodal novel starburst D-A-A systems with 1,3,5-triazine core as the non-conjugating spacer/acceptor with two arms having cyanoacetic acid (DTP-CYA), rhodanine-3-acetic acid (DTP-RHA), barbituric acid (DTP-BA) or thiobarbituric acid (DTP-TBA) as anchoring acceptor groups. Electrochemical, photophysical studies and theoretical studies show that they have suitable properties for use as dyes in dye sensitized solar cells. The applicability of these dyes for the DSSC was tested by constructing the sandwich model cell. However, the observed efficiency was lower than that obtained for N719 dye under similar experimental conditions. This is attributed to the low absorption coverage of the solar spectrum and large

energy gap between the LUMO of the dyes and the conduction band of the TiO_2. The results suggest tuning of the LUMO energy by incorporating a better conjugating bridging group such as thiophene on the acceptor side of the design.The synthesised molecules have also showed very good NLO properties. Among the three donor-acceptor systems studied DTP-BA shows the highest NLO activity but an order less than the DTOP-BA.

3.4. Experimental

DPA-T (**1**) was synthesized using a previously reported procedure[30]

3.4.1. Synthesis of DPA-T-PH (3)

A solution 4-formylboronic acid (**2**, 200 mmol) tertakis (triphenylphosphene)palladium(0) (20 mmol) and K_2CO_3 (10 mmol) and compound **3** (100 mmol) in dichloromethane (50 mL) were stirred under N_2 atmosphere at room temperature for 24 h. The reaction mixture was treated with water (50 mL) and the organic layer was separated and washed with distilled water. The residue obtained was purified by column chromatography on silica gel. Elution with a mixture of (1:20) hexane and dichloromethane gave pale yellow powder of **3** in 60% yield. mp. 210 $^{\circ}$C (decomp.) FT-IR (cm^{-1}): 3348, 1703, 1584, 1370, 1199, 1108. ^{1}H NMR (400 MHz, DMSO, δ ppm): 10.10 (m, 2H), 8.48-8.46 (m, 4H), 8.06-8.04 (m, 4H), 7.53-7.48 (m, 8H), 7.40-7.36 (m, 2H). ^{13}C NMR (100 MHz, DMSO, δ ppm): 192.92, 169.68, 142.85, 140.87, 138.67, 134.46, 129.70, 129.17, 128.82, 128.33, 127.78, 126.76. ESI m/z:

455.49 (M-1). Anal Calcd.: $C_{29}H_{20}N_4O_2$: C, 76.30; H, 4.42; N, 12.27., Found: C, 76.10; H, 4.22; N, 12.17.

3.4.2. General procedure for DTP-CYA (4a), DTP-RHA (4b), DTP-BA (4c) and DTP-TBA (4d)

A mixture of the dialdehyde **3** (1 mmol) and cyanoacetic acid/ rhodanine-3-acetic acid/ barbituric acid/thiobarbituric acid (22 mmol) and ammonium acetate (19 mmol) were dissolved in 0.5 M acetic acid heated 120^0C for 12 h. After cooling, the precipitated target product was washed with chloroform and methanol to remove the unreacted reagents and starting materials.

DTP-CYA (**4a**): Yellow solid, Yield 58%, mp. 235 °C (decomp.); FT-IR (cm^{-1}): 3381, 1522, 1370, 1185. ^{1}H NMR (400 MHz, DMSO, δ ppm): 8.47-8.45 (m, 2H), 8.37-8.32 (m, 2H), 8.17-7.55 (m, 3H), 7.43-7.41 (m, 1H), 3.08-3.06 (m, 2H), ^{13}C NMR (100 MHz, DMSO, δ ppm): 179.43, 148.67, 142.99, 129.08, 129.04, 128.63, 127.82, 118.42, 73.51, 37.78, 22.48., Anal. Calcd. for $C_{35}H_{22}N_6O_4$; C, 71.18; H, 3.75; N, 14.23. Found: C, 71.00; H, 3.65; N, 14.13.

DTP-RHA (**4b**): Yellow solid, Yield 58%, mp. 245 °C; FT-IR (cm^{-1}): 3320, 2355, 1592, 1322, 1188, 1105. ^{1}H NMR (400 MHz, DMSO, δ ppm): 8.40-8.38 (m, 2H), 7.98-7.88 (m, 2H), 7.79-7.77 (m, 4H) 7.84-7.48 (m, 8H), 7.40-7.36 (m, 2H), 4.62 (m, 6H). ^{13}C NMR (100 MHz, DMSO, δ ppm): 169.19, 166.46, 129.11, 128.9,

127.74, 124.17., Anal. Calcd for $C_{39}H_{26}N_6O_6S_4$: C, 58.34; H, 3.26; N, 10.47; S, 15.97, Found: C, 58.30; H, 3.20; N, 10.40; S, 15.88

DTP-BA (**4c**): Yellow solid, Yield 58%; mp. 224 °C; FT- IR (cm^{-1}): 3185, 2350, 1671, 1520, 1390, 1209, 1209. ^1H NMR (400 MHz, DMSO, δ ppm): 11.42 (s, 1H), 11.26 (s, 1H), 8.32-8.30 (m, 3H), 8.10-8.08 (m, 2H), 7.51-7.36 (m, 5H). ^{13}C NMR (100 MHz, DMSO, δ ppm):163.07, 153.15, 150.15, 136.55, 132.60, 129.10, 127.78, 127.48. Anal. Calcd. for $C_{37}H_{24}N_8O_6$: C, 65.68; H, 3.58; N, 16.56., Found: C, 65.58; H, 3.50; N, 16.50.

DTP-TBA (**4d**): Yellow solid; Yield 58%. mp. 250 °C (decomp.) FT-IR (cm^{-1}): 3320, 2360, 1623, 1572, 1514, 1396, 1198, 1115. ^1H NMR (400 MHz, DMSO, δ ppm): 12.49 (s, 1H), 12.36 (s, 1H), 8.35-8.23 (m, 3H), 8.18-8.08 (m, 2H), 7.54-7.48 (m, 5H). Anal. Calcd. for $C_{37}H_{24}N_8O_4S_2$ C, 62.70; H, 3.41; N, 15.81; S, 9.05, Found: C, 62.60; H, 3.35; N, 15.79; S, 9.00.

3.5. References

1. Zhou, J.; Lukin, L. V.; Braun, C. L., *J. Phys. Chem. A.* **2008**, *112*, 7507.
2. Siders, P.; Cave, R. J.; Marcus. R. A., *J. Chem. Phys.* **1984**, *81*, 5613.
3. Siddarth, P.; Marcus, R. A., *J. Phys. Chem.* **1990,** *94*, 8430.
4. Siddarth, P.; Marcus, R. A., *J. Phys. Chem.* **1993,** *97*, 13078.
5. Marcus, R. A., *Rev. Mod. Phys. 65*, **1993**.
6. Marcus. R. A., *J. Chem. Phys.* **1956,** *24*, 966.
7. Cave, R. J.; Siders, P.; Marcus, R. A., *J. Phys. Chem.* **1986**, *90*, 1436.

8. Dickerson, R. E.; Timkovich, R.; Boyer, P. D., Ed.; Academic Press: New York, **1975**, *11*, 397.
9. Marcus, R. A.; Sutin, N. *Biochim. Biophys. Acta.* **1985**, *811*, 265.
10. Chang, C. K., *J. Heterocycl. Chem.* **1977,** *14*, 1285.
11. Netzel, T. L.; Kroger, P.; Chang, C. K.; Fujita, **I.;** Fajer, J. *Chem. Phys. Lett.* **1979,** *67***,** 223.
12. Fujita, I.; Fajer, J.; Chang, C.-K.; Wang, C.-B.; Bergkamp, M. A.; Netzel, T. L., *J. Phys. Chem.* **1982,** *86***,** 3754.
13. Netzel, T. L.; Bergkamp, M. A.; Chang, C. K. *J. Am. Chem. Soc*. **1982**, *104*, 1952.
14. Zhong, H.; Lai, H.; Fang, Q. *J. Phys. Chem. C.* **2011,** *115*, 2423.
15. Neil, G.; William, E. G. *Chem. Rev*. **1996**, *96*, 877.
16. Imahori, H.; Mori, Y.; Matano, Y. *J. Photochem. Photobiol*. C. **2003**, *4*, 51.
17. Yan, S. G.; Prieskorn, J. S.; Kim, Y.; Hupp, J. T. *J. Phys. Chem. B.* **2000**, *104*, 10871.
18. Bisquert, J.; Zaban, A.; Greenshtein, M.; Mora-Sero´, I. *J. Am. Chem. Soc.* **2004**, *126*, 13550.
19. Wang, Z. S.; Sayama, K.; Sugihara, H., *J. Phys. Chem. B.* **2005**, *109*, 22449.
20. Xie, Q. J.; Kuwabata, S.; Yoneyama, H. *J. Electroanal. Chem.* **1997,** *420*, 219.
21. Fermin, D. J.; Teuel, H.; Scharaifker, B. R., *J. Electroanal. Chem*. **1996,** *401*, 207.
22. Lee, C.; Yang, W.; Parr, R. G., *Phys. Rev. B.* **1988**, *37*, 785.
23. Becke, A. D., *J. Chem. Phys*. **1993**, *98*, 5648.
24. Teng, C.; Yang, X.; Yuan, C.; Li, C.; Chen, R.; Tian, H.; Li, S.; Hagfeldt, A.; Sun, L., *Organic Letters.* **2009,** *11*, 5542.
25. El-Agezt, M., El-Tayyana, A., Al-Kahlouta., Tayas, A., Abdel-Latif, M. S., **2012**, *2*, 105.
26. Yaoting, F. *J. Mol. Struct*. **2004**, *693*, 217.
27. Wang, J.; Gu, B.; Wang, H. T.; X. W. Ni. *Opt. Commun.* **2010,** *283*, 3525.

28. Sona, N.; Sreejesh, P. R.; Aby C. P.; Sebastian M., Sreekumar, K.; Sudha, K.; Rani, J., *New J. Chem.* **2015**, 39, 2795.
29. Prem Kiran, P.; Naga Srinivas, N. K. M.; Raghunath Reddy, D.; Bhaskar G. Maiya.; Aditya Dharmadhikari, Arvinder S. Sandhu, Ravindra Kumar, G.; Narayana Rao, D. *Opt. Commun.* **2002**, *202*, 347.
30. Patel, K. C.; Patel, S. K.; Shah, R. R.; Patel, R. M., *Iran Polym J.* **2005,** *14*, 323.

Chapter 4

Synthesis, characterization and studies on the photovoltaic and nonlinear optical properties of a series of thiophene bridged diphenylamine-*s*-triazine based Donor-Acceptor triads with different π -Acceptor groups

Contents

Abstract

A series of starburst D-A-A triads having 1,3,5-triazine as core and the terminal acceptor groups directly linked to triazine through a thiophene bridge were synthesised and their photovoltaic and nonlinear optical properties were studied. Diphenylamine was used as the donor in all the compounds and the acceptor/anchoring groups used were cyanoacetic acid, rhodanine-3-acetic acid, barbituric acid or thiobarbituric acid. The overall design uses a bipodal anchoring strategy to semiconductors in a potential DSSC construction. The photophysical, electrochemical and theoretical studies showed that these molecules possess excellent electronic

properties for use as dyes in DSSC applicaitons. DSSC constructed using these molecules show significant improvements in the performance than the cells described in the previous chapters. The inherent asymmetry in the electron density in the ground state and the excited state making them ideal for NLO applications and the experimental results suggest to use as potential optical limiters.

4.1. Introduction

The rigid phenyl-triazine direct bridging has proved to be effective for DTP-RHA and DTP-TBA. However, the structural modification did not cause any significant improvement in the properties and warrant further modification in the design of the dye.[1] Wan *et al*., have studied the effect of the structure of the π-bridge in a series of dyes **1-3** having the starburst design as in the triazine series of dyes in the present study. In their design they have studied the effect of phenyl, thiophene and furan as a conjugating-π-bridge in a series of dyes having two phenothiazine donors on a triphenylamine core with cyanoacetic acid as the single acceptor/anchoring group (Chart 4.1). This change in the π-bridge has resulted in a progressive decrease in the band gap and thus a red shift in the absorption spectrum and the electrochemical measurements show that with the change in the π-bridge the HOMO gets destabilized without affecting the LUMO energy level.

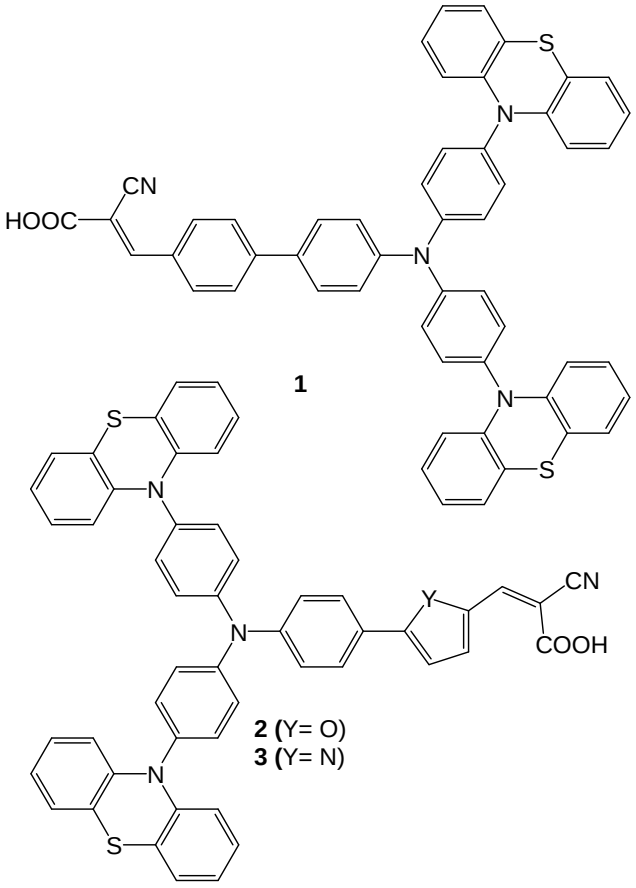

Chart 4.1.

In another report, Teng *et al.*, in a series of carbazol-π-cyanoacetic acid dyes **4, 5** (Chart 4.2) studied the effect of the π-bridge by introducing a thiophene bridge along with an increase in conjugation.[2] Here too the HOMO got destabilized along with a stabilization of the LUMO level leading to a red shifted absorption spectrum.[3-4] Both the studies report improvements in the photo conversion efficiencies. A similar strategy has been adopted by us

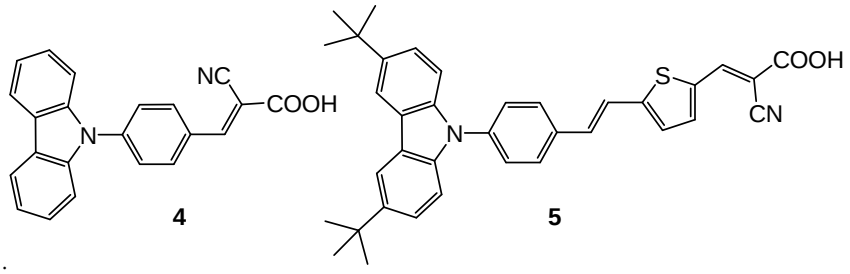

Chart 4.2.

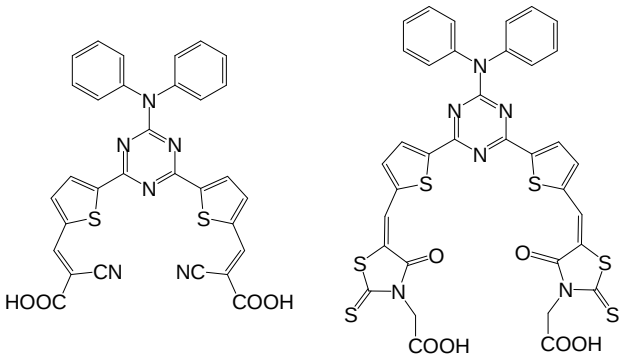

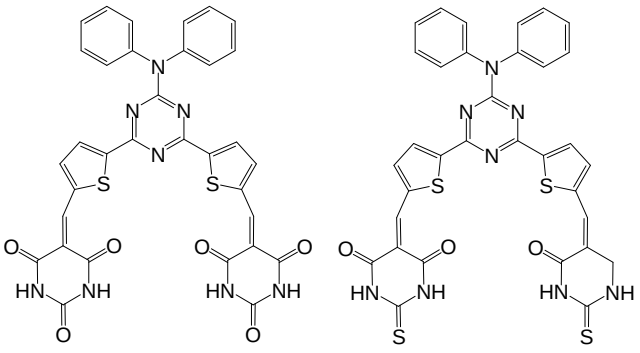

Chart 4.3.

and a series of dyes with thiophene as the π-bridge were designed, synthesised and studied (Chart 4.3). The proposed structural modification is expected to lower the HOMO-LUMO gap and subsequently improve the photoconversion efficiencies.

4.2. Results and discussion

4.2.1. Design and synthesis

The starburst D-A-A **6a-d** were synthesised by adopting the scheme illustrated in Scheme 4.1. By using the Suzuki coupling strategy the diphenylamine substituted 2,4-dichlorotriazine **7** was allowed to react with **8** in the presence of tetrakis (triphenylphosphine) palladium(0) and K_2CO_3 to prepare the dialdehyde (**9**). The dialdehyde (**9**) was subjected to Knoevenagel condensation with cyanoacetic acid, rhodanine-3-acetic acid, barbituric acid or thiobarbituric acid respectively, in the presence of ammonium acetate in glacial acetic acid at 95 $^{\circ}$C. The product DTT-CYA, DTT-RHA, DTT-BA and DTT-TBA (**6a-d**) were obtained with 50-60% yield. All the compounds were characterized by using ^{1}H NMR, ^{13}C NMR, FT-IR spectroscopy and elemental analysis.

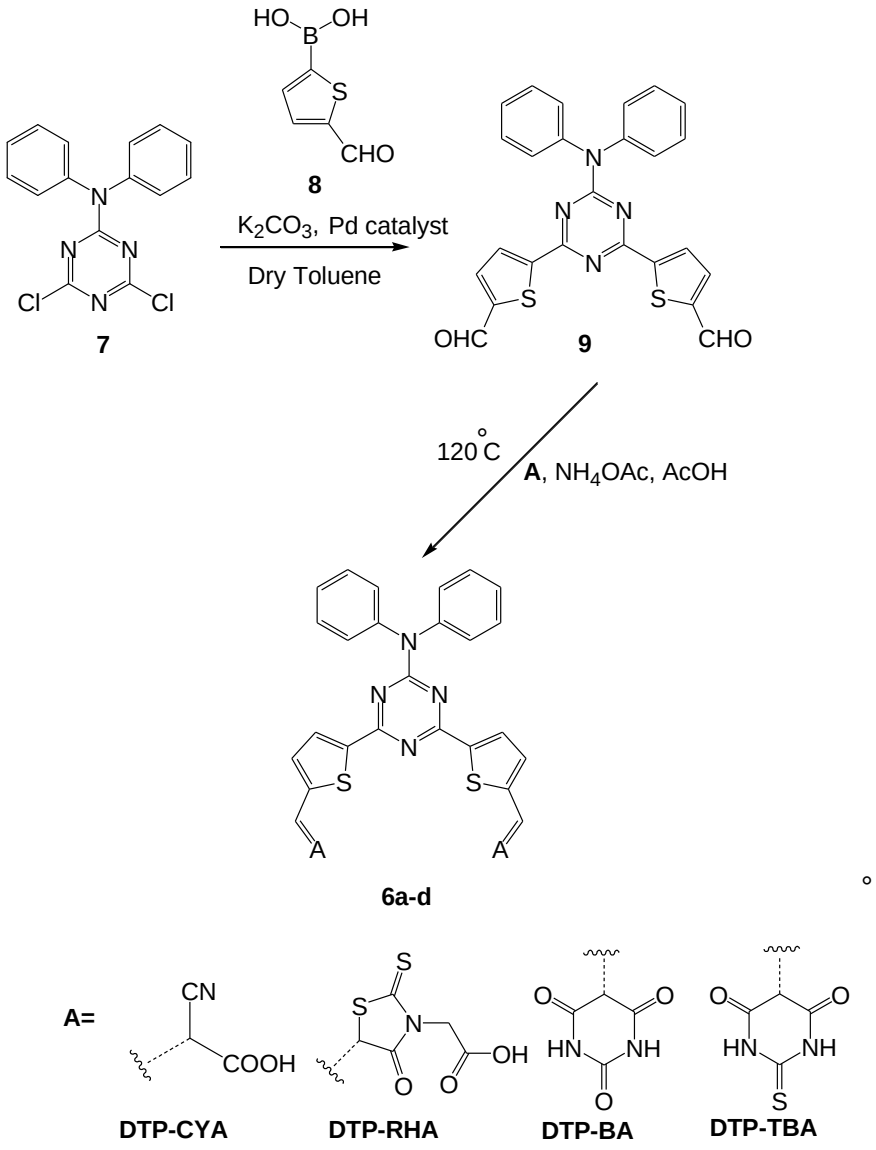
HO
B
OH
S
CHO
8
K_2CO_3, Pd catalyst
Dry Toluene
N
N
N
Cl
N
Cl
7
OHC
S
S
CHO
9
120 °C
A, NH_4OAc, AcOH
A
A
6a-d
A=
CN
COOH
S
S
N
OH
O
O
O
HN
NH
O
S
DTP-CYA
DTP-RHA
DTP-BA
DTP-TBA

Scheme 4.1.

4.2.2 Photophysical studies

All the starburst D-A-A triads with the thiophene bridge have good solubility in polar aprotic solvents such as DMF and DMSO and possessed very poor solubility in common organic solvents such as methanol, acetonitrile or chloroform. The absorption spectra of all compounds were recorded in DMF (Figure 4.1.) They all show characteristic absorption spectra for intramolecular charge transfer absorption at 422 nm, 496 nm, 480 nm and 514 nm, with the onset of absorption extending to 500 nm for DTT-CYA, 570 nm for DTT-RHA, 600 nm for DTP-BA and 700 nm for DTT-TBA. The diffuse reflectance spectra of all compounds in the powder form, show much broader absorption spectra with the onset of absorption extending to 750 nm (Figure 4.1 B).This red shift could be due to the stacking arrangement that facilitate intramolecular charge transfer.[5] Nano-crystalline TiO_2 thin films were made from a paste of TiO_2 purchased from Solaronix SA by doctor blading and annealing at 500 $^{\circ}C$ for 30 minutes in a muffle furnace. The dye coated TiO_2 thin films were prepared by immersing these thin films in respective dye solutions (~2 x 10^{-2} M) in DMF for 24 h, followed by washing successively with fresh DMF, water and ethanol. The diffuse reflectance spectra obtained for these dye coated thin films show red shift in their respective absorption maximum compared to that observed in DMF solutions. Figure 4.2 shows the diffuse reflectance spectrum obtained for these dyes when adsorbed on TiO_2 thin films. The singlet excitation energy $E_{0\text{-}0}$ was calculated from the onset of the

respective absorption bands in DMF solutions.[6] Photophysical properties of these compounds are summarized in Table 4.1.

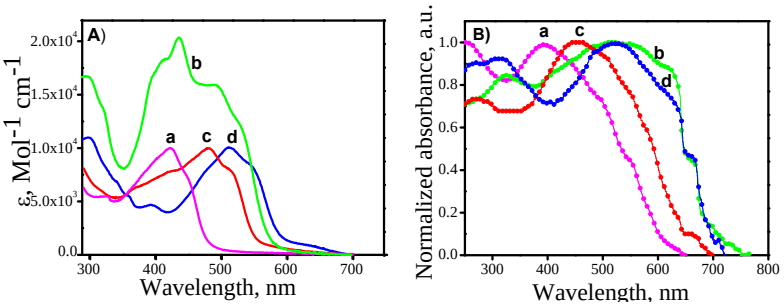

Figure 4.1. Absorption spectrum of compounds DTT-CYA (a), DTT-RHA (b), DTT-BA (c) and DTT-TBA (d), A) in DMF solution, B) in powder form

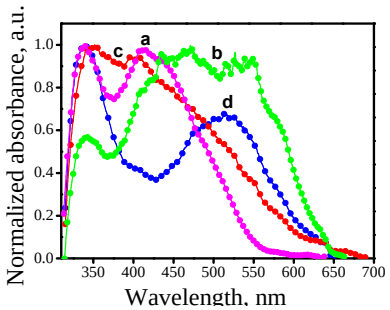

Figure 4.2. Normalized diffuse reflectance spectra of compounds DTT-CYA (a), DTT-RHA (b), DTT-BA (c) and DTT-TBA (d) adsorbed on TiO_2 thin film

Table 4.1. Photophysical properties of the compounds DTT-CYA, DTT-RHA, DTT-BA and DTT-TBA

Compounds	**λ_{max}(Abs), nm**	**λ_{onset}, nm**	**ε_{max}, dm^3mol^{-1} cm^{-1}**	**E_{0-0}, V**
DTT-CYA	422	480	1 x 10^4	2.6
DTT -RHA	438, 496 (sh)	554	2 x 10^4	2.2
DTT -BA	480	557	1 x 10^4	2.2
DTT -TBA	514	600	1 x 10^4	2.0

4.2.3 Electrochemical properties

The oxidation potentials of these compounds were determined from the square wave voltammograms of these compounds in DMF by using glassy carbon electrode as the working electrode, platinum counter electrode and tetrabutylammoniumhexafluorophosphate as the supporting electrolyte. The potential obtained were corrected by using ferrocene as an internal standard and referenced to NHE. The square wave voltammograms obtained are given in Figure 4.3. They exhibit characteristic oxidation potentials at 1.23, 1.29, 1.21 and 1.29 V, respectively *vs*. NHE. These values are lower than the redox potential of the electrolytes I^-/I_3^- and Br^-/Br_3^- used in the construction of DSSC's.[7] The energy gap between the redox couple and oxidation potential of the dye is significant in determining the current as well as the fill factor. For the compounds used in the present study, the energy gap obtained is very large and in the range 0.68-0.76 V for I^-/I_3^-. For Br^-/Br_3^-, this difference ranges between 0.12-0.2 V. This energy difference is conductive for an exergonic regeneration of the oxidized during the operation of the cell (Figure 4.5).[8] The values of HOMO energy levels of these compounds referenced to NHE were calculated from the oxidation potentials of these compounds. The values are comparable to that observed for the DTOP and DTP series of compounds. The LUMO energies were calculated by adding their respective singlet energy to the HOMO energies. Estimations of HOMO and LUMO energies against vacuum continuum have also been done and all the

values are presented in Table 4.2. An important feature of the present series of compounds is the lowering of LUMO levels achieved by incorporating the thiophene bridge in lieu of phenyl in the DTP series of compounds. For DTT-CYA, LUMO level has been lowered by 0.83 V and for DTT-RHA it is 0.74 V. For the barbituric acid conjugate DTT-BA and the thiobarbituric acid conjugate the lowering achieved was 0.95 V and 0.93 V, respectively. This dramatic effect could be due to the efficient electronic coupling between the donor and the acceptor moiety offered by thiophene bridge. Thus the use of thiophenyl bridge has proved as a viable strategy to properly tune the LUMO levels to match the conduction band of the TiO_2 *i.e.*, -0.5 V. As illustrated in Figure 4.4, the newly synthesised dyes possess the best electronic characteristics to be used as sensitizers in DSSC.

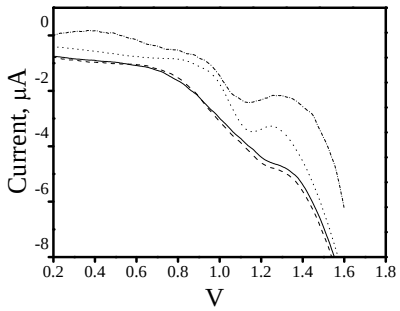

Figure 4.3. Square wave voltammograms obtained for compounds DTT-CYA (⋯), DTT-RHA (----), DTT-BA (-·-·-) and DTT-TBA (—) in DMF

Table 4.2. Electrochemical properties of the compounds DTT-CYA, DTT-RHA, DTT-BA and DTT-TBA in DMF[9-11]

Compounds	E_{onset}/V in DMF	E_{onset} (ox) *Vs.* E_{FOC}/V	$E_{(S+/S)}$ *vs* NHE/ V	LUMO *vs.* NHE/eV	E_{gap}/ V
DTT-CYA	1.14	1.03	1.23	-1.37	0.87
DTT -RHA	1.20	1.09	1.29	-0.91	0.41
DTT -BA	1.12	1.01	1.21	-0.99	0.49
DTT -TBA	1.20	1.09	1.29	-0.71	0.21

E_{FOC} = –0.11 V *vs.* Ag/Ag^+ the ground-state oxidation potentials $E_{(S+/S)}$ (HOMO) were measured in DMF containing 0.1M tetrabutylammonium hexaflourophosphate as supporting electrolyte using a glassy carbon working electrode, a Pt counter electrode and a Ag/Ag^+ reference electrode; the E_{0-0} value was estimated from the onset of absorption, E_{gap} is the energy gap between LUMO of the dye and the conduction band level of TiO_2 (−0.5 V *vs*. NHE)

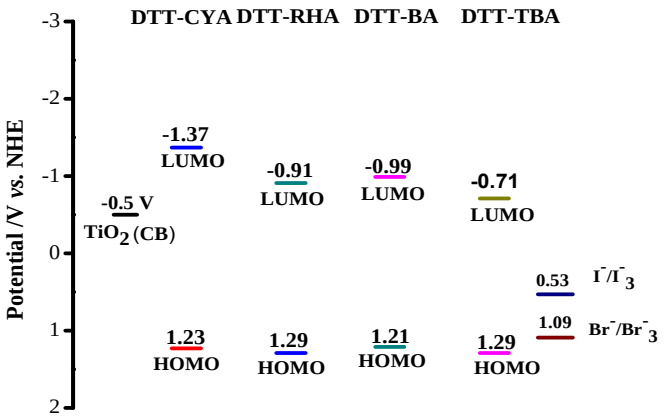

Figure 4.4. Schematic energy level diagram for compounds DTT-CYA, DTT-RHA, DTT-BA and DTT-TBA along with the conduction band of TiO_2 and the respective redox levels of electrolytes

4.2.4 Theoretical study

The optimized geometry of the compounds as well as the frontier orbitals and their energies are computed by density functional theory (DFT)[12] with B3LYP exchange-correlation functionaland 6-31+G(d) basis set.[13-15] The stationary points are characterized by frequency calculation. To include the effects of solvation, the polarization continuum model (PCM) for DMF has been used in the calculations. All calculations were performed with the GAUSSIAN 09 quantum chemistry package. The optimized geometry along with the frontier orbital representation and their respective energies against vacuum continuum is given in Figure 4. 5. As seen in the frontier orbital maps, a change from phenyl to thiophene did not affect much the delocalisation of HOMO and LUMO surfaces. As observed for DTOP and DTP series, HOMO is mainly localised on the diphenylamine and the triazine core. The LUMO is delocalised over two acceptor arms. The theoretically calculated energy levels are also found to be matching with the experimental values obtained from electrochemical measurements (Table 4.3).The low HOMO-LUMO gap explains the red shifted absorption spectrum of these compounds in comparison to the spectrum obtained for compounds described in the previous chapter. Thus the present series of dyes ensure better coverage of the solar spectrum in the visible region.

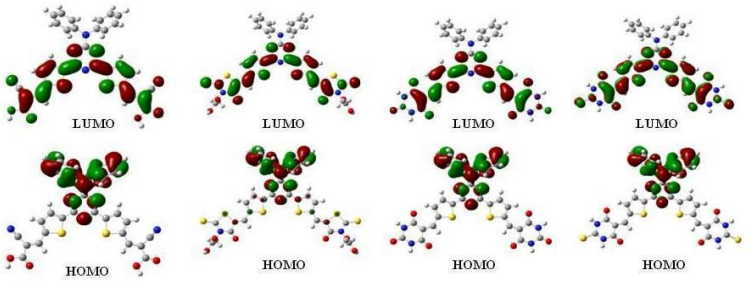

Figure 4.5. Optimized geometries of the compounds DTT-CYA, DTT-RHA, DTT-BA and DTTTBAcomputed using DFT theory at the B3LYP/6-31G + (d) level

Table 4.3. Comparison of the frontier orbital energies of DTT-CYA, DTT-RHA, DTT-BA and DTT-TBA in DMF

Compounds	Experimental		Theoretical	
	HOMO[a], eV	LUMO[b], eV	HOMO, eV	LUMO, eV
DTT-CYA	-6.03	-3.05	-6.24	-3.77
DTT-RHA	-6.09	-3.82	-5.89	-3.66
DTT-BA	-6.01	-3.67	-6.26	-3.48
DTT-TBA	-6.09	-3.93	-6.26	-3.52

[a]Ionization potential: IP = – 4.8 – (E_{onset} (ox) – E_{FOC}); [b]electron affinity: EA − $E_{0\text{-}0}$= IP

4.2.5 Photoelectrochemical properties

An AM 1.5 light source was used to illuminate the cells constructed using the DTT series of dyes. A few representative J-V curves obtained for compounds DTT-RHA, DTT-BA and DTT-TBA when Br^-/Br_3^- was used as the electrolyte are given in Figure 4.6.

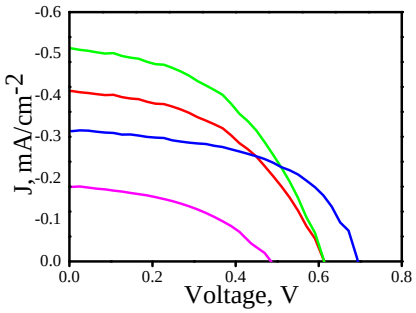

Figure 4.6. Photocurrent density–voltage curves of the compounds DTP-CYA(——), DTP-RHA(——), DTP-BA(——) and DTP-TBA(——) using Br^-/Br_3^- electrolyte

Table 4.4. DSSC Performance data obtained forthe compounds DTT-CYA, DTT-RHA, DTT-BA and DTT-TBA

Compounds	J_{sc}, mA cm^{-2}	V_{oc},mV	FF, %	η, %
DTT-CYA	0.1850 (±0.002)	0.4923 (±0.002)	43	0.04
DTT-RHA	0.5112 (±0.001)	0.5966 (±0.003)	49	0.15
DTT-BA	0.5178(±0.001)	0.6116 (±0.001)	47	0.15
DTT-TBA	0.3133 (±0.002)	0.6923 (±0.002)	55	0.12

The solar cell parameters obtained from the photocurrent measurements were summarized in Table 4.4. The solar energy to electrical energy conversion efficiency was calculated by the method described in the previous chapters. A photoconversion efficiency of 6.6 % was obtained for the standard dye N719 when I^-/I_3^- was used as the electrolyte and 3% when Br^-/Br_3^- as the electrolyte. Though lower the results obtained for the DTT series of compouds gave marked improvements in the photoconversion efficiency compared to DTOP and DTP series of compounds. The

cells prepared using I^-/I_3^- did not perform well and cell parameters were very low to be measured. V_{oc} value upto 0.69 V was achieved in the case of DTT-TBA, where thiobarbituric acid was used as the acceptor/anchoring unit. However, the short circuit current density (J_{sc}) observed was lower than that of the cells fabricated with DTT-RHA and DTT-BA. This could be due to a more exergonic electron injection from DTT-RHA and DTT-BA where the E_{gap} between the TiO_2 conduction band and the LUMO of these dyes were 0.4 V *vs.* 0.2 for DTT-TBA. In this series of compounds DTT-RHA and DTT-BA gave better efficiency than the rest of the compounds. Overall the design of the dye adopted here gave much better efficiency when compared to dyes of DTOP and DTP series. Hence the present dye design with the thiophene bridge with a direct coupling to triazine is proved to have suitable LUMO levels to be used with a DSSC constructed with TiO_2 as the semiconductor. The reduced efficiency in comparison to the standard dye may be due to other limiting factors such as regeneration of the dye via a back electron transfer from the conduction band of the semiconductor to the HOMO of the dye or short circuiting via a direct hole transfer to the electrolyte by the semiconductor.[16-17] A good strategy to avoid the later is to introduce more hydrophobicity to the dye thus making dye adsorbed TiO_2 surfaces more hydrophobic causing a barrier to the approach of ionic electrolyte to the semiconductor.

4.2.6 Non Linear optical properties

Similar to the compounds reported in the previous chapters all compounds show asymmetry in the electron density due to the basic donor-acceptor nature of the structure. This is further confirmed by the DFT calculations. One important difference between the DTOP series and the present compounds is in the geometry of the molecule where the thiophene π-bridge and the triazine unit are coplanar with the arylidne acceptor unit. Moreover the molecule is more rigid and the difference in the electron distribution between the HOMO and LUMO is not as pronounced as it is seen in the DTOP series. Figure 4.4 show the HOMO and LUMO orbitals of these compounds. In all the compounds the HOMO is centered on the diphenylamine and the triazine core. The LUMO is delocalized over the phenyl bridge and two acceptor moieties. These molecules were tested for their nonlinear optical behaviour by Z-scan technique using 532 nm second harmonic of an Nd-YAG laser with a pulse width of 7 ns. A ~1 mM solution in DMF was used for the experiment. No appreciable optical damages were observed after the Z-scan measurements. Experimentally the nonlinear behaviour is manifested in the observation of reverse saturable absorption (RSA), two photon absorption (TPA) and saturable absorption (SA), depending on the variation (increase or decrease) in transmission of the sample as a function of intensity of the laser. For a molecule, decreased transmittance or increase in the light absorption for a given laser light due to an enhanced light absorption property of the excited state in comparison to the ground state is the result of TPA and RSA with increasing laser intensity.[18] All compounds show RSA closer to the focus i.e., decreased transmittance as the excited state absorption becomes dominant. As evident from the solid lines in the figures (Figure 4.7), the

theoretical fit to the two photon absorption theories showed very good correlation. This shows that TPA is the main mechanism involved in the nonlinear absorption process for all these molecules. The nonlinear absorption coefficient (β) was determined by fitting the data obtained from the open aperture measurements to the equation (4.2). The results are tabulated in Table 4.4. The β value obtained for DTT-RHA and DTT-BA are higher compared to other two compounds but one order less than the DTOP series.

$$T_Z = \frac{C}{q_{0\sqrt{\pi}}} \int_{-\infty}^{\infty} In(1 + q_0\, e^{-r^2}) dt \ldots. \qquad (4.2)$$

Where $q_0(z, r, t) = bI0(t)\ L_{eff}$ and $L_{eff} = (1+e^{-\alpha I})/\alpha$ is the effective thickness of linear absorption coefficient α, I_0 is the irradiance at focus.

The nonlinear refractive index and nonlinear susceptibility of NLO active materials at high laser fluences can also be measured by the Z-scan technique. Since the excitation wavelength 532 nm was at the edge of the ground state absorption by these molecules, multiphoton absorption and the optical limiting behaviour lead to limited transmission of laser photons to obtain poor quality transmission data in the closed aperture Z-scan making the measurement of nonlinear susceptibility and nonlinear refractive index almost impossible.

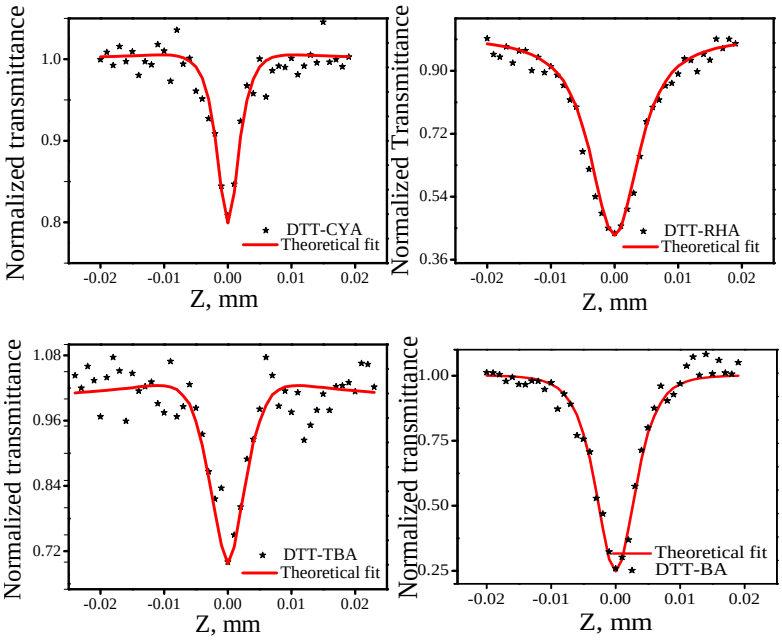

Figure 4.7. Open aperture Z-scan profile of DTT-CYA, DTT-RHA DTT-BA, and DTT-TBA in DMF

Table 4.4. Nonlinear absorption of the compounds DTT-CYA, DTT-RHA, DTT-BA, and DTT-TBA in DMF solution

Compounds	Nonlinear absorption coefficient (β), mW^{-1}	σ_2, GM	Optical limiting threshold, GW/cm^2
DTT-CY	0.17×10^{-10}	795	0.14
DTT-RHA	1.72×10^{-10}	12425	0.03
DTT-BA	2.57×10^{-10}	13727	0.02
DTT-TBA	0.68×10^{-10}	3313	0.13

4.2.7 Optical limiting property

Since all the studied moelcules show third order nonlinear optical properties these are suitable systems for optical limiting applications. The transmittance of a material with higher light

intensities is termed as the optical limiting property.[19] Among the donor-acceptor systems studied, all showed optical limiting behaviour with the DTT-BA and DTT-RHA showing a lower and early threshold value compared to other two dyes. A plot of normalised transmittance against the input intensity is given in Figure 4.8.

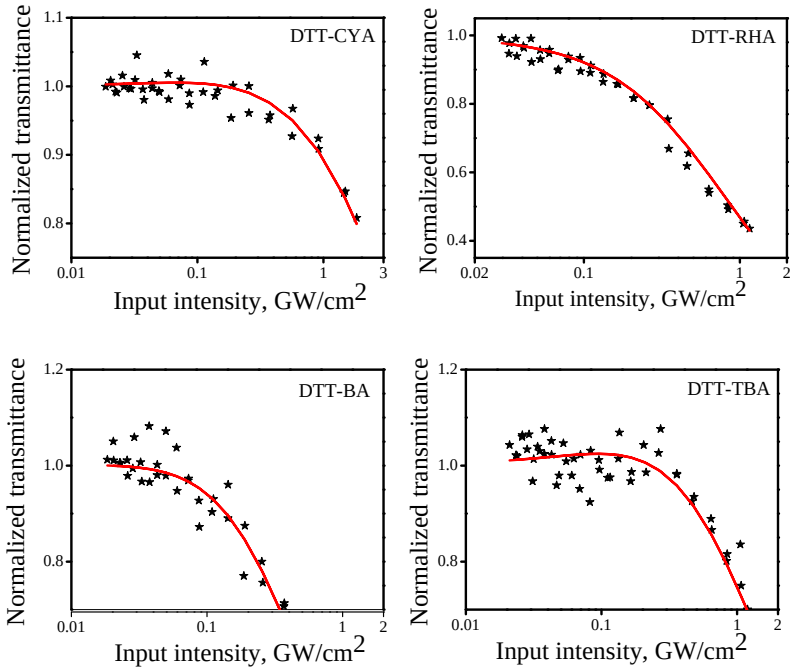

Figure 4.8. Optical limiting profile of DTT-CYA, DTT-RHA, DTT-BA, and DTT-TBA

4.3. Conclusion

Four starburst D-A-A triads with 1,3,5-triazine core as the non-conjugating spacer/acceptor with thiophene bridged cyanoacetic acid (DTT-CYA), rhodanine-3-acetic acid (DTT-RHA), barbituric acid (DTT-BA) or thiobarbituric acid (DTT-

TBA) as anchoring acceptor groups were synthesised. Electrochemical, photophysical and theoretical studies show that they have improved electronic properties for use as dyes in dye sensitized solar cells compared to dyes reported in the previous chapters. The applicability of these dyes for the DSSC was tested by constructing the sandwich model Photovoltaic cell. However, the observed efficiency was lower than that obtained for N719 dye under similar experimental conditions. Though the newly synthesised compounds show very good absorption coverage of the solar spectrum the lower efficiency obtained may be due to other efficiency limiting factors such as short circuiting and back electron transfer. The results suggest increasing hydrophobic character of the dye by appropriate structural modifications. All compounds show good threshold for optical limiting applications.

4.4. Experimental

4.4.1. DPA-T was synthesized using previously reported procedure[20]

4.4.2. Synthesis of DTT (9)

A solution 5-formyl 2-thienyl boronic acid (**8**) (200 mmol) tertakistriphenylphosphenepalladium(0) (20 mmol), K_2CO_3 (10 mmol) and a solution of compound **7** (100 mmol) in dichloromethane (50 mL) were stirred under N_2 atmosphere at room temperature for 24 h. The reaction mixture was treated with water (50 mL) and the organic layer was separated and washed with distilled water. The residue obtained was purified by column

chromatography on silica gel. Elution with a mixture of (1:20) hexane and dichloromethane gave pale yellow powder of **9** in 65% yield. mp. 255 $^{\circ}$C

FT-IR (cm^{-1}): 3329, 2815, 1688, 1350, 1054. ^{1}H NMR (400 MHz, DMSO, δ ppm):10.01 (s, 1H), 8.13 - 8.12 (d, 1H) 7.85 - 7.84 (d, 1 H), 7.69-7.63 (m, 5H); ^{13}C NMR (100 MHz, DMSO, δ-ppm): 192.9, 169.6, 142.8, 140.8, 138.6, 134.4, 129.7, 129.1, 128.8, 128.3, 127.1, and 126.; Anal Calcd: C_{29} H_{20} N_4 O_2 :- C, 76.30; H, 4.42; N, 12.Found: C, 76.10; H, 4.22; N, 11.10.

4.4.3. General procedure for DTT-CYA (6a), DTT-RHA (6b), DTT-BA (6c) and DTT-TBA (6d)

A mixture of aldehyde **9** (1mmol) and of rhodanine-3-acetic acid/ barbituric acid/thiobarbituric acid (22 mmol) and ammonium acetate (19 mmol) were dissolved in 0.5 M glacial acetic acid heated 120 $^{\circ}$C for 12 h. After cooling, the precipitated target product was washed with chloroform and methanol to remove the unreacted reagents.

OTT-CYA (**6a**): Orange red solid, Yield 58%, mp. 280 $^{\circ}$C (decomp.), FT-IR (cm^{-1}): 3320, 2915, 1588, 1390, 1105. ^{1}H NMR (400 MHz, DMSO, δ ppm): 7.69-7.66 (m, 1H), 7.65-7.51, (m, 1H), 7.48-7.44 (m, 1H), 7.35-6.08 (m, 1H); Anal. Calcd.for $C_{35}H_{22}N_6O_4$; C, 71.18; H, 3.75; N, 14.23; Found: C, 71.15; H, 3.63; N, 14.18.

OTT-RHA (**6b**): Purple, Yield 58%, mp. 287 °C (decomp.), FT-IR (cm^{-1}): 3330, 2926, 2858, 1390, 1105. ^{1}H NMR (400 MHz, DMSO, δ ppm): 8.17 (s, 1H), 7.82 -7.80 (d, 2H), 7.62-7.33 (m, 5H), 4.74 (s, 1H) Anal. Calcd.for $C_{39}H_{26}N_6O_6S_4$: C, 58.34; H, 3.26; N, 10.47;S, 15.97; Found: C, 58.24; H, 3.14; N, 10.35;S, 15.90.

OTT-BA (**6c**): Purple solid, Yield 58%, mp. 275 °C (decomp.); FT-IR (cm^{-1}): 3325, 2926, 1592, 1339, and 1105. ^{1}H NMR (400 MHz, DMSO, δ ppm): 11.36-11.35 (d, 1H), 8.5 (s, 1H), 8.19-8.18 (1H, d), 7.85-7.84 (1H, d), 7.47-7.36) (m, 5H) Anal.Calcd.for $C_{37}H_{24}N_8O_6$; C, 65.68; H, 3.58; N, 16.56; Found: C, 65.55; H, 3.47; N, 16.49.

DTT-TBA (**6d**): Purple solid, Yield 58%, mp. 280 °C (decomp.); IR (cm^{-1}): 3336, 2920, 1588, 1385, 1245, 1115, 1063. ^{1}H NMR (400 MHz, DMSO, δ ppm): 12.56-12.45 (d, 1H), 8.6 (s, 1H), 8.32-8.22 (1H, d), 7.99-7.89 (1H, d), 7.65-7.4) (m, 5H); Anal.Calcd.for $C_{37}H_{24}N_8O_4S_2$ C, 62.70; H, 3.41; N, 15.81; S, 9.05; Found: C, 62.60; H, 3.31; N, 15.78; S, 9.00.

4.5. References

1. Wan, Z.; Jia, C.; Duan, Y.; Zhou, L.; Lin, Y.; Shi, Y., *J. Mater. Chem.* **2012,** *22*, 25140.
2. Teng, C.; Yang, X.; Yuan, C.; Li, C.; Chen, R.; Tian, H.; Li, S.; Hagfeldt, A.; Sun. L., *Org. Lett.* **2009,** *11*, 5542.
3. Malytskyi, V.; Simon, J.-J.; Patrone, L.; Raimundo, J.-M., *RSC Advances.* **2015**, *5*, 354.

4. Liu, Q.; Kong, F.-T.; Okujima, T.; Yamada, H.; Dai, S.-Y.; Uno, H.; Ono, N.; You, X.-Z.; Shen, Z. *Tetrahedron Lett.* **2012,** *53*, 3264.
5. Zhong, H.; Lai, H.; Fang, Q., *J. Phys. Chem. C.* **2011,** *115*, 2423.
6. Marszalek, M.; Nagane, S.; Ichake, A.; Humphry-Baker, R.; Paul, V.; Zakeeruddin, S. M.; Graetzel, M. *J. Mater. Chem.***2012,** *22*, 889.
7. Wang, Z. S.; Sayama, K.; Sugihara, H., *J. Phys. Chem. B.* **2005,** *109*, 22449.
8. Neil, G.; William, E. G., *Chem. Rev*. **1996**, *96*, 877
9. Xie, Q. J.; Kuwabata, S.; Yoneyama, H., *J. Electroanal. Chem.* **1997,** *420*, 219.
10. Fermin, D. J.; Teuel, H.; Scharaifker, B. R., *J. Electroanal. Chem*. **1996,** *401*, 207.
11. Parr, R. G.; Yang, W., Density-Functional Theory of Atoms and Molecules; Oxford University Press, **1989**, New York.
12. Becke, A. D., *J. Chem. Phys.***1993**, *98*, 5648.
13. Lee, Yang, W.; Parr, R. G., *Phys. Rev. B.***1994**, *37*, 785.
14. Stephens, P. J.; Devlin, F. J.; Chabalowski, C. F.; Frisch, M. J., *J. Phys. Chem.***1994**, *98*, 11623.
15. Liu, D.; Fessenden, R. W.; Hug, G. L.; Kamat, P. V. *J. Phys. Chem.* B **1997**, *101*, 2583.
16. Burfeindt, B.; Hannappel, T.; Storck, W.; Willig, F. *J. Phys. Chem.* **1996**, *100*, 16463.
17. Sayama, K.; Tsukagochi, S.; Hara, K.; Ohga, Y.; Shinpou, A.; Abe, Y.; Suga, S.; Arakawa, H. *J. Phys. Chem. B*. **2002**, *106*, 1363.
18. Srinivas, N.; Rao, S. V.; Rao, D.; Kimball, B. K.; Nakashima, M.; Decristofano, B. S.; Rao, D. N., *J Porphyr Phthalocyanines.* ***2001,*** *5*, 549.
19. Lin, T.-C.; Zheng, Q.; Chen, C.-Y.; He, G. S.; Huang, W.-J.; Ryasnyanskiy, A. I.; Prasad, P. N., *Chem. Commun.* **2008**, *3*, 389.
20. Patel, K. C.; Patel, S. K.; Shah, R. R.; Patel, R. M., *Iran Polym J.* **2005**, *14*, 323.

Chapter 5

Synthesis, characterization and studies on the photovoltaic and nonlinear optic properties of a series of phenyl and thiophene bridged Donor-Acceptor systems based on dioctylaniline-*s*-triazine-rhodanine-3-acetic acid triad

Contents

Abstract

Two 1,3,5-triazine cored bipodal starburst D-A-A traids were designed and synthesized where octylaniline as the donor and a phenyl or thiophene bridged rhodanine-3-acetic acid as the acceptor/anchoring group. The photophysical and electrochemical studies showed that these molecules possess suitable electronic properties for use as dyes in DSSC applications. The photovoltaic properties of the DSSC devices constructed using TiO_2 as the semiconductor gave up to 0.3% as the photoconversion efficiency. The marked improvement in the efficiency over DTT-RHA shows that the presence of hydrophobic n-octyl groups has a significant role in enhancing the efficiency of the cells. Both compounds have

good two photon absorption coefficients and are good optical limiters.

5.1. Introduction

Through a systematic variation of the structure of starburst type dyes with 1,3,5-triazine as the core, diphenylamine as the donor and a series of acceptors with varying electron affinities we have demonstrated the importance of HOMO-LUMO energy levels in obtaining optimal photoconversion efficiencies in this class of D-A-A systems. Among these, the thiophene bridged system yielded best results. However, the overall photoconversion efficiencies were much lower than that obtained for standard dye such as N719 under identical experimental conditions. A major factor that controls the photoconversion efficiency is the back electron transfer within the dye as well as between the semiconductor and the electrolyte species.[1] Koumura *et. al.*, in their study of a series of carbazole-π-cyanoacetic acid dyes addressed this issue (Chart 5.1). They have identified the back electron transfer to the electrolyte as the efficiency limiting process in this type of dyes. To overcome this, they have introduced long alkyl substituents on the dye so that overall hydrophobicity of the TiO_2 surface increases upon adsorption of the dye. This increased hydrophobicity was acting as a barrier to the approach of the ionic electrolyte species to the semiconductor photoanode.[2-4] Similarly Cheng-Yong Su reported the effect of long alkyl chains on a series of triphenylamine-π-cyanoacetic acid dyes[5] (Chart 5.2). Here the

two phenyl rings on the triphenylamine bear alkyl substituents with varied chain length and the photo conversion efficiency improved from 4.99% for a methyl substituent to 6.04% for a nonyl substituent. We have employed this strategy in the design of dye reported in the present chapter. Here the donor group has been changed to a dioctylaniline and rhodanine-3-acetic acid as the acceptor on a 1,3,5-triazine core with either phenyl or thiophene as the acceptor/anchoring group (Chart 5.3).

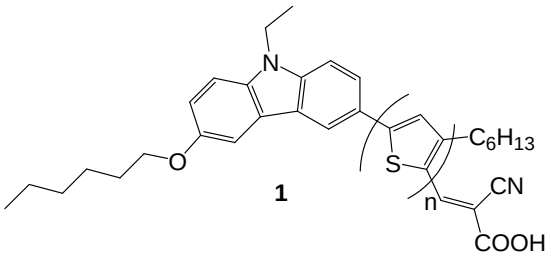

1

Chart 5.1.

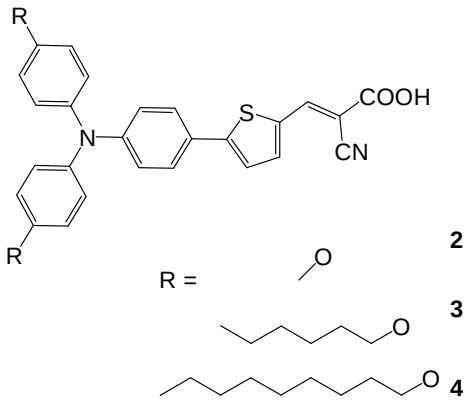

2

3

4

Chart 5.2.

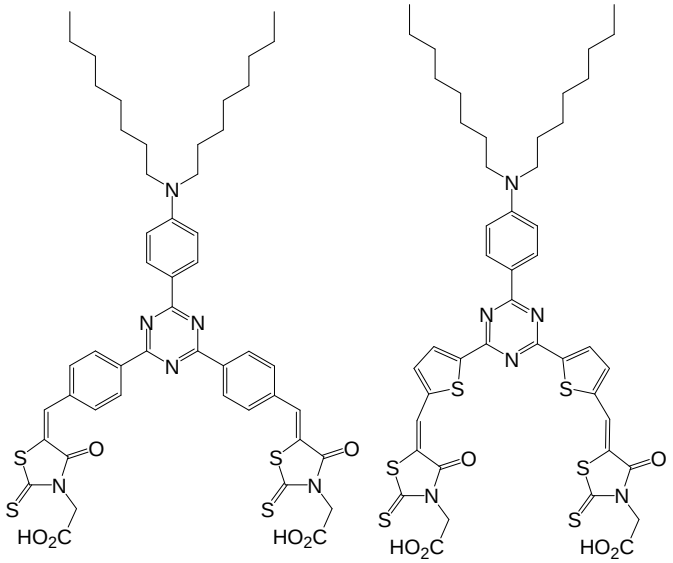

OTP-RHA (5) **OTT-RHA (6)**

Chart 5.3.

5.2. Results and discussion

5.2.1. Design and synthesis

The starburst D-A-A triads with triazine core and thiophene bridge or phenyl bridge were synthesised by adopting the synthesis scheme illustrated in Scheme 5.1. By using the Suzuki coupling strategy the octylaniline substituted 2,4-dichlorotriazine **8** was allowed to react with **9** or **10** in the presence of tetrakistriphenylphosphinepalladium(0) and K_2CO_3 to prepare the

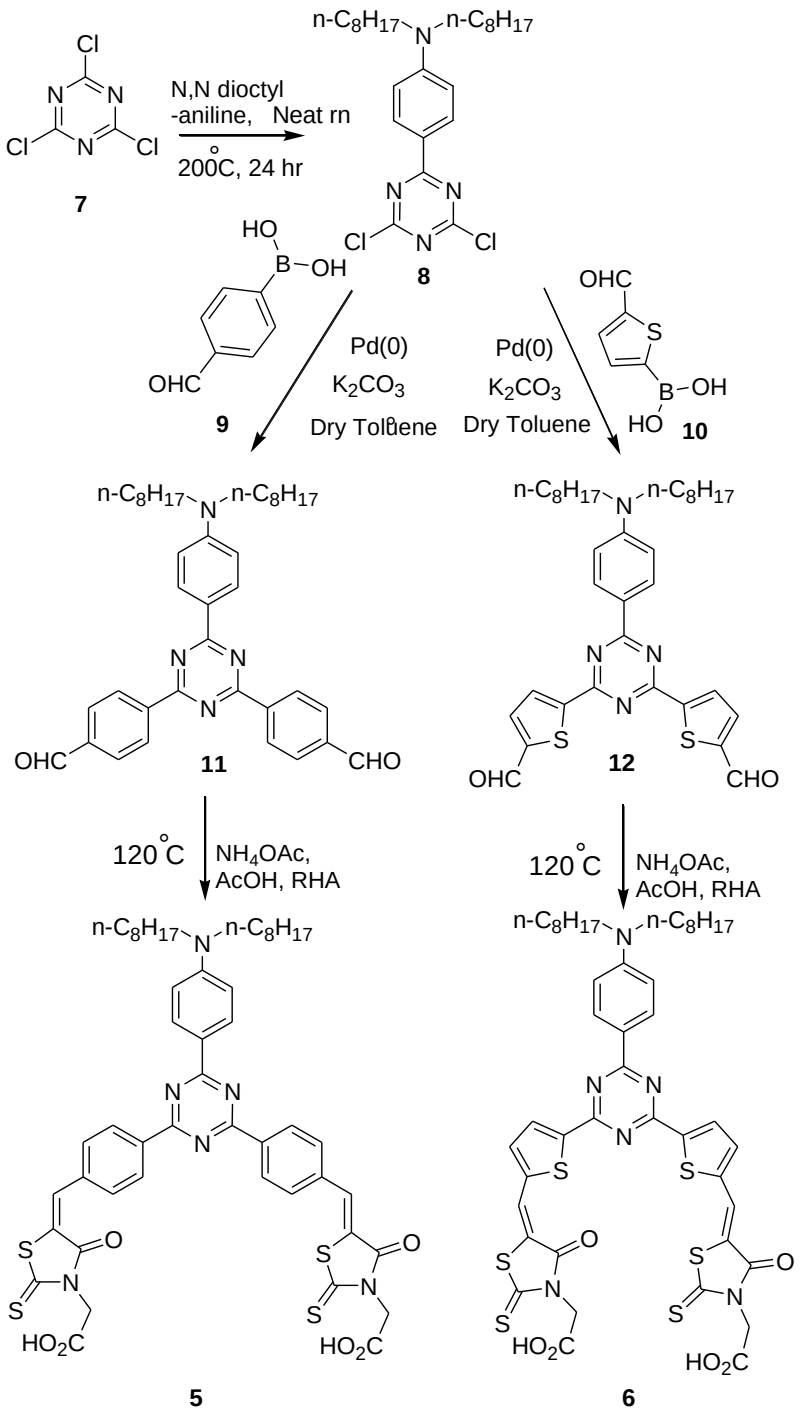
N,N dioctyl
-aniline, Neat rn
200°C, 24 hr
7
8
9
10
Pd(0)
K2CO3
Dry Toluene
Pd(0)
K2CO3
Dry Toluene
11
12
120°C
NH4OAc,
AcOH, RHA
120°C
NH4OAc,
AcOH, RHA
5
6

Scheme 5.1.

dialdehyde (**11** or **12**). The dialdehyde **11** or **12** was subjected to Knoevenagel condensation with rhodanine-3-acetic acid, in the presence of ammonium acetate in glacial acetic acid at 120 $^{\circ}$C. The products **5** (OTP-RHA) and **6** (OTT-RHA) were obtained with 50-60% yield. All the compounds were characterized using ^{1}H NMR, ^{13}C NMR, FT-IR spectroscopy and elemental analysis.

5.2.2. Photophysical studies

Absorption spectra of OTP-RHA and OTT-RHA show characteristic intramolecular charge transfer absorption band at 382 nm and at 381 nm. In addition to the band at 381 nm, OTT-RHA showed two additional weak absorptions at 445 nm and 502 nm, with onset of absorption extending to 600 nm (Figure 5.1A). The diffuse reflectance spectra of all the compounds in the powder form however, show broad absorption spectra with maximum at 390 nm and the onset of absorption extending to 650 nm (Figure 5.1B). Both the compounds shows emission at 430 nm for OTP-RHA and 409 nm for OTT-RHA at an excitation wavelength at 370 nm (Figure 5.2). The ability of these compounds in binding with TiO_2 was probed by diffuse reflectance spectroscopy of dye coated nano-crystalline TiO_2 thin films (Figure 5.3) prepared by immersing in respective dye solutions in DMF for 24 h. All films showed light red color and washed thoroughly with DMF, water and ethanol and dried in air prior to measurement and the spectra obtained showed characteristic red shift in the absorption maximum.[6]

The singlet excitation energy $E_{0\text{-}0}$ was calculated from onset of the absorption spectrum obtained in DMF solution. Photophysical properties of these compounds were summarized in Table 5.1.

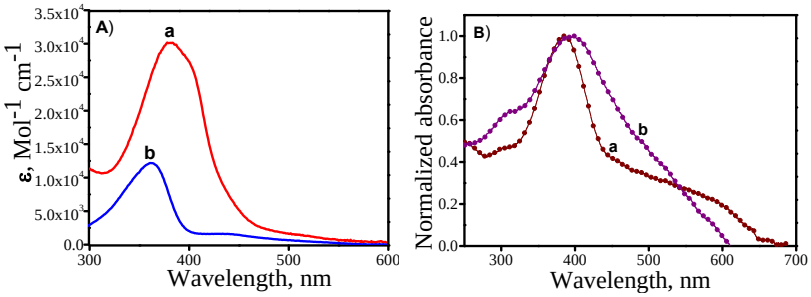

Figure 5.1. Absorption and diffuse reflectance spectrum of compounds OTT-RHA (a), OTT-RHA (b) A) in DMF, B) in powder form

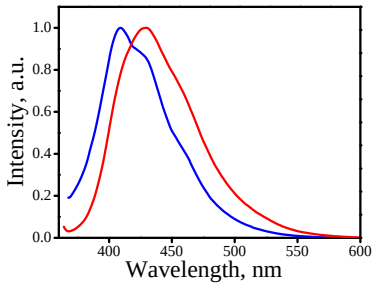

Figure 5.2. Fluorescence spectrum of OTP-RHA (——) and OTT-RHA (——) in DMF (concentration ~1 X 10^{-8} M)

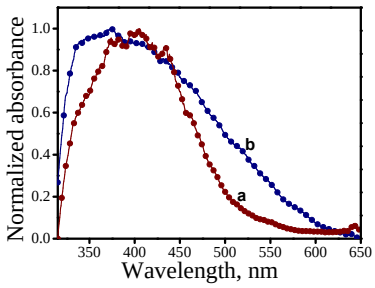

Figure 5.3. Diffuse reflectance spectra of OTP-RHA (a) and OTT-RHA (b) adsorbed TiO_2 thin films

Table 5.1. Photophysical properties of OTP-RHA and OTT-RHA

Compounds	λ_{max} (Abs), nm	ε_{max}, dm^3mol^{-1} cm^{-1}	λ_{max} (Em) , nm	E_{0-0}, eV
OTP-RHA	382	3×10^4	410	2.53
OTT-RHA	381, 445 (Sh_1), 502 (Sh_2)	1.35×10^4	430	2.18

5.2.3. Electrochemical properties

The oxidation potentials of these compounds were determined from the square wave voltammograms of these compounds in DMF by using glassy carbon electrode as the working electrode, platinum counter electrode and tetrabutylammonium hexafluorophosphate as the supporting electrolyte. The potential obtained were corrected by using Ferrocene as an external standard and are referenced to NHE. The square wave voltammograms obtained were given in Figure 5.4. They exhibit characteristic oxidation potentials at 1.23 V and 1.24 V *vs.* NHE respectively, for OTP-RHA and OTT-RHA. These values are lower than the redox potential of the electrolytes I^-/I_3^- and Br^-/Br_3^- used in the construction of DSSC's. The energy gap between the redox couple and oxidation potential of the dye is significant in determining the current as well as the fill factor. For the compounds used in the present study the energy gap obtained is very large (0.73 V) for I^-/I_3^- and very low (0.14 V) for Br^-/Br_3^-. This energy difference is conductive for an exergonic regeneration of the oxidized during the operation of the cell.[7] The values of HOMO energy levels of these compounds referenced to NHE were

calculated from the oxidation potentials of these compounds. The values are comparable to that observed for the DTOP, DTP and DTT series of compounds. The LUMO energies were calculated by adding their respective singlet energy to the HOMO energies. Estimations of HOMO and LUMO energies against vacuum continuum have also been done and all the values are presented in Table 5.2. An important feature is the lowering of LUMO levels achieved when thiophene bridge is incorporated in lieu of phenyl in OTP-RHA. This dramatic effect could be due to the efficient electronic coupling between the donor and the acceptor moiety offered by thiophenyl bridge.[8-9] Thus the use of thiophenyl bridge has proved as a viable strategy to properly tune the LUMO levels to match the conduction band of the TiO_2 *i.e.* -0.5 V. A comparison of the energy levels of the dye, semiconductor and the redox couples were presented in Figure 5.5. As illustrated OTT-RHA possess the best electronic characteristics to be used as sensitizer in DSSC.

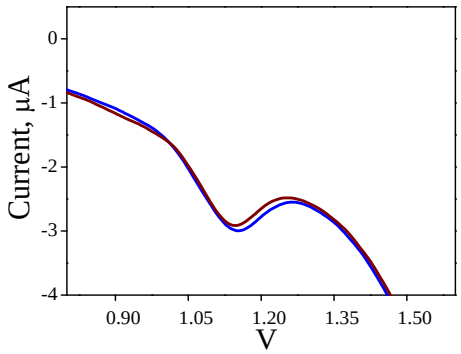

Figure 5.4. Square wave voltammograms of the of OTP-RHA (——) and OTT-RHA (——) in DMF (concentration 4 x 10^{-5} M)

Table 5.2. Electrochemical properties of OTP-RHA and OTT-RHA in DMF[10]

Compounds	[a]E_{onset} /V in DMF	[b]E_{onset} (ox) *Vs.* E_{FOC}/V	[c]$E_{(S+/S)}$ *vs.* NHE/ V	LUMO *vs.* NHE/eV	[d]E_{gap}/ V
OTP-RHA	1.14	1.03	1.23	-1.30	0.80
OTT-RHA	1.15	1.04	1.24	-0.94	0.74

[a]Observed reduction potentioan in DMF, [b]E_{FOC}= –0.11 V *vs.* Ag/AgCl. [c]The ground-state oxidation potentials $E_{(S+/S)}$ (HOMO) were measured in DMF containing 0.1 mol tetrabutylammonium hexafluorophosphate as supporting electrolyte using a glassy carbon working electrode, a Pt counter electrode and a Ag/AgCl reference electrode. [d]E_{gap} is the energy gap between LUMO of the compound and the conduction band level of TiO_2 (−0.5 V *vs.* NHE).

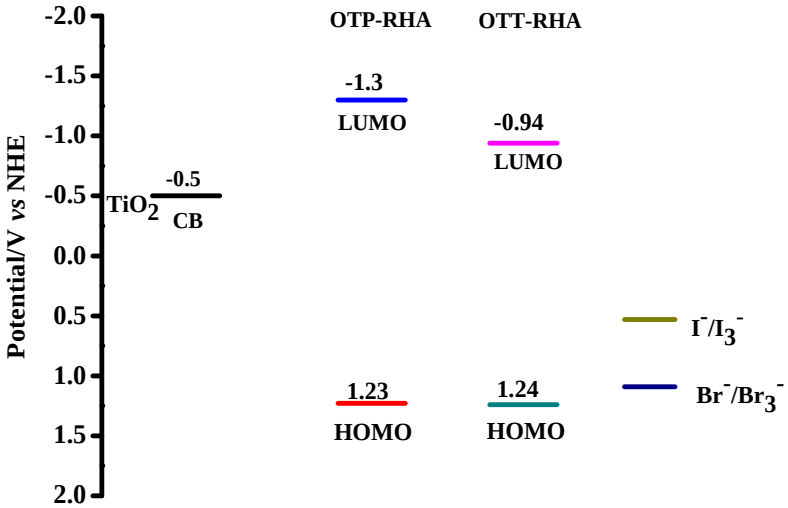

Figure 5.5. Schematic energy level diagram for a DSSC based on dyes coated nanocrystalline TiO_2 film on conducting FTO

5.2.4 Theoretical study

The optimized geometry of the compounds as well as the frontier orbitals and their energies are computed by density functional theory (DFT)[11] with B3LYP exchange-correlation functional and 6-31+G(d) basis set.[12-13] The stationary points are characterized by frequency calculation. To include the effects of solvation the polarization continuum model (PCM) for DMF has been used in the calculations. All calculations were performed with the GAUSSIAN 09 quantum chemistry package. The optimized geometry along with the frontier orbital representation and their respective energies against vacuum continuum is given in Figure 5.6. Delocalization of HOMO among the aniline moiety and the triazine has a profound effect in the lowering of HOMO energies as well as on the observed oxidation potential of these compounds. As seen in the DTP and DTT series, the LUMO is delocalised on both branches of the acceptor/anchoring part of the molecule. All the compounds show better directionality of charge transfer as the HOMO and LUMO are localized on different regions of the molecule. The theoretically calculated energy levels are also found to be matching with the experimental values obtained from electrochemical measurements Table 5.3.

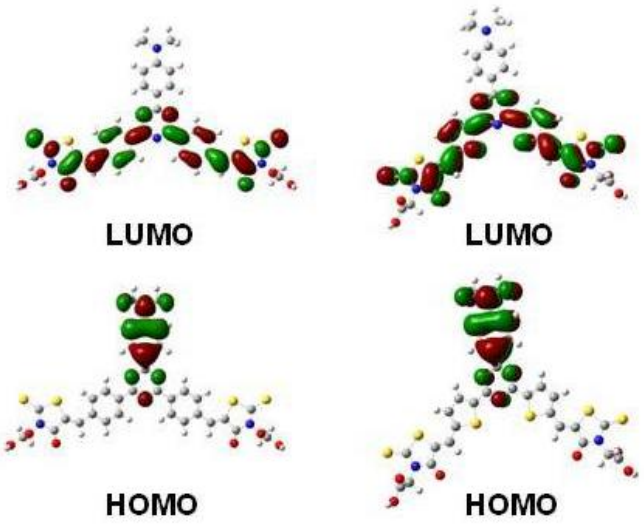

Figure 5.6. Optimized geometries of the compounds computed using DFT theory at the B3LYP/6-31G + (d) level

Table 5.3. Comparison of theoretical and experimental frontier orbital energies of of OTP-RHA and OTT-RHA

	Experimental		Theoretical	
Compounds	**HOMO[a]**	**LUMO[b]**	**HOMO**	**LUMO**
OTP-RHA	-6.03	-3.50	-5.56	-3.09
OTT-RHA	-6.04	-3.86	-5.94	-3.27

[a]Ionization potential: IP = – 4.8 – (E_{onset} (ox)– E_{FOC}); [b]electron affinity: EA − $E_{0\text{-}0}$ = IP

5.2.5. Photoelectrochemical properties

The DSSC devices constructed using dye adsorbed TiO_2 thin films and a Pt counter electrode with either I^-/I_3^- or Br^-/Br_3^- were illuminated by an AM 1.5 light source.[14-15] J-V characteristics typical for photodiodes were obtained for both compounds. The J-V curves obtained for OTT-RHA and OTP-RHA are given in Figure 5.7. The solar cell parameters obtained are summarized in

Table 5.4. Under our experimental conditions an efficiency of 6.6 % was obtained for the N719 compound when I^-/I_3^- was used as the electrolyte and 3% for Br^-/Br_3^-. The results show that the observed conversion efficiency of OTP-RH**A** was 0.12 and for OTT-RHA the efficiency was 0.3 when Br^-/Br_3^- was used as the electrolyte. The data obtained for the cells with I^-/I_3^- as the electrolyte were very low in comparison to the data obtained for Br^-/Br_3^- in terms of V_{oc} and η. This is expected as the potential difference between the Fermi level of TiO_2 and the redox potential of I^-/I_3^- is low compared to Br^-/Br_3^- redox couple. The improved efficiency obtained for OTT-RHA further proves the importance of thiophene as the bridging group in the design of the dye. The improved efficiency data observed to that obtained for dyes of DTT series reported in the previous chapter also signifies important role of increased hydrophobicity in reducing energy wasting short circuiting caused by the interaction of the electrolyte with the semiconductor. Relatively better performance of OTT-RHA suggests a similar design strategy for the synthesis of better performing sensitizers for DSSC applications.

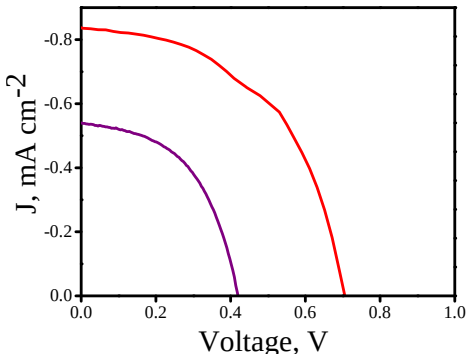

Figure 5.7. Photocurrent density-voltage curves of the compounds OTP-RHA (——) and OTT-RHA (——) using Br^-/Br_3^- electrolyte

Table 5.4. DSSC Performance data for the compounds OTP-RHA and OTT-RHA

Dyes	J_{SC}, mA cm^{-2}	V_{oc}, V	FF, %	η, %
OTP-RHA	-0.0543[a] (±0.002)	0.4190[a] (±0.002)	44[a]	0.01[a]
	-0.5373[b] (±0.002)	0.4228[b] (±0.002)	53[b]	0.12[b]
OTT -RHA	-0.3818[a] (±0.003)	0.4099[a] (±0.004)	45[a]	0.07[a]
	-0.8424[b] (±0.002)	0.7081[b] (±0.002)	50[b]	0.3[b]

[a] I^-/I_3^- electrolyte; [b] Br^-/Br_3^- electrolyte

5.2.6 Nonlinear optical properties

The third-order NLO properties of compounds OTP-RHA and OTT-RHA were investigated by Z-scan technique using second harmonic 532 nm laser beam of the Nd:YAG laser. The open-aperture (OA) Z-scan results and their fit to the two photon absorption theories suggest that these compounds are good NLO materials that show third order nonlinear optical properties in ~1 mM DMF solutions. The OA Z-scan data for both compounds are given in Figures 5.8a and 5.8b, respectively. The fitted curves

(solid lines in Figure 5.8a and 5.8b) to two photon absorption theory gave the β values as 0.22 x 10^{-10} and 0.64 x 10^{-10}. The optical limiting thresholds were also determined (Figure 5.9) and the results are presented in Table 5.5. Attempts to perform the closed aperture scan were failed due to the overlapping absorption spectra of the compouds at the excitation wavelength, 532 nm.

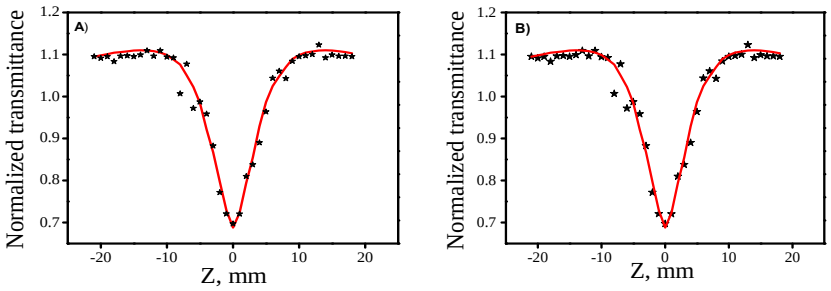

Figure 5.8. Open aperture Z-scan profile of OTP-RHA (A) and OTT-RHA (B) in DMF

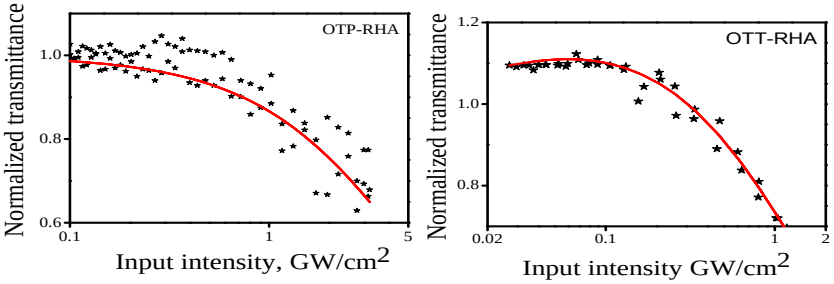

Figure 5.9. Optical limiting profile of OTP-RHA and OTT-RHA in DMF

Table 5.5. NLO properties of the compounds of OTT-RHA and OTT-RHA in DMF

Compounds	**Nonlinear absorption coefficient (β), mW^{-1}**	**σ_2, GM**	**Optical limiting threshold, GW/cm^2**
OTP-RHA	0.22 X 10^{-10}	142302	0.22
OTT-RHA	0.64 x 10^{-10}	401995	0.10

5.3 Conclusion

Two starburst D-A-A triads with 1,3,5-triazine core as the non-conjugating spacer/acceptor with phenyl/thiophene bridged (OTT-RHA and OTT-RHA) with rhodanine-3-acetic acid as anchoring/acceptor groups were synthesised. Electrochemical, photophysical and theoretical studies show that they have improved electronic properties for use as dyes in dye sensitized solar cells compared to dyes reported in the previous chapters. The applicability of these dyes for the DSSC was tested by constructing the sandwich model photovoltaic cell. However, the observed efficiency was lower than that obtained for N719 dye under similar experimental conditions. Though the newly synthesised compounds show lesser absorption coverage of the solar spectrum than the DTT series compounds, the improved efficiency obtained may be due to the effect of increasing hydrophobic character of the dye by incorporating alkyl chain on the dye structure. Both the compounds show good nonlinear optical properties and can be used as material for optical limiters.

5.4 Experimental

5.4.1. Synthesis of OCT-T (8)

2,4,6-trichloro-1,3,5-triazine (**1,** 100 mmol) and N,N-dioctylaniline (200 mmol) were refluxed at 70^0C for 20h and treated with water (100 mL). The organic layer was extracted with chloroform. The extract was washed several times with water and dried over anhydrous sodium sulphate prior to evaporation under

vacuum in a rotary evaporator. The residue was purified by column chromatograpy using hexane-ethyl acetate (1:4) to yield **8** in 68% yield as an red viscous liquid. FT-IR (cm^{-1}); 2910, 1195. ^{1}H NMR 8.3 (1H, d, J = 12 Hz), 6.3 (1H, d, J = 8 Hz), 3.36 (1H, t, J =16), 1.64-0.87 (15H, m), ^{13}C NMR (100 MHz, DMSO): 170.83, 153.18, 132.42, 118.74, 111.11, 51.14, 31.78, 31.78, 29.39, 29.24, 27.27, 27.04, 22.61, and 14.05. Anal. Calc. for. $C_{25}H_{38}C_{l2}N_4$ C, 64.50; H, 8.23; Cl, 15.23; N, 12.04, Found; C, 64.48; H, 8.17; Cl, 15.18; N, 12.00.

5.4.2. Synthesis of OCT-T-PH (11) or OCT-T-TH (12)

A solution 4-formyl phenylboronic acid (**9**) or 5-formyl 2-thienyl boronic acid (**10**) (200 mmol) tertakis(triphenylphosphene) palladium(0) (20 mmol) and K_2CO_3 (10 mmol) under N_2 atmosphere at room temperature followed by a solution of compound **8** (100 mmol) in dichloromethane (50 mL). The mixture was stirred for 24 h and the organic layer was separated and washed with distilled water. The residue obtained was purified by column chromatography on silica gel. Elution with a mixture of (1:20) hexane and dichloromethane gave pale yellow powder of **11** (68 %) or **12** (65%).

OCT-T-PH (11): FT-IR (cm^{-1}): 3330, 2915, 2858, 1592, 1396, 1105; ^{1}H NMR (400 MHz, DMSO, δ ppm): 8.3 (1H, d, J = 9.2 Hz), 6.63 (1H, d, J = 9.2 Hz 3.36 (1H, t, J = 8), 1.64-0.87 (15H, m); ^{13}C NMR (100 MHz, DMSO):170.83, 153.15, 132.42, 118.74, 111.11, 51.42, 31.78, 29.39, 29.24, 27.27, 27.04, 22.61, 14.05; MW= 604.

Anal. Calcd. for $C_{39}H_{48}N_4$; C, 77.45; H, 8.00; N, 9.26; Found: C, 77.25; H, 7.95; N, 9.16.

OCT-T-TH (12): FT-IR (cm^{-1}): 3330, 2915, 1598, 1103. ^1H NMR (400 MHz, DMSO, δ ppm): 11.08, (1s, 1H), 7.99 (s, 1H), 6.7 (s, 1H) 1.5-0.86 (m, 15H). ^{13}C NMR (100 MHz, DMSO, δ PPM): 178.46, 143.50, 110.72, 31.18, 28.78, 28.63, 22.03, 13.90.Anal. Calcd. for $C_{35}H_{44}N_4O_2S_2$ C, 68.15; H, 7.19; N, 9.08; O, 5.19; S, 10.40, Found: C, 68.10; H, 7.15; N, 9.00; O, 5.15; S, 10.35.

5.4.3. General procedure for OTP-RHA (5) and OTT-RHA (6)

A mixture of dialdehyde **11** or **12** (10 mmol) and of rhodanine-3-acetic acid (22 mmol) and ammonium acetate (19 mmol) were dissolved in 0.5 M acetic acid and refluxed for 12 h. After cooling, the precipitated target products **5** or **6** were washed successively with chloroform and methanol to remove the unreacted reagents.

OTP-RHA (5): Yield 60%, mp. 280 °C (decomp.); FT-IR (cm^{-1}): 3330, 2915, 1598, 1103. ^1H NMR (400 MHz, DMSO, δ ppm): 11.06 (s, 1H), 7.99-7.93 (m, 2H), 7.86-7.76 (m, 2H), 7.61-7.51(m, 1H), 6.76-6.68 (m, 1H), 4.76 (s, 2H), 1.52-0.85 (m, 15H) . ^{13}C NMR (100 MHz, DMSO, δ ppm): 180.87, 121.14, 106.74, 31.16, 28.82, 28.68, 26.67, 20.14, 22.02. Anal. Calcd. for $C_{49}H_{54}N_6O_6S_4$ -C, 61.87; H, 5.72; N, 8.83; S, 13.48, Found: C, 61.75; H, 5.64; N, 8.75; S, 13.40.

OTT-RHA (6): yield 68%, mp. 289 °C (decomp.) FT-IR (cm^{-1}): 3336, 2920, 1598, 1385, 1209, 711. ^{1}H NMR (400 MHz, DMSO, δ ppm):10.61(s, 1H), 8.17 (s, 1H), 7.99 (d, 1H, *J*=8.8 Hz) 7.82 -7.80 (d, 2H), 4.74 (s, 1H) 6.6 (s, 1 H), 3.28 (t, 5H, *J*=7.6 Hz), 1.84-0.80 (m, 15H).^{13}C NMR (100 MHz, DMSO, δ ppm): 178.95, 152.97, 111.45, 31.78, 29.41, 29.26, 27.21, 27.05, 22.62, and 14.06. Calcd. for $C_{45}H_{50}N_6O_6S_6$ - C, 56.11; H, 5.23; N, 8.72; S, 19.97, Found: C, 56.08; H, 5.19 N, 8.65; S, 19.85.

5.5. References

1. Koumura, N.; Wang, Z.-S.; Miyashita, M.; Uemura, Y.; Sekiguchi, H.; Cui, Y.; Mori, A.; Mori, S.; Hara, K. *J. Mater. Chem.* **2009,** *19*, 4829.
2. Yu, Q.-Y.; Liao, J.-Y.; Zhou, S.-M.; Shen, Y.; Liu, J.-M.; Kuang, D.-B.; Su, C.-Y. *J. Phys. Chem.C.* **2011,** *115*, 22002.
3. Wang, X.; Guo, L.; Xia, P. F.; Zheng, F.; Wong, M. S.; Zhu, Z. *J. Mater. Chem. A.* **2013**, *1*, 13328.
4. Yu, Q.-Y.; Liao, J.-Y.; Zhou, S.-M.; Shen, Y.; Liu, J.-M.; Kuang, D.-B.; Su, C.-Y., *J. Phys. Chem.* **2011,** *115* , 22002.
5. Wang, Z. S.; Hara, K.; Dan-Oh, Y.; Kasada, C.; Shinpo, A.; Suga, S.; Arakawa, H.; Sugihara, H. *J. Phys. Chem. B.* **2005,** *109* , 3907.
6. Koumura, N.; Wang, Z-S.; Mori, S.; Miyashita, M.; Suzuki, E.; Hara, K. *J. Am. Chem. Soc*. **2006**, *128,* 14256.
7. Hagfeldt, A.; Grätzel, M. *Chem. Rev*. **1995**, *95*, 49.
8. Hara, K.; Sato, T.; Katoh, R.; Furube, A.; Ohga, Y.; Shinpo, A.; Suga, S.; Sayama, K.; Sugihara, H.; Arakawa, H. *J. Phys. Chem. B*. **2003**, *107*, 597.
9. Hao, X.; Liang, M.; Cheng, X.; Pian, X.; Sun, Z; Xue, S. *Org. Lett.* **2011**, *13*, 5424.
10. Longhi, E.; Bossi, A.; Di Carlo, G.; Maiorana, S.; De

Angelis, F.; Salvatori, P. *Eur. J. Org. Chem.* **2013**, *84.*
11. Parr, R. G.; Yang, W., Density-Functional Theory of Atoms and Molecules; Oxford University Press, **1989**, New York.
12. Becke, A. D., *J. Chem. Phys*. **1993**, *98*, 5648.
13. Lee, Yang, W.; Parr, R. G., *Phys. Rev. B*. **1994**, *37*, 785.
14. Wang, Z.; Sayama, K.; Sugihara, H. *J. Phys. Chem. B.* **2005**, *109*, 22449.
15. Teng, C.; Yang, X.; Yuan, C.; Li, C.; Chen, R.; Tian, H.; Li, S.; Hagfeldt, A.; Sun, L.*Org. Lett.* **2009**, *11*, 5542.

Photovoltaic and nonlinear optical studies of a few Donor-π-Acceptor molecules with s-triazine core

Thesis submitted to the
Cochin University of Science and Technology
in partial fulfilment of the requirements
for the award of the degree of
Doctor of Philosophy in Chemistry
Under the Faculty of Science

by
SUMA, C. S.
(Reg. No. 3712)

DEPARTMENT OF APPLIED CHEMISTRY
COCHIN UNIVERSITY OF SCIENCE AND TECHNOLOGY
KOCHI – 682 022, KERALA, INDIA

June 2016

.....To my parents

Declaration

I hereby declare that the work presented in the thesis entitled "**Photovoltaic and nonlinear optical studies of a few Donor-π-Acceptor molecules with *s*-triazine core**" is an independent work carried out by me under the supervision of Dr. Manoj. N, Associate Professor, Department of Applied Chemistry, Cochin University of Science and Technology and the same has not been submitted elsewhere for any other degree, diploma or title.

Kochi-22 **Suma, C. S.**

20-06-2016

DEPARTMENT OF APPLIED CHEMISTRY
COCHIN UNIVERSITY OF SCIENCE AND TECHNOLOGY
Kochi – 682 022, KERALA, INDIA
Ph:-0091-484-2575804; Email: manoj.n@cusat.ac.in

Dr. Manoj, N.
Associate Professor

CERTIFICATE

This is to certify that the thesis entitled "**Photovoltaic and nonlinear optical studies of a few Donor-π-Acceptor molecules with *s*-triazine core**" is a genuine record of research work carried out by Ms. Suma, C. S., under my supervision, in partial fulfilment of the requirements for the degree of Doctor of Philosophy of Cochin University of Science and Technology, and further that no part thereof has been presented before for the award of any other degree. All the relevant corrections and modifications suggested by the audience and recommended by the doctoral committee of the candidate during the presynopsis seminar have been incorporated in the thesis.

Kochi-22 **Dr. Manoj,N.**
14-06-2016 (Thesis Supervisor)

Acknowledgements

The work presented in this thesis would not have been possible without my close association with many people who were always there

when I needed them the most. I take this opportunity to acknowledge them and extend my sincere gratitude for helping me to make this Ph.D. thesis a possibility. First and foremost, I express my sincere gratitude and obligation to my mentor Dr. Manoj, N. Associate Professor, Department of Applied Chemistry, Cochin University of Science and Technology, for giving me an opportunity to be in his research team, for his inspiration, excellent guidance, valuable suggestions and boundless support throughout my research work.

I am grateful to Dr. Prathapan, S. Doctoral committee member for his support and valuable suggestions.

I am very thankful to Prof. Dr. M. R. Prathapachandra Kurup, Head of the department and Prof. Dr. K. Girish Kumar and Prof. Dr. K. Sreekumar, former HODs of the Department of Applied Chemistry, CUSAT for providing the facilities of the department for carrying this work and encouragement.

My sincere thanks are also due to,

- Dr. P. A. Unnikrishnan for all the support and discussions at various stages of the work.
- All the teaching and nonteaching staff of the Department of Applied Chemistry, for their help and support.
- Dr. Gopidas K. R., NIIST, Thiruvananthapuram for valuable suggestions and support.
- Dr. Shibu, Dr. Adarsh and Mr. Saji, STIC & DST-SAIF, CUSAT, for NMR and CHNS analysis.
- Mrs. Thahira, A. for the LC-MS analysis.
- I owe greatly to my seniors Dr. Jomon, Dr. Eason, Dr. Sandhya, Dr. Sajitha and Dr. Reshma for their advice and support in many things within and beyond chemistry.

- Mr. Jaison and Ms. Sabitha, International School of Photonics, CUSAT, for Z-scan measurements.
- My colleagues, Ms. Seena, Ms. Pravitha, Mr. Senju, Ms. Kala, Mr. Rakesh, Ms. Minu, Ms. Soumya, Ms. Cisy, Ms. Nithya, Ms. Ligi, Mr. Shan, Mr. Tomson, Ms. Vineetha, Ms. Parvathy, Mr. Kiran, Mr. Jith, Mr. Fredi, Ms. Amrutha, Ms. Nishad, Ms. Jesna, Ms. Rani and Ms. Aswathy, Ms Nayana for their endless support during the work.
- My roommates Anjali and Bhavya for their care and love.
- Friends from the Department of Technical Education and Department of Collegiate Education for their inspiration.
- Dr. Mahesh, Dr. John, Dr. Jisha, Dr. Priya, Dr. Navya, Dr. Mangala, Dr. Manju, Ms. Mridula and other friends in the department and other departments in CUSAT.
- Principal, teachers and non-teaching staff of Govt. Women's Polytechnic College, Kalamasserry, Ernakulam for their encouragements and support.
- CSIR, Govt. of India for the financial assistance.
- SAIF, CUSAT for analytical support.

Words are inadequate to express my feelings for my family and teachers for their love and whole-hearted support throughout my academic career.

Above all, I thank God Almighty for the blessings.

Suma, C. S.

PREFACE

1,3,5-Triazine or *s*-Triazine and its derivatives have been recognized as synthons for the preparation of many pharmaceutical products, pesticides, dyestuffs, optical brighteners, explosives and surface active agents. Recently, triazine has been used as a core in starburst type blue fluorescent molecules for organic light emitting diodes. *s*-Triazines having unsymmetrical substitution pattern are promising structural unit for the synthesis of Donor-Acceptor systems. The unique structure of s-triazine donot permit direct coupling between the donor and acceptor moieties and this has been used as an effective tool for tuning HOMO and LUMO energy levels of such donor-acceptor molecules. Such donor-acceptor systems with acceptor groups which have affinity to semiconductor surfaces can be used as dyes for dye-sensitized solar cells (DSSC). Athanassios G. Coutsolelosand coworkers reported a triazine based D-A systems having porphyrin as a donor and triazine as the acceptor moiety having glycine anchoring unit for DSSC. In another report, triphenylamine coupled to triazine *via* direct arylation has been used in conjunction with rhodanine-3-acetic acid as the acceptor as well as the anchoring unit. DSSC devices fabricated with this design philosophy yielded efficiencies in the range of 0.35-1.81%. Some of the most efficient dyes reported for DSSC applications are based on inorganic complexes of Ruthenium and are very expensive to prepare. In this respect, triazine based dyes offer the cost advantage as the starting material 2,4,6-trichloro-1,3,5-triazine is a cheap synthon. This molecule can

undergo facile aromatic nucleophilic substitution, as well as Suzuki coupling reactions which offers the possibility of making symmetrically and unsymmetrically substituted triazine derivatives. Based on this design philosophy, we synthesized 1,3,5-triazine derivatives with diphenylamine as the donor and a series of heterocyclic cyclic amides as acceptors. The acceptor/anchoring groups used were rhodanine-3-acetic acid, barbituric acid and thiobarbituric acid along with cyanoacetic acid for comparison. We expected a strong binding interaction with TiO_2 surface as these cyclic amides are also strong acids which can deprotonate and bind as observed in dyes with cyanoacetic acid as the anchoring unit. Such molecules with an asymmetric polarization also show nonlinear optical properties. These molecules with unsymmetrical substitution in a starburst form are expected to have high non linearity with transparency and stability which are the major requirements for such applications. A systematic study of structural factors that control efficiency of DSSCs constructed using these dyes and third order nonlinear optical properties were carried out. The results of these studies are embodied in the thesis entitled "**Photovoltaic and nonlinear optical studies of a few Donor-π-Acceptor molecules with *s*-triazine core**".

The thesis is divided in to 5 chapters which are presented as independent units and therefore the structural formulae, schemes, figures and references are numbered chapter wise.

Chapter 1 is a review on the D-π-A systems and photovoltaic and NLO properties followed by introduction to the

chemistry and applications of s-triazine and the *s*-triazine cored donor-acceptor systems. The chapter is concluded with the objectives of the present work with a brief discussion on the design strategy adopted.

Chapter 2 describes the synthesis, characterization, photovoltaic and nonlinear optical properties of a series of starburst donor-acceptor systems having a *s*-triazine core with one diphenylamine unit as the donor and two benzylidene derivatives as acceptor moieties. The beznylidene acceptor units were linked to *s*-triazine through an oxa bridge. Three such derivatives were synthesized by the knoevenagel condensation of *p*-hydroxybenzaldehyde with rhodhanine-3-acetic acid, barbituric acid or thiobarbituric acid respectively. All these compounds were characterized by ^{1}H & ^{13}C NMR spectroscopy, FT-IR spectroscopy and elemental analysis. The photophysical, and electrochemical properties were studied and the experimental results were correlated to theoretical parameters obtained through DFT and TD-DFT calculations. The energies of the frontier orbitals were compared with that of the conduction and valence band of TiO_2 and the redox couples I^-/I_3^- and Br^-/Br_3^- used for the fabrication of the dye sensitized solar cells. All the compounds gave characteristic J-V curve for a photovoltaic system and yielded efficiencies that can be correlated to the electronic properties of these molecules. nonlinear optical properties were also studied using Z-scan technique and DTOP-BA was found to have good nonlinear absorption coefficient and nonlinear refractive index.

Chapter 3 of the thesis reports four donor-acceptor molecules where the benzylidine units having cyanoacetic acid, rhodanine-3-acetic acid, barbituric acid or thiobarbituric acid acceptor/anchoring groups are linked to the *s*-triazine core through a Suzuki–Miyaura aryl coupling reaction of N,N-diphenyl-2,6-dichlorotriazine. All the compounds gave characteristic J-V curve for a photovoltaic system and yielded efficiencies that can be correlated to the electronic properties of these molecules. Nonlinear optical properties were also studied using Z-scan technique. All the compounds were NLO active and among them DTP-BA was found to have good nonlinear absorption coefficient and nonlinear refractive index.

The absorption spectra of the compounds reported in chapter 2 and 3 showed the maximum only of 400 nm. To further improve the electronic coupling between the diphenylamine and the acceptor groups we have introduced thiophenylidene bridge instead of benzylidine bridge. In chapter 4 we report the synthesis, characterization, photovoltaic and nonlinear optical properties of these compounds. As expected these compounds showed an extended absorption maximum of 516 nm in the case of thiobarbituric acid conjugate. With this, we could achieve a better coverage of the solar spectrum up to 650 nm. All these compounds show photoconversion efficiencies better than the compounds reported in the previous chapters. All the dyes showed good nonlinear absorption properties with two photon absorption

mechanism and these compounds can be used as optical limiting materials in optoelectronic applications.

In the case of compounds reported in the previous three chapters the donor amine was linked to the *s*-triazine through the N atom of the amine. In chapter 5, to study the effect of electronic interaction between the donor and the triazine moiety as well as the effect of hydrophobicity of the dye in controlling the photoconversion efficiencies we have synthesized N,N-dioctylaniline–2,6–dichlorotriazine conjugate *via* a Friedel-Crafts arylation reaction. This was coupled with 4-formylphenylboronic acid or 5-formyl-2-thienylboronic acid to obtain the dialdehydes. The dialdehyde was coverted to the respective compounds by knoevenagel condensation with rhodanine-3-acetic acid. Absorption spectrum of these compounds did not show any dramatic change upon this modification. However, the photoconversion efficiencies showed improvements which could be due to the increased hydrophobicity which control the back electron transfer to the electrolyte. Both compounds showed NLO properties and can be used as optical limiters in optoelectronic applications.

A summary of the work is given towards the end of the thesis.

List of Abbreviations

AcOH	:	acetic acid
DCM	:	dichloromethane
DMF	:	Dimethylformamide
DMSO	:	Dimethyl sulfoxide
d	:	doublet
EtOH	:	ethanol
FTO	:	Florine dopped Tin Oxide
ICT	:	Intramolecular Charge Transfer
NMR	:	Nuclear Magnetic Resonance
HOMO	:	Highest Occupied Molecular Orbital
LUMO	:	Lowest Unoccupied Molecular Orbital
mg	:	milligram
mL	:	millilitre
nm	:	nanometer
NLO	:	NonLinear Optics
PET	:	Photoinduced Electron Transfer
PEDOT-PSS	:	poly(3,4-ethylenedioxythiophene) polystyrene sulfonate
s	:	singlet
Spiro-OMETAD	:	2,2',7,7'-Tetrakis[N,N-di(4methoxyphenyl)amino]-9,9'-spirobifluorene
TBAB	:	Tetrabutylammonium bromide
t	:	triplet

Contents

Chapter-5

Publication

1. Thiobarbituric acid dyes for dye sensitized solar cell application. **Suma, C. S**., Manoj, N., *Proceedings of the International Conference on Materials for the Millennium (MATCON 2016),Vol.2* , **2016**, *2*, 684-686, ISBN 978-93-80095-738

Papers presented in symposia

1. Thiobarbituric acid dyes for dye sensitized solar cell applications. **Suma, C.S**., Manoj N. poster presentation at International Conference on Materials for the New Millennium (MATCON-2016), held at Department of Applied Chemistry, Cochin University of Science and Technology, Kochi-22 during 14-16 January **2016**. PP. ENM175.

2. Novel twin legged D-A-π-A sensitizer molecules containing 1,3,5-traiazine core for DSSC applications'. **Suma Chemben Subramanyan**, Manoj Narayanapillai. Presented a poster at. International Conference on Green Chemistry (ICGC-2015) held at Department of Chemistry, Goa University, GOA. January **2015**, PP-79.

3. Novel twin legged D-A-π-A sensitizer molecules containing 1,3,5-traiazine as p spacer for dye sensitized solar cell applications. **Suma Chemben Subramanyan**, Manoj Narayanapillai . an oral presentation at National Seminar "Trends in Physics" (Trips-2015) held at the Department of Physics, Sree Sankarachayra College, Kalady, Ankamaly, Ernakulam, **2015,** OP-V.

4. Ship in a bottle synthesis of 2,6-diphenyl-4-pyridile pyrilium cations encapsulated in zeolites Y and beta, **Suma, C. S**. , Manoj N., presented a poster at National Conference "Current Trends in Chemistry" (CTriC-2012) held at the Department of Applied Chemistry, Cochin University of Science and Technology, Kochi during 20-21 January **2012**, PP-27

SUMMARY

The thesis entitled "**Photovoltaic and nonlinear optical studies of a few Donor-π-Acceptor molecules with *s*-triazine core**" embodies the results of the investigations carried out to study unsymmetrically substituted *s*-Triazine cored starburst donor – acceptor systems with a bipodal acceptor/anchoring group design. The thesis opens with a review on the application of organic donor-acceptor systems in photovoltaics with special emphasis on applications in dye sensitised solar cells. The review also briefly discusses the application of such systems in the development of nonlinear optical materials.

The unique structure of s-triazine do not permit direct coupling between the donor and acceptor moieties and this has been used as an effective tool for tuning HOMO and LUMO energy levels of such donor acceptor molecules. The effect of nature of the π-bridge and the acceptor groups on the photovoltaic properties was studied and the results are presented in chapters 2, 3 and 4. Among the three types of π-bridges studied, thiophene served as the best in terms of improving absorption spectral properties. Thiophene bridged dyes (DTT-CYA, DTT-RHA, DTT-BA and DTT-TBA) showed better coverage of the solar spectrum. Photovoltaic properties of these dyes were studied by constructing sandwhich model dye sensitized solar cells with nanocryasalline thin film of TiO_2 on FTO coated with the respective dye as the photoanode, I^-/I_3^- and Br^-/Br_3^- as the redox couple/electrolyte and a platinized FTO as the cathode. The cell parameters and the

photoconversion efficiency calculated show that the thiophene bridged dyes when used with Br^-/Br^{3-} as the redox couple/electrolyte have the optimal performance.

In chapter 5, the effect of hydrophobicity of the dye in reducing the back electron transfer to the electrolyte was studied by choosing di-octylaniline as the donor group. The long hydrocarbon chain can increase the hydrophobicity of the dye molecules. Among the two dyes synthesised and studied OTT-RHA with the thiophene π-bridge showed optimal performance. Though these dyes have poor coverage of the solar spectrum the measured photoconversion efficiencies were higher than the dyes in the DTOP, DTP and DTT series. This shows that the back electron transfer to the electrolyte is a major efficiency limiting process in these series of dyes. Based on the results presented better dyes can be designed and synthesised. A prospective design of the dye with optimal efficiency can be made with the following aspects in mind.

- A bithiophene π-bridge can be used for further lowering of LUMO energy and thereby achieving a better coverage of the solar spectrum
- Diphenylamine donor group can be replaced with a bis (4-alkoxy-phenyl)amine having long alkyl chains. This will introduce the hydrophobic barrier which will reduce the efficiency limiting back electron transfer to the redox couple.

All dyes prepared were thermally and optically stable and studied for their nonlinear optical properties by Z-scan technique.

Among the acceptor groups studied barbituric acid based dyes show better NLO properties. In particular, DTOP-BA was found to have excellent third order NLO properties. The thiophene bridged dyes show very good optical limiting behaviour. The results of the study show that unsymmetrically substituted triazine is a good structural motif for the design of better NLO active materials.